MICROCOPY RESOLUTION TEST CHART
NATIONAL BUREAU OF STANDARDS-1963-A

AFOSR·TR· 83-1045

EFFECTS OF BLOWING SPANWISE FROM
THE TIPS OF LOW-ASPECT RATIO WINGS
OF VARYING TAPER RATIO, WITH APPLICATION
TO IMPROVING STOL CAPABILITY OF
FIGHTER AIRCRAFT

by

R. G. Schwind and M. M. Briggs

83 12 13 128

DTIC
SELECTED
DEC 15 1983

D

NIELSEN ENGINEERING
AND RESEARCH, INC.

OFFICES: 510 CLYDE AVENUE / MOUNTAIN VIEW, CALIFORNIA 94043 / TELEPHONE (415) 968-9457

#11

⑫

EFFECTS OF BLOWING SPANWISE FROM
THE TIPS OF LOW-ASPECT RATIO WINGS
OF VARYING TAPER RATIO, WITH APPLICATION
TO IMPROVING STOL CAPABILITY OF
FIGHTER AIRCRAFT

by

R. G. Schwind and M. M. Briggs

NEAR TR 294

February 1983

DTIC
ELECTE
DEC 15 1983

D
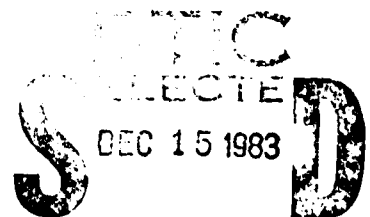
D

REPORT DOCUMENTATION PAGE		READ INSTRUCTIONS BEFORE COMPLETING FORM
1. REPORT NUMBER AFOSR-TR- 83-1045	2. GOVT ACCESSION NO. AD-A135688	3. RECIPIENT'S CATALOG NUMBER
4. TITLE (and Subtitle) EFFECTS OF BLOWING SPANWISE FROM THE TIPS OF LOW-ASPECT RATIO WINGS OF VARYING TAPER RATIO, WITH APPLICATION TO IMPROVING STOL CAPABILITY OF FIGHTER AIRCRAFT		5. TYPE OF REPORT & PERIOD COVERED Final 1 Apr 82 – 30 Sep 82
		6. PERFORMING ORG. REPORT NUMBER TR 294
7. AUTHOR(s) R. G. Schwind M. M. Briggs		8. CONTRACT OR GRANT NUMBER(s) F49620-82-C-0061
9. PERFORMING ORGANIZATION NAME AND ADDRESS Nielsen Engineering & Research, Inc. 510 Clyde Avenue Mountain View, CA 94043		10. PROGRAM ELEMENT, PROJECT, TASK AREA & WORK UNIT NUMBERS 61102F 2307/A1
11. CONTROLLING OFFICE NAME AND ADDRESS Air Force Office of Scientific Research/NA Bolling Air Force Base Washington, DC 20332		12. REPORT DATE February 1983
		13. NUMBER OF PAGES 86
14. MONITORING AGENCY NAME & ADDRESS(if different from Controlling Office)		15. SECURITY CLASS. (of this report) Unclassified
		15a. DECLASSIFICATION/DOWNGRADING SCHEDULE

16. DISTRIBUTION STATEMENT (of this Report)

Approved for public release
distribution unlimited.

17. DISTRIBUTION STATEMENT (of the abstract entered in Block 20, if different from Report)

18. SUPPLEMENTARY NOTES

19. KEY WORDS (Continue on reverse side if necessary and identify by block number)

Wind Tunnel Test	Jet Flow
Wings	Jet Fighters
Wing Tips	Short Takeoff Aircraft
High Lift	

20. ABSTRACT (Continue on reverse side if necessary and identify by block number)

Parametric low-speed wind tunnel testing of several low aspect ratio half-span wings featuring outboard-blowing wing-tip jets has been accomplished. This effort was performed to extend the existing information base regarding lift augmentation of low aspect ratio wings to encompass tapered wings suitable for application to high-performance fighter aircraft. At an angle of attack typical for fighter aircraft takeoff, operation of the wing-tip jets was found to augment the lift coefficient of aspect

DD FORM 1473 EDITION OF 1 NOV 65 IS OBSOLETE

ratio two wings by 25% to 35%, depending upon the value of the jet momentum coefficient and the wing taper ratio. At low angles of attack, the wing lift coefficients were augmented by as much as 120%, but the amount of lift augmentation decreased in inverse proportion to wing angle of attack. The worth of blowing outboard from the wing tips of fighter aircraft as a means of enhancing STOL performance was assessed. Diverting 70% of the engine bypass airflow to the wing tips reduced predicted takeoff and landing distances by 15%. Differential left-wing-tip-to-right-wing-tip modulation of the jet momentum can immediately produce up to 15,000 ft-lbs of additional roll control torque during low-speed landing approaches.

NOMENCLATURE

a_o, a_1, a_2	equation constants (see Table 2) fitting measured jet momentum components
A	total area of wing panels outboard of airplane fuselage
A_J	wing tip jet exit area, in^2
$\mathcal{R}$	aspect ratio of two wing semispan panels joined together at their roots $= b^2/S$
b	wing total span, in. (of two wing panels)
$b/2$	wing panel semispan, in.
$\bar{c}$	mean aerodynamic chord, ft
C_B	semispan wing root bending coefficient based upon C_R
C_D	drag coefficient
C_f	coefficient of rolling friction during takeoff roll
C_J	wing tip jet momentum coefficient, $2(\rho_J V_J^2 A_J / \rho_\infty V_\infty^2 S)$ (per tip jet)
C_L	lift coefficient
ΔC_L	lift coefficient increment of aircraft components other than the wings
C_M	semispan wing pitching moment about leading edge of root chord, based upon C_R
C_R	wing root chord, in.
C_T	wing tip chord, in.
DOTM, $\dot{m}$	jet mass flow, slugs/sec
DMX, DMY	local jet momentum flux in X and Y directions
F_g	gross thrust, lbs
F_n	net thrust, lbs
F_T	wing tip jet thrust, lbs

NOMENCLATURE (Continued)

FX1J + FX2J	reaction to Y-component of jet momentum (see Figure 4), lbs
FYJ, FZJ	reaction to components of jet momentum as defined in Figure 4, lbs
K	proportion of engine bypass duct mass flow that is diverted to the wing tip jets
$K_{B(W)}$	wing-body interference factor
$K_{W(B)}$	body upwash factor on wing lift
L/D	wing lift-to-drag ratio
$\dot{m}$, DOTM	jet mass flow, sl/sec
MXJ, MYJ, MZJ	reaction moments (X, Y, and Z components, see Figure 4) to jet momentum, in-lb
S	complete wing plan-view area, $(C_T + C_R)b/2$, in^2 (two semispans joined at root)
u_x, u_y	X- and Y-components of local jet velocity
UTUN	wind tunnel corrected free stream velocity
V_J, V_∞	jet velocity, free stream velocity, ft/sec
w	local jet slot width
W	weight, lbs
WMJX, WMJY, WMJZ	Jet momentum components in X, Y, Z wing coordinates
x	distance along wing tip chord (Figure 1), inches
X	landing or takeoff distance, feet (sections 5 and 6)
X,Y,Z	wing coordinates (see Figure 4)
α	wing corrected angle of attack, deg
δ, γ	tip jet momentum vector sweepback angle and angle of deflection below plane of the wing, degrees
λ	wing taper ratio, C_T/C_R
ρ	density, slugs/ft^3

TABLE OF CONTENTS

1. INTRODUCTION

When plane jets are directed spanwise from the tips of a wing, the wing under consideration essentially becomes the central part of a complex "virtual" wing composed of a rigid center section and fluid dynamic outer portions. The outer portion cannot directly transmit loads to the center portion, but the flowfield over the center portion behaves much the same as if it were part of a wing of much larger aspect ratio; accordingly, the rigid center portion of this wing carries increased loading that provides increased lift coefficient and lift/drag ratio. This phenomenon may have many applications. In particular it may serve to reduce the takeoff and landing rolls of advanced fighter aircraft.

Improved STOL capability is desirable for future fighter aircraft owing to the need for continuing operations in the presence of potential runway denial tactics of attacking enemy forces. Other benefits may accrue from adoption of wing-tip blowing on fighter aircraft; these include augmented roll control in landing approach, and small increases in endurance and ferry range associated with lift/drag ratio increases.

The current information base regarding the lift augmentation produced by blowing outboard from the tips of wings is limited to rectangular wing data. Experimental data regarding tapered wings with leading edge sweepback is needed to determine the utility of wing-tip blowing in application to fighter aircraft that require supersonic capability.

This report presents results for the effects of wing-tip blowing on eight half-span wing models. These wings had both rectangular planforms and tapered planforms typical of

high-performance fighter aircraft. The results are applied to estimating the reduction in takeoff and landing distance required in the presence of wing-tip jet blowing for a typical high-performance fighter airplane.

2. RELATED INVESTIGATIONS

Blowing outboard from the tips of rectangular wings has been shown by several investigators (refs. 1, 2, and 3) to be effective in markedly increasing the lift coefficient of wings at a given angle of attack if the wing aspect ratio is relatively small. Brooks (ref. 1) worked with rectangular fins of 0.62 and 1.24 aspect ratio in a water medium and showed very large increases in lift curve slope at what were apparently small angles of incidence. Carafoli (ref. 2) conducted experiments using rectangular wings of aspect ratio 0.6, 1.0, 1.5, and 2.0 using a very large range of wing tip jet momentum coefficient; his results showed lift amplification ratios of up to 7 resulted from blowing from the wing tips at extreme momentum coefficient levels for low angles of attack and an aspect ratio of 0.6, but that the lift amplification ratio was reduced to the order 1.25 above 10° angle of attack with aspect ratio 2.0 and blowing rates consistent with jet engine bypass airflow rates. Lloyd (ref. 3) worked with an aspect ratio 2.0 rectangular wing using a very wide range of jet momentum coefficient; his results were in general agreement wth those of Carafoli, but showed lower lift augmentation levels at many of the same test conditions. Lloyd also demonstrated that lift/drag ratio was increased by more than a factor of two with high blowing rates and lift coefficients in the 0.2 to 0.5 range.

3. APPARATUS AND PROCEDURES

3.1 Apparatus

Eight semispan wing models were designed and fabricated having a combination of aspect ratios (0.62 to 4) and taper ratios (0.25 to 1). The principal dimensions of the models are given in Table 1. The planform areas of these untwisted, semispan wings were all approximately 0.5 ft^2. The NACA 0015 airfoil section was selected to allow adequate internal space for passage of the compressed air to the tip and an internal balance. This is the same airfoil section as used in reference 3. It was necessary to thicken the base region of Wing 10, which had the smallest base chord, to provide adequate internal room. The base section of this wing was a 20.6 percent thick airfoil tapering to the NACA 0015 airfoil at 25 percent of the span.

One of three tip-jet slot-nozzle designs was selected for each model depending upon the size of the tip section. The designs are shown in Figure 1 and the jet dimensions and areas are included in Table 1. Figure 2 shows various views of the wings and tip jet nozzles.

A variety of design problems were encountered and resolved in the preliminary design phase of the investigation. These included:

(1) The large variety of wing shapes required for this study combined with the need for a wide range for the tip-jet momentum parameter drove the need for sweepback of wing internal flow passageways on the tapered wings, and further led to a fan-shaped flow passage on most rectangular wings.

3

(2) the adequate resolution of measured forces into two
categories, wing force components (in the presence of an
airflow altered by the tip jet) and reaction forces to
the jet momentum required extensive calibration of the
reaction forces prior to wind tunnel testing. Also, for the
sizing of the wing models it was necessary to consider that
wall corrections applied to the data should not be unduly
large.

(3) adequate clearance had to be provided between the wing
tip and opposite wind tunnel wall so that flow of the jet was
mostly subject to free interaction with th .in stream flow.

(4) the provision of pressurized air (to `3 psig) to the wing
models in a manner that caused repeatabl ; ·ce interactions
on the balance amenable to calibration wa. a challenging
design problem that was resolved by utilizing custom-made
bellows; the wing/balance/bellows combinations were calibrated
as assemblies for each wing model.

(5) the contract cost constraint called for a relatively
inexpensive method of model fabrication, yet the designs
had to accommodate large loads arising from internal
pressures and internal surface areas. A two-piece aluminum
sand casting joined with epoxy adhesive provided the
needed solution.

(6) the design of an aerodynamically-shaped passageway from
the mounting base and around the balance to the wing tip
to assure a uniform tip jet flow drove the need for two-piece
wing model castings with built-in streamline shapes for the
flow channel and the balance centerbody.

To measure the model lift, drag, and various moments it was

4

necessary to use the NEAR 5-component 3/4-inch-diameter force balance. Its rated capacities are (mounted parallel to the wing span) 50 lbs axial and normal force, 50 in-lb pitching moment, and 80 in-lb root bending and drag moments. For the selected wing semispan planform area of 0.5 square feet, a wind tunnel velocity of 200 fps, and $C_L = 1.0$, the model lift would be 23.8 lbs. The balance capacity would then just be limiting if the model center of pressure were located 2 to 3 inches from the balance center. This required that the balance be mounted inside the wing and that the wing be at least 0.9 inches thick at the mounting location.

The models were tested in the Nielsen Engineering & Research Water/Wind Tunnel operated in the wind tunnel mode. The test section size was 20 x 14 in. and the maximum test section velocity approximately 210 fps. The flow loop contained two honeycomb flow straighters (one in the plenum), four turbulence-damping screens in the plenum, and an 8:1 area ratio nozzle. The typical inlet test section flow distortion in velocity was ±0.2 percent and ±0.2° flow angle. Very little inlet flow degradation was anticipated with the models at maximum angle of attack due to the relatively high flow loss around the circuit and the extra honeycomb and screens for flow straightening. Standard wind tunnel wall corrections for blockage (for the typical semispan wing tested) and at maximum lift were 1.2 percent on velocity and 2.0 percent on the lift coefficient for the typical semispan wing of this study.

Based upon an assessment of the engine bypass airflow available from typical fighter aircraft propulsion units, and the wing-tip blowing studies of Brooks (ref. 1), a maximum design jet momentum coefficient $C_J = 0.2$ was selected. Tip jet nozzle areas between 0.7 and 1.7 in were used to provide a

5

maximum jet momentum of 9 lb-sec and maximum jet velocities of 1000 fps. The most appropriate of the three jet nozzle designs shown in Figure 1 was selected for each wing tip. It was necessary to use design "A" (see Table 1) to obtain the maximum required nozzle area for the tapered wings because they had the smallest tip chords, and design "C" for the wings with the longest chords to spread the jet over the tip chord from 3.5 to 80 percent.

The path of the tip jet was considered during the design phase. The unobstructed path of the jet-in-a-crossflow was estimated using the data and analysis of Marguson (ref. 4) for round jets, modified by the data of Mosher (ref. 5) for round and oblong jets. The position of the jet centerline is approximately:

$$\frac{X}{D} = 1.2\left[\frac{V_e^2}{4\,\sin^2\beta}\left(\frac{Z}{D}\right)^3 + \frac{Z}{D\,\tan\beta}\right]$$

where

$$\frac{1}{V_e} = \sqrt{\frac{\rho_j V_j^2}{\rho_\infty V_\infty^2}}$$

and other terms are defined in the sketch.

6
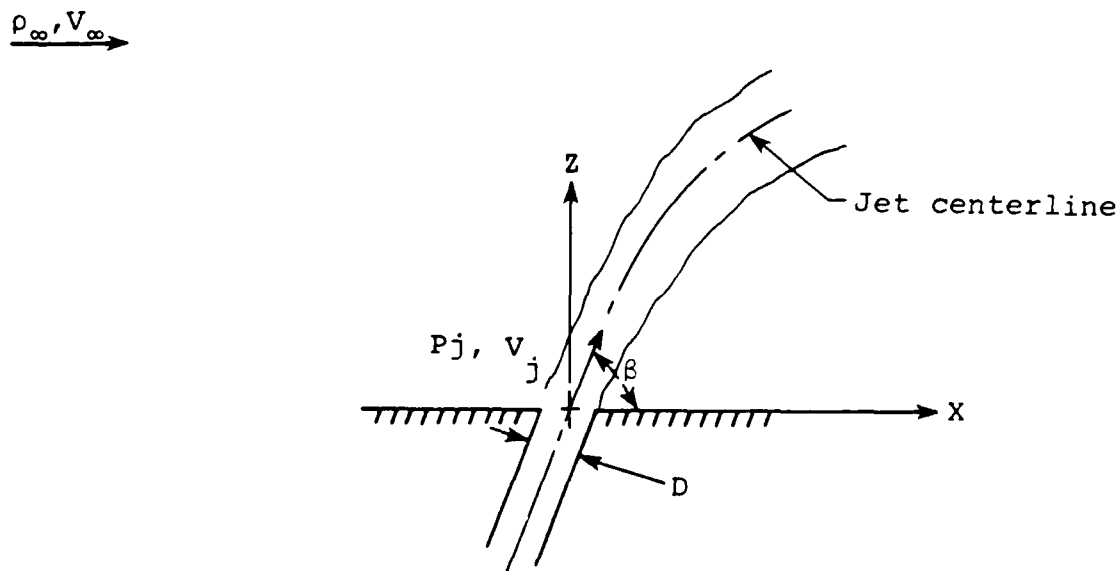
The wings were supported upside-down in the test section with the base mounted close to the top 14-inch wide wall. With this orientation th 20-inch test section height was available for the model plus the jet flow. For the maximum jet momentum coefficient C_J = 0.20 (and no wing lift) the intersection of the jet centerline with a plane parallel to, and 1 inch above the far wind tunnel wall, was calculated to be at least a tip chord behind the swept wings, half a chord behind rectangular wings nos. 6 and 7, and behind the trailing edge for rectangular wings 8 and 10.

The NEAR balance was located in the models parallel to the trailing edge at the 40 percent base chord position as shown in Figure 1. This placed the balance closest to the chordwise center of pressure. A rotatable housing was located outside the test section wall. The connection to the test section wall was made with a base plate. The balance was attached to this housing via a 3/4-inch diameter sting. To minimize tares on the balance due to the incoming air flow for the tip jet, the air was introduced coaxially and essentially symmetrically about the balance sting. An approach was taken of making a flexible air passage connection between the housing and the model by using a soft metal bellows with axial spring rate of 18.6 lb/in. This was a 2.0-in I.D. x 2.5-in O.D. x .003-in. wall nickel-cobalt bellows from the Servometer Corporation. A round-to-elliptical metal tube completed the air passageway into an elliptical hole in the base of the model. The interaction of the bellows on the balance was found to be small and reproducible, and so could be accounted for by calibration of each wing/balance/bellows assembly.

To fabricate model patterns, 1/8-in thick metal templates were machined for the base and tip chords. With these templates in proper alignment, balsa wood was glued in between and shaped with the end templates as guides. Any resulting depressions were filled and reshaped. Next, the interior air passageway was roughed out. One side of the model pattern was then cut out to expose the air passageway for final shaping, resulting in two pattern pieces. A wood block was glued in place in the passageway to provide the balance housing pattern (see Figure 1). The final air passageway shape, with the balance housing located within it, was the design result of layouts of the cross sections to assure a smooth approach to the tip nozzle section.

After the aluminum sand castings of the two pieces for each model were made, the interior flow passageway smoothed, the side piece glued in place, the base and tip ends milled flat and parallel, and the exterior surface sanded and shaped final. The base elliptical hole and tip jet shapes were machined, the balance housing and pin holes machined, and finally, the bellows with the round-to elliptical adapter was glued in place. The model was then ready for mounting onto the balance and clamping the nonmetric end of the bellows to the housing. Wing no. 4 is shown in Figure 3 as an example. The final typical model finish was approximately 16 microinch roughness.

Housing assembly rotation, designed as a means for varying wing model angle of attack, was provided by a gear motor driving a fine-pitch lead screw to provide a stiff drive mechanism. To keep the base of the model essentially out of the wall boundary layer, a 13-inch-diameter splitter plate (see Figs. 1 and 4) was attached to the tunnel wall with a 1/2-inch gap to the wall (unobstructed boundary layer thickness was 0.61 in.). The wing models were installed with approximately 1/32-inch gap to this splitter

8

plate. This gap was frequently checked to assure that no contact was made with the splitter plate. Some of the jet air introduced into the tunnel circuit at the wing tip could escape from the wall boundary layer flow via a slot on the front side of the sting housing. The remainder escaped from holes at the end of the test section.

Pressurized air was provided to the model from the NEAR auxilliary air supply, which consists of a 550-CFM roots-type blower driven by a 75-HP electric motor. This 15 psig air was routed through a water-cooled heat exchanger to drop the air supply temperature to the 60-75° F range. A bypass valve arrangement was used to control the flow rate provided to the the models.

As described in Section 3.3 the housing with balance and each wing attached was mounted on a static test stand before installation in the test section. Wing and jet forces and moments were calibrated on the test stand and pilot traverses of the tip jet were accomplished to determine the jet mass and momentum flow distributions.

3.2 Instrumentation

A total of fifteen force, pressure, temperature and position sensors were employed that produced electrical signals. These sensors are listed here:

Symbol	Group/Function	Transducer	Calibrated range
	Jet Blowing Parameters		
PDB	orifice pressure difference	0.5 psi Validyne	0-0.87 psi
PTB	" total pressure	12.5 " "	0-15 psi
TB	" total temperature	therminstor	63-124 °F
PTC, PSBEL	wing cavity, bellows total pressure	12.5 psi Validyne	0-15 psi
	Wind Tunnel Velocity Parameters		
PDW	plenum-test section static	0.3 psi Validyne	0-0.44 psi
PSMA	test section static minus atmosphere	12.5 psi "	-0.3 to 15 psi
TW	tunnel air temperature	thermistor	60-130 °F
	Wing Loads and Angles		
FZ	normal force	NEAR 5-component balance	-5 to 30 lbs
FY	side force	↓	0-10 lbs
MY	pitching moment		0-80 in-lbs
MX	bending moment		-5 to 55 in-lbs
ALPHA	wing angle of attack	10-turn pot	-3° to 20°
	Calibration Stand Sensors		
FX1	load cell 1	Celesco	0-10 lbs
FX2	load cell 2	"	0-10 lbs
PTJET	jet total pressure	same as PSMA	-0.3 to 15 psi

Jet mass flow was determined using one of two ASME flat plate orifices with flange pressure taps (PDW), upstream total pressure Kiel probe (PTB) and temperature-measurement Themistor (TB). The orifice was located in a 10 ft section of 3-in ID. pipe with honeycomb at the start of the pipe to remove any swirl in the flow. The wind tunnel velocity as calculated from the plenum-minus-test-section static pressure (PDW, corrected for area ratio), the test section total minus atmospheric pressure (PSMA, the tip blowing caused an excess tunnel static pressure), tunnel air temperature TW, plus barometric pressure and humidity.

The NEAR 5-component balance was oriented in the wing as shown in Figures 1 and 4. Figure 4 shows the wing coordinate system and balance force and moment system. The Y-component of reaction to the jet momentum (spanwise force) was not measured by the balance. This force was obtained during calibration from the two load cells FX1 and FX2 upon which the housing was mounted on the calibration test stand. Chordwise centerline velocity distributions were obtained using a 3-hole pressure probe.

All of the electrical signals from the sensors described above were sampled and processed by the NEAR LSI 11/23 minicomputer system with its A/D system, hard disk storage unit, terminal, and printer. The pressure transducers were all of the interchangeable diaphram, variable reluctance type. They were operated by Validyne CD 90 carrier-demodulators. Power supply- filter-amplifier units powered the balance, load cell gages, and thermistors and conditioned their signals. Two 5-digit digital voltmeters were used to visually monitor the various sensor signals.

3.3 Procedures

All of the sensors described above were calibrated prior to this experimental program after the integration and debugging of the electronics system. The calibration was performed using the power supplies, signal conditioners and computer connections used for the entire test.

The 12.5 psi Validyne pressure transducers were calibrated against a 15 psi, 10-in diameter Heise gage, the calibration of which had just been certified, traceable to NBS standards. Smaller-pressure-difference Validyne pressure transducers were calibrated using a micromanometer. For best sensitivity several diaphragms were operated to 140 percent of full scale and well below pressure levels where hysterisis effects might have been encountered. All calibrations were fitted with second-degree (least-squares) equations that represented the data within ±0.15 percent.

The thermistors were calibrated over the full temperature range to be experienced using a water bath. A mercury-in-glass laboratory thermometer was used for the standard. The overall uncertainty of the analytic fit to the data with respect to the standard was 1.3°F. The mass flow was determined from pressure and temperature readings associated with the ASME orifices. Since the ASME orifices were certified by the manufacturer, no attempt was made to independently determine the orifice coefficients, though they were checked against each other in the overlapping flow range. Standard installation practices were followed in the plumbing upstream and downstream of the orifice and in the use of honeycomb far upstream of the orifice to eliminate any swirl. From Benedict, chapter 24 (ref. 6) the

maximum uncertainty in flowrates calculated from the orifice pressures is ±1.5 percent relative to the true value of flow rate.

The wing angle of attack was determined in two steps: (a) geometric measurements, and (b) in situ determination of the angle setting for zero normal force. First, relative angles were determined by mounting the apparatus (housing and balance) so the balance was horizontal. A wing was mounted and pinned to the balance and a gunner's quadrant was attached and used to determine angles. The angle-of-attack data was correlated against the leadscrew drive position pot output, and so represented a smooth but nonlinear function due to the lead screw drive arrangement. A tabular lookup with linear interpolation was employed to determine the relative angle ±.05 degrees.

Determination of the wing zero angle was dependent upon several factors, especially the balance pin hole orientation in each wing model. Upon mounting each wing in the wind tunnel a preliminary run was made to find the approximate $\alpha = 0$ location based upon the sign change on the balance normal force (FZ) gage. This was adequate for establishing the run schedule, which involved taking data in two degree increments. Afterward, the final location of the $\alpha = 0$ condition in the relative angle of attack data was selected based upon determining the lead-screw drive angle for $C_L = 0$ graphically. The total maximum uncertainty of the absolute wing angle is estimated to be ±0.1 degrees. The effect of angle correction due to tunnel walls, a function of the lift, is described later.

13

The test of each wing model involved a five-part procedure:

1) In-place calibration of the balance
2) Jet momentum calibration   } calibration test stand
3) Jet velocity profile traverse
4) Wind tunnel test
5) Post-test data reduction

These steps are described below.

With a load check on the first wing it was found that the bellows, which seemed orders of magnitude more flexible than the balance when unrestrained, actually created signficant interactions with the balance. This was due both to the bellows stiffness in torsion about its centerline (the convolutions increase its resistance to buckling with torsion) and its greatly increased lateral stiffness when both ends are clamped. The end clamping was necessary to make an air-tight conduit for the jet air supply. Also, the bellows interaction was somewhat dependent upon internal pressure of the bellows. This required that the balance be calibrated in place in each wing with the bellows mounted, at two or three internal pressures. The bellows adapter was temporarily expoxied to each wing in turn. This joint was broken for reuse on each succeeding wing. It was found necessary to complete the entire test process including the wind tunnel test with this joint undisturbed; breaking and regluing the bellows-to-wing joint produced different balance interactions. So long as the glue joint was not disturbed, the calibration repeatability was found to be excellent.

To accomplish the calibration three small holes were drilled and tapped into each wing on the suction side for use as pull points for balance calibration. These points were

14

precisely located to load the balance with known combinations of bending and pitching moments plus side force. A special screw-cable connection was constructed to precisely apply the load. With the wing and balance mounted on the static test stand several pull loads were applied at each location at 2 or 3 internal pressures (usually 0, 5 and 10 psi, the tip jet being sealed during this process). Wing axial loads were also applied. The balance calibration data was first analyzed manually to extract the zero shifts due to bellows pressurization. With this effect in large measure removed from the data a matrix inversion yielded the balance coefficients (including force and moment interactions) at each pressure level. During subsequent tests involving the calculation of balance forces a linear interpolation with pressure was performed using the results from the bracketing matrices. The test apparatus, consisting of wing, balance, and housing was actually bolted to two load cells which in turn were bolted to the calibration test stand. Calibrated weights mounted on top of the wing were used to check the combined load cell calibrations.

By rereducing calibration data through the derived matrices to determine uncertainties, and then allowing a margin of twenty percent of the uncertainty on all measured parameters, the uncertainties in force and moment measurement are (balance coordinates):

	F (lb)	F (lb)	F (lb)	M (in-lb)	M (in-lb)	M (in-lb)
average uncertainty	.06	.12	.18	.96	.40	.25
maximum "	.12	.31	.29	2.1	.74	.54

It was anticipated that the tip jet momentum could not be correctly measured while the model was mounted in the test section. During such a calibration it would be necessary for

15

there to be no through flow in the test section as this would create wing loads, yet the recirculating jet exhaust would create such loads. Therefore, the jet momentum was calibrated versus the mass flow (as determined from the orifice sensors) while the apparatus was mounted to the calibration test stand in a large room.

It would appear that loads could be carried out of the system through the air supply hose in addition to the load cells. However, the hose, which was a long, flexible plastic tube, contained a loop as sketched here. Vertical loads could not be transferred across the bottom of the loop, as $dy/dx = 0$ at that location. A control volume has been sketched around the apparatus, cutting through the load cells and through the supply tube where $dy/dx = 0$. The location of the control volume
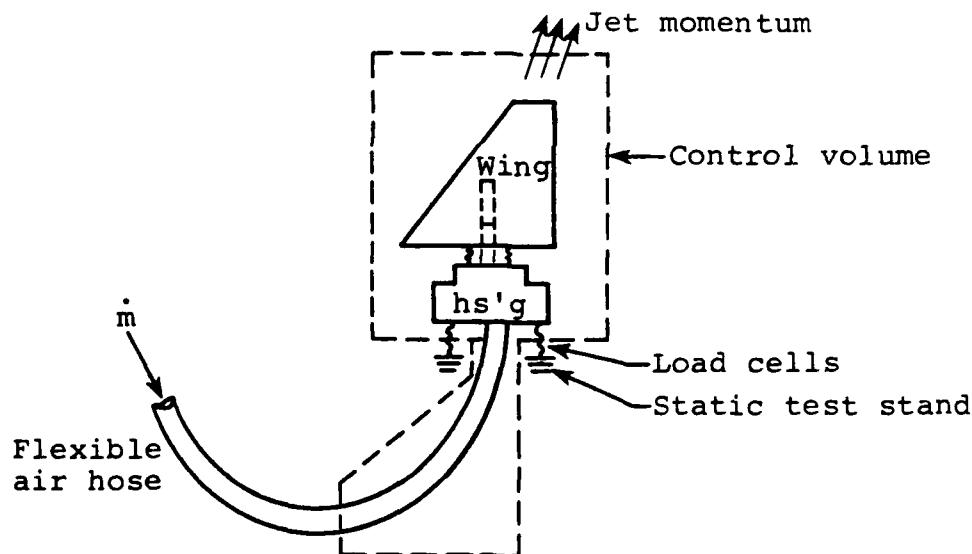
top surface is far enough from the wing tip to assure that the static pressure through the jet at this location is atmospheric. A vertical momentum balance, then, will simply equate the Y-momentum to the sum of the load cell readings.

All force and moment readings other than vertical force were obtained from the balance. The momentum of the flow entering the base of the wing was symmetric to the balance and parallel to it, so again there was no momentum component on the balance forces and moments due to the air flowing into the wing.

16

For the jet momentum calibration the bellows pressure
PSBEL, orifice sensors, load cells, and balance readings were
recorded and reduced by the minicomputer using the program
called JETMOM. The momentum components were correlated against
mass flow rate using a quadratic equation fitted to the data:

$$F_i \text{ or } M_i = a_{oi} + a_{1i} \text{ DOTM} + a_{2i} \text{ DOTM}^2$$

While each wing was still mounted on the test stand a
manual chordwise traverse was made along the jet centerline
using a calibrated, 3-hole total pressure-yaw probe. The probe
was oriented to the null yaw position and angle, total pressure,
and orifice flow quantities measured. The traverse was made at
a constant mass flow condition with the probe tip within 0.1 in.
of the jet slot.

The local Y- and X-components of velocity (u_y, u_x) and momentum
(DMY, DMX) were calculated using the orifice total temperature,
probe total pressure minus atmospheric pressure (for the static
pressure), barometer and specific himidity readings, probe
angle, and local jet slot nozzle width(w). No allowance was
made for the effect on the jet of the very thin boundary layers on the
flow passage walls. The local momentum components are then:

$$DMY = \rho u_y^2 w \qquad DMX = \rho u_x u_y w$$

The local mass flow and these local momentum components were
also integrated along the jet nozzle length using linear
interpolation to obtain total flux values. Comparisons with the
calculated orifice mass flow and measured jet reactions are
presented in Section 4.1.

Upon completion of the calibration test stand tests the
entire apparatus assembly was moved from the calibration stand and
mounted in the wind tunnel. As with the data acquisition on the
test stand, before each run the sensor excitation voltages were
checked, zeros set, and amplifier gains ("R-cals") checked. The
wind tunnel velocity was run up and maintained at approximately

17

200 fps. (Setting an exact value was unimportant as the final data is in coefficient form.) The Reynolds number at this velocity and a typical wind-tunnel air-circuit temperature of 100°F was 1.12×10^6 per foot. The model angle of attack and blowing rates were first increased to maximum values to exercise the balance and minimize any hysteresis errors. A first test run was made at small angles to locate the approximate angle for zero lift. An angle schedule was then established for taking data at approximately two degree increments. Several levels of tip blowing would be repeated at each angle.

During conduct of the wind-tunnel tests, The program ATOD was used to acquire data from all the sensors previously described. The minicomputer analog-to-digital unit sampled each channel 200 times at a 200 hertz rate and the samples were averaged. Just before starting to run, a set of data samples was obtained using ATOD and the resulting averages were then used as tare values for subtracting off all subsequent averages. Finally, the data-taking runs were accomplished. The tunnel cooling capacity was inadequate to maintain constant temperature, so the test section temperature increased at approximately 1°F per minute. Testing was interrupted at 130°F, where a set of zero values was taken. Usually, the test sequence was completed in two runs, or one run if the velocity were decreased for a short while to drop the temperature. For monitoring purposes during a run, the average "counts" ouput of the instruments, counts reduced to basic units (i.e. psi, °F, etc), and a few important quantities (forces, uncorrected velocity, mass flow) were printed. The raw, averaged counts were stored for further processing.

After the test was completed the best value for zero alpha, α_o, was selected based upon C_L/α at low angles. Programs REDUCE and SAVER were then run to obtain final data with all wind tunnel wall corrections included. These corrections included effects for model and model wake blockage (the jet blockage

18

was negligible) and induced angle effects. The correction
procedures presented by Pope (ref. 1) were employed. The ouput
from program SAVER is presented in the following section.

4. EXPERIMENTAL DATA

4.1 Tip Jet Characteristics

Two types of data were acquired for each of the eight wings
tested. Described in this section are the jet momentum forces
and moments and the jet centerline surveys, both of which were
obtained while the model was mounted in the calibration test stand.
The wind tunnel data showing the effects of tip jet momentum
upon the various wing aerodynamic coefficients are presented
in the following section.

As previously noted, the effects of jet momentum upon
balance measurements, as measured on the calibration test stand,
were fitted with a quadratic equation as a function of DOTM so
the jet momentum effects could be removed from the total loads
and produce wing alone results.

The constants a_o, a_1, and a_2 are listed in Table 2 for the
balance forces and moments FZJ, FYJ, MYJ, MZJ, MXJ, and the load
cell forces FX1J and FX2J. With these constants the jet
conditions can be calculated for any test condition.

Figure 6 presents momentum vectors for the wings, the
vector sum of the local Y- and X-momentum components, DMY and
DMX. These vectors are all to the same scale as indicated on
the Wing 1 drawing. Some remaining wake from the balance
housing is evident (decreased velocity near $x/C_T = 0.4$),

19

particularly for Wings 1, 4, 6, and 10. For the smaller aspect
ratio untapered wings (Wings 6, 7, 8) the flow diverges rapidly
from the inlet ellipse at the base to the tip jet slot. The
result is a fanning-out of the tip flow with considerable
forward-directed momentum for $x/C \leq 0.4$, and rearward-directed
momentum over the rest of the slot.

The ratio of the running chordwise sum of the Y-momentum
(spanwise component) to the total spanwise jet momentum is
presented versus x/C_T in Figure 7. The data has been spread to
facilitate reading by raising the ordinate as indicated for each
wing and a reference line (an approximate average for the wings)
drawn at the identical location for each wing. Wings 2 and 6
deviate the most from the reference line.

Table 3 contains a summary of the jet characteristics.
Lines 2, 3, and 4 contain the mass flow determined from the
orifice, and the jet momentum reactions WMJY and WMJX as
measured by the balance and load cells in the calibration test
stand tests. Line 5 shows that the integrated mass flow ranged
from 8 percent low to 7 percent high, compared to the orifice
measurements. This provides a good check of the jet velocity
and mass flow measurement system. Line 6 shows the integrated
momentum flux to range from 7 to 48 percent higher than the
orifice/load-cell measurements. This appears to be related to
the relative size of the tip jet slot (listed in the following
line) and may be related to a slightly reduced static pressure
caused by the jet induced flow. Line 8 shows the difference, in
pounds, between the integrated and measured X-momentum
(chordwise) component. The maximum difference is 0.09 lbs.
Lines 9 and 10 indicate the total jet momentum vector angles
(degrees), δ and γ, as defined here. Only Wings 2 and 6 have
significant jet deviation from the wing plane.
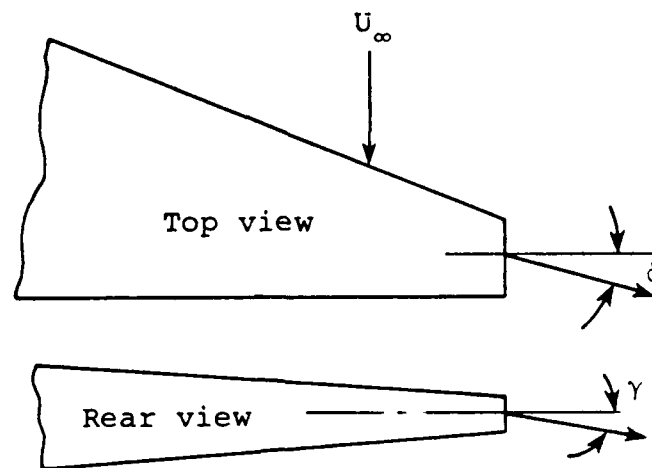
Lines 11 and 12 of Table 2 contain the percent of Y-momentum forward of $x/C_T = 0.25$ and 0.4. Line 13 shows the percent of X-momentum forward of $x/C_T = 0.4$. This is approximately the location for the dividing streamline about the center body, and the division where the momentum vectors point either more upstream or downstream than the average momentum vector. The percent X-momentum on line 13 is based upon the total Y- momentum. While the total X-momentum for the untapered wings is essentially zero, line 13 documents the significant deviations from the average for Wings 6, 7 and 8, as is shown in Figure 6.

4.2 Wing Force and Moment Characteristics

Table 4 contains the reduced wind tunnel data. The header for each section indicates (in order) the run number, wing number, and flow orifice number, barometric pressure and specific humidity. The zero angle of attack, which has been subtracted from all the data, ALPHA 0, is indicated. The column titles are ALPHA - corrected angle of attack; DOTM - jet mass flow; UTUN - corrected tunnel velocity; CJ, CL, CD, CM, and CB - coefficients of jet momentum, lift, drag, pitching moment, and bending moment; and L/D - lift-to-drag ratio. Wing 10 data showed a larger than usual effect on C_L and C_D at zero angle of attack due to blowing. The C_L effect has been corrected in the

tabular data and the drag data is not presented, but the drag for no blowing is included in Figure 8.

All wing coefficient data in Table 4 reflect wing loads with the appropriate jet momentum reaction components (as determined from the bench tests) deducted. The results, then, represent the wing loads influenced by the freestream airflow as influenced by the tip jet, but not the jet reaction.

Balance force and moment uncertainties were described in Section 3.3. The uncertainty in drag force data is essentially the uncertainty in F_Y determination, which is 0.12 lb, or $\Delta C_D = 0.005$ at $U_\infty = 200$ fps. This is approximately twenty percent of the typical drag near zero angle of attack. Also, the uncertainty in L/D at zero tip blowing and low α will be at least this great, depending on the angle of attack and the lift uncertainty ($\sim$10 percent at $\alpha = 1°$ due to 0.18 lb average uncertainty). For swept wings the jet (chordwise) X-momentum is as much as an order of magnitude greater than the drag force, greatly increasing the uncertainties in C_D and L/D.

Figure 8 provides a plot of C_D vs. α at $C_J = 0$. Wings 1 and 2 exhibit the lowest drags, and Wing 6 has the greatest drag up to $\alpha \approx 8°$. Figure 9 presents C_D vs C_J, in each case for the set of constant α-data closest to zero. At α near zero C_D should be independent of C_J. Considering the magnitude of the momentum term that has been removed the results appear to be very good. For example, Wing 1 with $C_J = 0.19$ has DOTM = 0.010 (Table 4). From Table 3 the X-momentum (-FY) is calculated to be 4.63 lbs, or an equivalent $C_D = -.18$. This compares with a change in C_D in Figure 9, as C_J increases from 0 to 0.9, of $\Delta C_D = 0.006$, which amounts to a 3 percent overcorrection for the X-momentum reaction.

The following procedure has been applied for improving the C_D and L/D data from those listed in Table 4. The wing C_D for no blowing at $\alpha = 0$ has been selected (as one example) from Figure 8. The difference between this value and the C_D values

in Table 4 at the $\alpha \simeq 0°$ angles (Figure 9) have been determined versus C_J. These corrections were used as if they remained oriented with the wing axis, so ΔC_D was multiplied by the cosine of the angle of attack to yield corrections at $\alpha \neq 0$.

Figure 10 shows the combined effects of wingtip blowing and angle of attack upon the lift coefficients for all the wings tested. The data in these figures is displayed in "carpet plot" format, wherein the scale for increasing angle of attack but constant momentum coefficient runs diagonally up and to the right, and the scale for increasing jet momentum coefficient runs from right to left. The resulting lines of constant jet momentum coefficient (C_J) run diagonally upwards and to the right as angle of attack is increased, whereas the lines of constant angle of attack run slightly upwards and to the left as the jet momentum coefficient is increased. This type of graph is useful in interpolating in bivariant parameter data $(C_L$ in this case) to find constant independent variable lines, especially when both independent variables were subject to scatter.

Considerable differences are observable in the seven plots of Figure 10. The width of each plot indicates the maximum C_J to which the wing could be tested before encountering one of the blowing design limitations described earlier. The height indicates the maximum lift coefficient at maximum angle of attack. The most striking characteristic of the plots is that the constant angle of attack curves have two basic shapes. For the wings with jet slot designs A and B (Figure 1) the rate of C_L increase is greatest at $C_J = 0$, with the C_L slope continuously decreasing with greater blowing rates. Essentially the opposite is true for the wings with jet slot design C (6, 7 and 8) where there is virtually no effect on lift for small amounts of blowing. Because of the large tip chord of the wings 6, 7, and 8 they have the narrow jet slot (configuration "C") covering one-tenth to one-fourteenth of the exposed tip area (Table 3). The velocity in these with their large jet perimeter will dissipate

23

rapidly with turbulent viscous action. The tapered wings have small tips with a relatively thin perimeter around the slot, so the jets initially have an airfoil shape and are much thicker. There are some differences in the jet Y-momentum distribution along the slot (see Figure 7) but without any consistent trend with the data. Another effect is the significant component of forward momentum in the front portion of the jets for Wings 6, 7 and 8 and the resulting fanning out of an already thin jet.

The lines of varying C_L at constant C_J in Figure 10 tend to be nearly straight. A decrease in slope near the top of the plot indicates the wing is approaching stall. An increase in slope indicates that rate of blowing is having a more positive effect on lift. By comparing Wings 1 versus 4, both of aspect ratio 2, the lift augmentation for the taper ratio 0.5 wing is noted as greater than for the taper ratio 0.25 wing at any combination of momentum coefficient and angle of attack.

Figure 11 shows the increment in rectangular wing lift coefficient associated with wingtip blowing at $\alpha = 12°$. The lift coefficient increment increases with increasing aspect ratio.

Figure 12 compares the lift augmentation ratio, (ratio of C_L with tip blowing to C_L without tip blowing) at $\alpha = 12°$ for the aspect ratio 2.0 wings, as influenced by tip-jet momentum coefficient. The 12° angle of attack case is of interest because it is in the range of take-off angles of attack utilized by modern fighter aircraft. When the momentum coefficient is less than about 0.1, the $\lambda = 0.5$ wing provides the highest lift augmentation ratio of the three wings considered. Figure 7 compares the lift augmentation ratios of all the wing configurations tested for cases where $\alpha = 12°$ and $C_J = 0.1$; these data indicate that the lift augmentation ratio of tapered wings

24

decreases more rapidly with increasing aspect ratio than is the case with untapered wings. Some of the effects noted in Figures 11 and 12 are likely to be influenced by the jet X- and Y-momentum distributions as previously discussed.

The current results regarding lift augmentation by wing tip blowing are compared with those of earlier investigators (refs. 1, 2, and 3) in Figures 13 and 14. General agreement with the rectangular-wing archival data base is indicated, although there exist important source-dependent differences among all of the data. Possibly these data differences result from variations in the jet momentum distribution.

Wing 4 yielded a favorable lift augmentation performance and provides a planform suitable for a fighter aircraft wing. The lift amplification performance of this aspect ratio 2, $\lambda =$ 0.5 wing is summarized in Figure 14, where the variation of lift amplification ratio with angle of attack is shown for several values of the jet momentum coefficient.

An example of the augmentation in the lift-to-drag ratio (L/D divided by $(L/D)_{C_J = 0}$) is plotted in Figure 15 versus the jet momentum coefficient for several different wings for $C_L \approx 0.35$. The magnification in drag errors involved from subtracting out a large momentum component with a resulting small net difference was previously described. To minimize the error, the procedure described for correcting C_D was applied to L/D. The same type of correction was also applied to C_L in several cases (taking into account the real effects of jet blowing at angles near zero). Significant augmentation in L/D is observed for the tapered wings, but generally there was a degradation in L/D for the untapered wings.

25

5. APPLICATIONS TO FIGHTER AIRCRAFT LIFT AND STOL CAPABLITY IMPROVEMENT

To provide a basis for assessing the potential military worth associated with blowing outboard from the wing tips of fighter aircraft, the F-15 airplane was selected as a baseline for predicting improvements in takeoff and landing performance. The following information was extracted from References 8 and 9 combined with some analysis:

X_{TO} (nominal takeoff roll) = 900 ft at 41,500 lbs gross weight, full power (augmented)

X_L (nominal landing roll) = 2,500 ft (no parachute) at nominal landing weight

V_a (approach speed) = 144 mph (211 ft/sec) at nominal landing weight

α_{TO} (nominal takeoff angle-of-attack) = 12 deg

$C_{L_{TO}}$ (takeoff lift coefficient) = 0.83

S (reference area) = 608 ft^2

W_{TO} (takeoff weight) = 41,500 lbs (interceptor mission)

$\bar{c}$ (mean aerodynamic chord) = 14.5 ft

$C_{D_{TO}}$ (drag coefficient at takeoff) = 0.14

Æ_{wg} (gross wing aspect ratio) = 3.0

Æ_{wp} (aspect ratio of two wing panels, portion outboard of the fuselage) = 2.0

A_w (total area of wing panels outboard of fuselage) = 496 ft^2

$F_{g_{max}}$ (maximum gross thrust at S/L) 47,620 lbs (augmented)

$F_{n_{TO}}$ (liftoff net thrust of engines at sea level) = 43,810 lbs (augmented)

BPR   (engine bypass ratio) = 0.6

FPR   (fan pressure ratio) 2.0 minimum

C_f (aircraft coefficient of rolling friction) = 0.025

The relationship between wing lift and complete airplane lift was derived using the upwash and interference factors of Reference 10 as follows:

$$C_{L_{A/C}} = \Delta C_L + C_{L_W}[K_{B(W)} + K_{W(B)}]$$

where: ΔC_L = Lift coefficient increment due to fuselage, air inlets, & empennage

for the F-15, $K_{B(W)}$ = 0.3

$$K_{W(B)} = 1.225$$

so that at takeoff ($\alpha = 12°$):

$$C_{L_{TO}} = .83 = \Delta C_L + .56(1.525); \quad \Delta C_L = 0.117$$

where the F-15 wing-alone lift coefficient was assigned a value of 0.56 based upon wing-alone data base information. Therefore the effects of blowing outboard from the wing tips upon complete aircraft lift augmentation may be written:

$$C_{L_{A/C}}(C_J) = \Delta C_L + C_{L_W}[K_{B(W)} + K_{W(B)}] \frac{C_L(C_J)}{C_L(C_J = 0)}$$

The $\lambda = 0.5$ data of Figure 12 can be adequately represented by the quadratic:

$$\frac{C_L(C_J)}{C_L(C_J = 0)} = 1 + 3.725 \, C_J - 9.75 \, C_J^2$$

so that the takeoff lift coefficient ($\alpha = 12°$) of an F-15 fitted with an aspect ratio ~ 2.0, taper ratio 0.5 wing may be written:

$$C_{L_{A/C}}(C_J) = .117 + .789 (1 + 3.725 \, C_J - 9.75 \, C_J^2)$$

28

Diversion of airflow from the engine bypass ducts reduces net thrust according to the following relationship:

$$F_n(K) = F_n(1 - .375K) + F_T \sin\delta$$

where: .K = fraction of bypass airflow diverted to wing tips

.F = delivered thrust of wing tip jets = .1626 $F_n K$

.δ = sweepback angle of wing tip jet moment vector
(27.5° for $\mathbb{R}$ = 2.0, λ = 0.5 wing)

. The engine exhaust nozzles are adjusted to provide sonic flow at the throat.

Figure 16 shows the extent to which the net axial thrust of two augmented F-100 engines operating at full power is degraded by varying the fraction of engine bypass air that is diverted to the wingtip jets.

5.1 Takeoff Roll Reduction

The total lifting force normal to the runway that operates to effect liftoff is composed of aerodynamic lift and thrust vector components. In the case of a baseline F-15 airplane in interceptor configuration without benefit of wing tip-jet lift augmentation, about 900 ft takeoff roll is required to reach the 236 ft/sec takeoff speed (assuming α_{TO} = 12 degrees and $C_{L_{T/O}}$ = 0.83); at this liftoff condition, the airplane develops 32,400 lbs of aerodynamic lift, whereas the component of engine thrust normal to the runway is about 9100 lbs (41,500 lbs

gross weight at liftoff). Figure 17 shows the variation of
total liftoff force, aerodynamic lift, and the thrust component
normal to the runway with the fraction of engine bypass airflow
diverted to the wingtip jets for 210 ft/sec runway speed,
these data show that whereas aerodynamic lift can be augmented
by about 23% at K = 0.7, the loss of thrust-component liftoff
force constrains the total liftoff force improvement to about
15%. Figure 18 shows the variation of total liftoff force with
runway speed and fraction of bypass air diverted to the wingtip
jets. The data of Figure 18 llustrate the fact that the maximum
liftoff force is achieved at decreasing values of the diverted
bypass fractions as runway speed is reduced; this occurs because
the momentum coefficient (C_J) is increased as runway speed is
reduced at constant wingtip-jet blowing rate, and this results
in less lift augmentation per lb of thrust loss at the higher
levels of wingtip blowing due to the quadratic variation of
lift augmentation ratio with C_J (Figure 12). The implication
of this result is that if reduced takeoff speeds can be
achieved through nonpropulsive aerodynamic improvements, then
the full benefits of lift augmentation produced by wingtip
jet blowing can be provided at lower bypass airflow diversion
fractions.

The relationship between diverted mass flow and the momentum
coefficient is: $C_J = 6046 \ K/V_\infty^2$, where an assumed 10% total
pressure loss in the tip-jet ducting yields a wing tip jet
Mach number of 0.98.

The takeoff condition was specified as:

$$\sum F_Z = W_{TO} - C_L q_\infty s - F_n(C_J) \sin\alpha_{TO} = 0$$

The equation used for longitudinal acceleration is:

$$a = \left[F_n(C_J = 0) - C_D qs - C_f W_{TO} \right] \frac{q}{W_{TO}}$$

where the equation assumes application of full thrust without wing-tip blowing until takeoff velocity is achieved; at this point, engine bypass air is diverted to blow outboard from the wing tips and the airplane is assumed rotated to the takeoff angle of attack. The acceleration relationship was integrated in time via finite differencing to obtain takeoff velocity and distance traveled.

The takeoff roll analysis results are displayed in Figure 19 relative to the nominal values of F-15 takeoff roll and velocity. Apparently, diverting 70% of the engine bypass airflow so as to blow outboard from the wing tips augments the airplane lift coefficient by about 24%; this in turn reduces the takeoff roll by 15%. The reduction in takeoff distance is less than would result from inverse proportionality to lift augmentation due to the loss in net thrust associated with diverting engine bypass air to the wing tips.

31

Figure 20 shows how takeoff roll and velocity are affected by
variation of the fraction of bypass and airflow diverted to
the wing tips; these data were developed under the assumption
that the F-15 can be fitted with $\cancel{R} = 2.0$, $\lambda = 0.5$ wing panels
with provisions for wingtip blowing. The resulting takeoff
roll for zero wingtip blowing is some 140 ft less than that of
the F-15 baseline owing to the higher lift coefficient at
takeoff (0.906 vs. 0.83) associated with the different wing
configuration.

5.2 Landing Roll Reduction

The landing roll of an airplane varies in proportion to
landing speed (or approach speed) squared and in inverse
proportion to the deceleration level available after touchdown.
In the simplest terms, the landing roll, X may be stated:

$$X_L \cong V_L^2 / 2\bar{a}$$

where: V_L = landing velocity
approach velocity (ft/sec)

$\bar{a}$ = average deceleration (ft/sec) from touchdown
to zero runway speed.

In landing approach, a high-performance fighter aircraft such
as the F-15 would be configured for high drag (full flaps) with
the throttles set for 80% or   re of full military power, this
to enable the slowest possible s.fe approach speed while providing
for rapid transition to full augmented power in the event the
landing must be aborted. The maximum military power rating of

32

two Pratt & Whitney F-100 engines as installed in the F-15 is 26,450 lbs net thrust. Assuming 87% throttle, and that the resulting total thrust of 23,000 lbs can be maintained by throttle adjustment when engine bypass air is diverted to the wing-tip jets, the thrust component of forces acting normal to the airplane flight path at $\alpha = 12$ degrees is 4780 lbs.

If the airplane weighs 28,000 lbs in final approach, the approach speed can be computed from the lift coefficient as augmented by wing-tip blowing; the results of such calculations are provided as Figure (21), which shows the predicted variation of approach speed for the F-15 with the fraction of engine bypass airflow diverted to the wing-tip jets. Also shown in Figure (21) is the percent reduction in landing roll expected due to wingtip blowing at varying airflow rates. It therefore appears that the effect of lift augmentation (due to wingtip blowing) upon landing roll (23% reduction) is significantly greater than its effect upon takeoff distance (15% reduction); this occurs because net axial thrust is less of a factor in determining the total force opposing weight normal to the airplane flight path. The actual values of landing distance required depend upon knowledge of $\bar{a}$, the average deceleration value. Deceleration can be provided by braking, thrust reversing and/or drag chute deployment. Regardless of the deceleration measures employed, the landing distance reduction percentages shown in Figure 21 apply.

5.3   Roll Control Augmentation During Landing Approach

The ability of pilots to control roll attitude in final approach constitutes a limiting factor in attaining reduced landing speeds; although lower approach speeds may apparently be possible due to lift augmentation, the associated reduction

33

in dynamic pressure can result in sluggish control response and degraded handling qualities. If wing tip-jet blowing is adopted as a means of reducing takeoff and landing speeds and distances, then a large measure of roll control authority can be made available by modulating the wing-tip jet momentum balance between the left and right wings. For example, up to 15,000 ft-lbs of roll control torque is available on demand by diverting different amounts of bypass air to each wing tip so as to produce a left-to-right difference in wing panel lift coefficient of 0.05 while satisfying the lift-equals-weight condition. The resulting rolling moment coefficient is about 0.035.

6. INTEGRATION OF WING TIP BLOWING IN FIGHTER AIRCRAFT, TOGETHER WITH OTHER MEASURES, TO GREATLY IMPROVE STOL CAPABILITY.

High-performance fighter aircraft that must provide unsurpassed interceptor and air-superiority mission capabilities generally exhibit the following aerodynamic performance features:

1. High transonic energy-maneuverability, and ability to execute high-angle-of-attack "corner-velocity" maneuvers.

2. Limit speeds above Mach 2.5 (35 Kft altitude or greater).

It is clear that airplane wing configurations and equipment added to effect STOL capability must not compromise either of these two essential aerodynamic qualities. This means that air-superiority fighter aircraft will continue to utilize thin, highly swept wings of low aspect ratio and low drag at lift coefficients in the 0.1 to 0.3 region. Further provision of STOL capability must not involve complex mechanisms and service-

intensive techniques such as tangential blowing through slender, close-tolerance slots due to the attendant reliability and life-cycle cost considerations.

The above-noted requirements constitute constraints as regards selection of methods for lift augmentation applied to improve STOL capability of high performance fighter-aircraft. For example, a circulation-controlled wing must be excluded from consideration for this application because the supersonic drag of such blunt-trailing-edge wings is excessive, and complex, retractable mechanisms would be required to configure the wing for low drag after takeoff; this is unfortunate because the circulation-controlled airfoil (ref. 11) provides the greatest lift augmentation per unit jet momentum coefficient of any known fluid injection method.

Blowing outboard near the wing root does not significantly augment wing lift below the stall region, and so will not be considered here.

Three methods remain that are relatively simple to implement:

1. The jet-flap (ref. 12) wherein engine bypass airflow, (or other fluid) is ejected from the wing trailing edge deflected downward at some substantial angle to provide a fluid-dynamic flap. This affects wing pressure distribution very much as would a mechanical flap. This method traditionally utilizes very large values of jet momentum coefficient that could not be provided in a practical, effective high-performance fighter, but at low jet momentum levels the technique is still effective, providing

35

$$\frac{\partial C_L / \partial C_J}{C_{L_\alpha}} \approx 1.06 \ (C_J \leq 0.1)$$

for a jet flap deflection of 30° (2-D wing).

2. A wing lower surface jet that exhausts normal to the chord line has been shown by Leopold, Krothapalli, and Tevella of Stanford University (ref. 13) to be very effective in augmenting the lift of 2-D wings. Presence of the jet on the wing lower surface somewhere between midchord and the trailing edge separates the flow over the aft portion of the wing lower side, signficantly reducing the local pressure at the trailing edge; this region of low pressure significantly reduces pressures over the wing upper surface, consistent with the analytic procedure of enforcing the Kutta condition at the wing trailing edge. The reference 13 data indicate the efficiency of this technique to be:

$$\frac{\partial C_L / \partial C_J}{C_{L_\alpha}} \approx 1.49 \ (C_J \leq 0.1)$$
for 2-D wings

3. Blowing outboard from the wing tips was investigated in the present experiments documented in section 4 of this report. For low-aspect ratio, tapered wings suitable for application to high-performance fighter aircraft, the efficiency was found to be:

$$\frac{\partial C_L/\partial C_J}{C_{L_\alpha}} \approx 0.96 \ (C_J \geq .05)$$

for $\text{Æ} = 2.0$, $\lambda = 0.5$ wing

Given all due regard for the fact that the jet-flap and lower-surface slot-jet techniques have not been investigated in the context of low aspect ratio wings with substantial leading edge sweepback, it appears that the three methods provide about the same levels of lift augmentation efficiency. However, providing a jet exhaust along the trailing edge of a wing poses some severe integration problems with respect to trailing-edge control surfaces and mechancal flaps, structural design, and air ducting.

The wing tip-blowing technique is the most straight forward in terms of integration into the wing because the wing tip region is unfettered with control equipment, and an enlarged wing spar can be utilized as a passageway for pressurized air from the engine bypass ducts. The lower-surface slot-jet technique would also be relatively easy to integrate with the wing over its inboard portions (flap region); experimental data are needed to characterize the lift augmentation effectiveness of this technique in application to swept, low-aspect ratio wings with flaps for the fighter aircraft application. Use of lower-surface jets ahead of the wing ailerons may or may not affect aileron effectiveness in an adverse way, but this also needs further investigation.

37

The lift augmentation due to wing tip blowing has been shown herein to be sensitive to jet geometry and direction, and so it is believed that the lift augmentation performance of this technique can be improved somewhat; also, the current data base needs to be extended to include the effects of section camber.

Based upon the present aerodynamic augmentation results, we believe that takeoff speed can be reduced to about 180 ft/sec with a takeoff roll less than 500 ft for a 41,500 lb-class fighter takeoff weight without propulsive improvements or vectored-thrust measures. Increasing wing area by 20% and integration of the F-401 derivative of the F-100 engine would reduce takeoff roll to about 375 ft with a takeoff velocity of about 160 ft/sec. The recommended approach is to utilize combined wingtip blowing and wing lower surface slot-jets, each operating at jet momentum coefficients of about 0.1 (0.2 total); this would provide the maximum possible lift augmentation at minimum utilization of engine bypass air because both of the lift augmentation measures would be operating in regions of maximum efficiency.

Figure 22 illustrates the F-15 planview wth AR = 2.0, λ = 0.5 wing panels superposed. The baseline F-15 wing leading edge sweepback could be duplicated by utilizing a slightly smaller wing aspect ratio. Wing area would be added at constant aspect ratio and taper. Figure 23 illustrates the wing features needed to integrate wing tip and lower surface blowing. Since the enlarged wing spar reduces the wing internal volume needed for fuel storage, increasing wing area slightly would be required to maintain range performance.

7. CONCLUSIONS AND RECOMMENDATIONS

The following conclusions were derived from the present experimental results and application studies:

1. Blowing outboard from the tips of low-aspect-ratio wings augments the wing lift coefficient by an amount that depends strongly upon wing geometry, angle of attack, jet momentum coefficient, and the tip-jet geometry and direction.

2. Wing lift was augmented by as much as a factor of 2.2 at low angles of attack ($\alpha = 2°$) with $C_J = 0.2$ for an AR = 1.24, rectangular wing.

3. At angles of attack close to those typical of fighter takeoff conditions ($\alpha \approx 12°$), up to 35% lift augmentation was measured.

4. The lift augmentation decreased monotonically with increasing angle of attack, but the lift coefficient increment due to wing tip blowing was roughly constant with angle of attack in the $\alpha = 6°$ to $16°$ range for all wings tested.

5. Strong effects of wing tip jet geometry were observed; the reasons for this remain to be determined, and are obscured by superposed wing taper effects. This occurred because differing jet geometries were necessary to provide the desired range of momentum coefficient as wing tip chord was increased.

6. Increasing wing taper and sweepback (decreasing taper ratio) slightly reduced (apparently) lift augmentation between $\lambda = 1.0$ and $\lambda = 0.5$. Decreasing taper ratio from 0.5 to 0.25 significantly reduced wing lift augmentation for $C_J \geq 0.05$.

7. Increasing wing aspect ratio systematically reduced the lift augmentation associated with wing tip blowing.

8. Integration of wing tip blowing (as characterized by the present experimental results) on an F-15-class fighter can reduce takeoff roll by 15% and reduce landing roll by about 23%. Additional relatively straightforward lift augmentation measures are available for use in conjunction with wing tip blowing to provide further STOL capability improvements.

The following recommendations are made regarding work that should be accomplished in the second phase of this Defense Small Business Advanced Technology Program:

1. Additional experiments should be conducted to parametrically characterize the effects of wing tip jet geometry and direction. One of the existing half-span wing models could be modified for this purpose.

2. Experiments should be conducted to parametrically measure the lift augmentation performance of lower-side slot jets on low-aspect-ratio tapered wings, alone as well as in conjunction with wingtip jets. This can be accomplished by modifying existing hardware.

3. The effects of wing camber should be measured for an aspect ratio 2.0, $\lambda = 0.5$ wing. This would require fabrication of an additional wing with a prescribed camber distribution; this wing would be tested using existing instrumentation and equipment.

4. A design study needs to be accomplished to trade off and select the preferred means of integrating wing tip and lower-side slot-jet blowing with fighter aircraft wings. This study would include structural design, aerodynamic performance, provision of needed internal volume for displaced fuel capacity, and integration of flow control equipment.

5. Planning should be initiated for wind tunnel testing of a high performance fighter aircraft model that incorporates wing tip and wing lower-side blowing.

REFERENCES

1. Waugh, J. G., Kelly, H. R., and Fabula, A. G.:
    Recent Hydrodynamic Research at the Naval Ordnance Test
    Station (sub-section on Fin LIft Augmentation by
    Spanwise Fluid Ejection-Reprise of J.B. Brook's work).
    ONR-9, Vol. 2, p. 504, presented at 5th Navy Science
    Symp., Naval Academy, Annapolis, MD.

2. Carafoli, E. and Camarasesen: New Researches on Small
    Span-Chord Ratio Wings with Lateral Jets. Studii si
    Cercetari de Mecanica Aplicata, 1970, Vol. 29, No. 4,
    pp. 947-962, also available in English from NTIS as
    AD-733858.

3. Lloyd, A.: The effect of Spanwise Blowing on the
    Aerodynamic Characteristics of Low Aspect Ratio Wing.
    von Karman Institute for Fluid Dynamics Project Report
    1963-90, 1963.

4. Margason, R. J.: The Path of a Jet Directed at Large
    Angles to a Subsonic Free-Stream. NASA TN D-4919, Nov.
    1968.

5. Mosher, D. K.: An Experimental Investigation of a
    Turbulent Jet in a Cross Flow. Georgia Institute of
    Technology Report 70-7, Dec. 1970.

6. Benedict, R. P.: Fundamentals of Temperature, Pressure
    and Flow Measurements, 2nd ed. Wiley, 1977.

7. Pope, A.: Wind Tunnel Testing, 2nd ed., Wiley 1954.

8. Janes's All the World's Aircraft, 1976-77, Jane's Yearbooks, Paulton House, London.

9. Abercrombie, J. M.: Flight Test Verification of F-15 Performance Prediction. AGARD CP-342, Paper No. 17, presented at the Flight Mechanical Panel Specialists Meeting on Performance Prediction Methods, Paris, France, Oct. 1977.

10. Pitts, W. C., Nielsen, J. N., and Kaattari, G. E.: Lift and Center of Pressure of Wing-Body-Tail Combinations at Subsonic, Transonic, and Supersonic Speeds. NACA Report 1307, 1957.

11. Wood, N. J. and Conlon, J. A.: The Performance of a Circulation-Control Aerofoil at Transonic Speeds. AIAA Paper 83-0083. AIAA 21st Aerospace Sciences Meeting, Reno, NV, January 1983.

12. Halsey, N. D.: Methods for the Design and Analysis of Jet-Flapped Airfoils. AIAA J. Aircraft, Vol. 11, No. 9, Sept. 1974.

13. Leopold, D., Krothapalli, A. and Tavella, D.: Some Observations on the Aerodynamics of an Airfoil with a Jet Exhausting from the Lower Surface. AIAA Paper 83-0173. Presented at the AIAA 21st Aerospace Sciences Meeting, Reno, NV, January 1983.

Table 1.- Wing Dimensions

Wing Number		1	2	4	5	6	7	8	10
λ		0.25	0.25	0.50	0.50	1.00	1.00	1.00	1.00
Æ		2.00	3.00	2.00	4.00	0.62	1.24	2.00	4.00
b/2 (in)		8.23	10.16	8.35	11.82	4.55	6.55	8.40	11.78
C_R (in)		13.37	10.85	11.13	7.81	14.73	10.73	8.36	5.93
C_T (in)		3.25	2.68	5.55	3.93	14.75	10.74	8.33	5.89
S (in²)		68.42	68.72	69.65	69.40	67.10	70.33	70.05	69.61
Tip Jet Design		A	A	B	B	C	C	C	B
Jet Area (in²)		0.733	0.456	1.276	0.647	1.721	0.844	0.685	1.466
Jet Dimensions (in)	w	0.364 max	0.278 max	0.328	0.230	0.150	0.104	0.080	0.357
	x_1	0.17	0.09	0.16	0.11	0.53	0.39	0.26	0.206
	x_2	---	---	3.44	2.57	---	---	---	3.59
	x_3	2.93	2.24	4.44	3.17	12.02	8.53	6.84	4.80
	d_3	---	---	0.095	0.06	0.150	0.104	0.080	0.093

Note: Wing nos. 3 and 9 were not tested, so have been deleted from this Table.

44

Table 2.- Wing Tip Jet Force and Moment Equation Constants

Force or Moment Coefficient = $a_0 + a_1 DOTM + a_2 DOTM^2$

Wing		EZJ	FYJ	MYJ	MZJ	MXJ	FX1J	FX2J
1	a_1	0.325	-7.503	-1.055	17.189	-4.391	7.328	-.559
	a_2	-.2639E3	.4552E5	.1728E4	-.1441E6	.7026E4	-.6546E5	.3671E4
2	a_0	0.003	0.038	-0.025	0.165	-0.037	0.043	0.051
	a_1	0.531	1.523	0.234	26.130	-4.601	4.814	4.608
	a_2	-.4137E4	.2936E5	-.3100E5	-.1746E6	.1480E5	-.6684E5	-.1363E5
4	a_1	-7.180	0	3.476	1.933	0	-0.112	-1.609
	a_2	0	.2289E5	.5380E1	-.4284E5	0	-.2807E5	-.1593E5
5	a_0	-0.002	0.008	0	-0.075	0.012	-0.020	-0.051
	a_1	-0.350	0.284	-0.834	-7.675	2.216	-0.018	-4.103
	a_2	.5576E3	.1395E5	.2839E4	-.3305E5	.2698E4	-.4661E5	-.2101E5
6	a_0	0	0	0	0	-.234	0	0
	a_1	-.693	-.256	1.107	1.068	-.485	0	0
	a_2	.9336E3	.1642E4	-.7083E3	-.2519E4	.3463E4	-.1421E5	-.1073E5
7	a_0	-0.039	-0.016	0.183	-0.013	0	0.054	0.138
	a_1	0.316	0.731	-3.631	0.849	0	0.994	-1.876
	a_2	.9636E3	.2037E4	.3950E4	-.2696E4	0	-.2685E5	-3.002E5
8	a_0	0.051	0.001	-0.172	0.032	0	-0.186	-0.155
	a_1	-0.650	-1.112	4.671	6.528	129.0	1.218	-0.940
	a_2	.9438E3	-.1328E3	.1699E5	-.2151E5	0	-.3075E5	-.3952E5
10	a_0	0.005	0.040	-0.065	0.214	-0.186	0.025	-0.025
	a_1	0.240	0.377	-0.952	2.586	-1.355	0.616	0.162
	a_2	-.7530E3	-.1735E4	.5673E4	-.4421E5	-.7482E4	-.1261E5	-.2833E5

Table 3.- Jet Characteristics

Wing No.	1	2	4	5	6	7	8	10
1. TRAVERSE U_{jmax}, fps	478	555	594	452	455	679	592	387
2. $\dot{m}_{ORIFICE}$ $\mathrm{sl/sec}$	.00506	.00417	.01046	.00421	.01005	.00989	.00506	.00704
3. WMJY, lbs	1.75	2.39	4.83	1.49	2.52	5.39	2.14	2.05
4. WMJX, lbs	1.18	.97	2.48	0.28	0.16	0.20	-0.01	-0.05
5. $\int_0^{x_3} \dot{m}dx/\dot{m}_{ORIFICE}$	.975	1.0	1.00	1.00	1.00	.919	.975	1.07
6. $\int_0^{x_3} DMYdx/WMJY$	1.13	1.07	1.11	1.21	1.48	.988	1.31	1.20
7. Tip Section Area/Jet Area	1.48	1.62	2.48	2.45	12.95	14.05	10.48	2.43
8. $\int_0^{x_3} DMXdx$ - WMJX, lbs	.01	-.07	-.07	.07	-.02	-.09	.03	.01
9. $\delta^\circ = \tan^{-1}(WMJX/WMJY)$	34.0	22.1	27.2	10.6	3.6	2.1	-.03	-1.4
10. $\gamma^\circ = \tan^{-1}(WMJZ/WMJY)$	0.4	3.0	0.8	-0.4	-1.5	-0.8	-1.2	1.0
11. %Y-momentum$_{x/C_T}$ = .25	27	30	29	27	23	25	27	30
12. %Y-momentum$_{x/C_T}$ = .40	51	56	50	51	48	47	47	47
13. $\%\int_0^{x/C_T = 0.4} DMX\cdot C_T\cdot d\left(\frac{x}{C_T}\right)/WMJY$	39	16	24	9	-23	-12	-13	-3

46

Table 4.- Wind Tunnel Data[1]

Wing 1 λ = 0.25, AR = 2

IDATA IWING IDORF BARM SPFHUM ALPHA 0
30 1 3 29.96000 0.01000 1.67000   11-FEB-83   16:27:04

ALPHA	DOTM	UTUN	CJ	CL	CD	CM	CB	L/D
0.76	0.00000	192.23	0.0000	0.0276	0.0161	-0.0303	0.0093	1.72
1.85	0.00000	192.17	0.0000	0.0713	0.0170	-0.0515	0.0212	4.21
2.87	0.00000	190.80	0.0000	0.1143	0.0197	-0.0727	0.0327	5.81
3.99	0.00000	190.66	0.0000	0.1609	0.0230	-0.0966	0.0458	6.99
8.02	0.00000	192.80	0.0000	0.3529	0.0410	-0.1957	0.0987	8.60
12.52	0.00000	193.90	0.0000	0.5840	0.0783	-0.3196	0.1618	7.46
16.45	0.00000	193.15	0.0000	0.7616	0.1202	-0.4119	0.2093	6.34
13.17	0.00676	198.44	0.1425	0.7602	0.0529	-0.3918	0.2136	14.38
0.79	0.00000	0.00	0.0000	0.0000	0.0000	0.0000	0.0000	0.00

IDATA IWING IDORF BARM SPFHUM ALPHA 0
32 1 3 29.96000 0.01000 1.67000   11-FEB-83   16:28:15

ALPHA	DOTM	UTUN	CJ	CL	CD	CM	CB	L/D
-0.07	0.00000	195.57	0.0000	-0.0019	0.0108	-0.0227	-0.0010	-0.18
-0.03	0.01064	201.69	0.2001	0.0124	0.0173	-0.0205	-0.0013	0.71
-0.03	0.00877	200.36	0.1382	0.0117	0.0149	-0.0235	-0.0008	0.79
-0.02	0.00667	200.49	0.0799	0.0102	0.0111	-0.0253	-0.0002	0.92
-0.00	0.00507	200.16	0.0464	0.0083	0.0084	-0.0259	0.0001	0.99
0.01	0.00364	198.68	0.0241	0.0066	0.0097	-0.0265	0.0000	0.68
0.02	0.00000	197.49	0.0000	0.0007	0.0115	-0.0254	0.0001	0.06
2.00	0.01044	202.79	0.1943	0.1253	0.0122	-0.0759	0.0340	10.28
2.03	0.00869	201.99	0.1356	0.1250	0.0155	-0.0786	0.0336	8.07
2.03	0.00653	200.42	0.0777	0.1215	0.0119	-0.0790	0.0327	10.20
2.05	0.00491	197.69	0.0451	0.1174	0.0099	-0.0792	0.0318	11.84
2.07	0.00352	197.74	0.0229	0.1099	0.0125	-0.0764	0.0302	8.76
2.05	0.00000	198.85	0.0000	0.0872	0.0099	-0.0701	0.0235	8.77
4.06	0.01049	203.93	0.1962	0.2350	0.0205	-0.1275	0.0689	11.48
4.08	0.00862	202.80	0.1343	0.2343	0.0209	-0.1287	0.0669	11.24
4.10	0.00651	200.55	0.0782	0.2271	0.0188	-0.1266	0.0644	12.11
4.11	0.00489	199.58	0.0443	0.2187	0.0172	-0.1260	0.0621	12.72
4.11	0.00342	200.13	0.0215	0.2067	0.0199	-0.1238	0.0585	10.36
4.10	0.00000	198.11	0.0000	0.1781	0.0153	-0.1096	0.0481	11.66
5.99	0.01039	204.27	0.1939	0.3536	0.0270	-0.1885	0.1040	13.11
6.01	0.00855	204.02	0.1318	0.3411	0.0294	-0.1881	0.1027	11.59
6.03	0.00661	202.74	0.0795	0.3368	0.0291	-0.1869	0.0989	11.58
6.04	0.00496	201.88	0.0450	0.3271	0.0277	-0.1819	0.0950	11.79
6.05	0.00366	200.42	0.0247	0.3120	0.0290	-0.1770	0.0901	10.75
6.03	0.00000	197.77	0.0000	0.2691	0.0243	-0.1548	0.0736	11.09
8.04	0.01039	205.01	0.1938	0.4823	0.0434	-0.2569	0.1412	11.12
8.03	0.00863	204.27	0.1346	0.4639	0.0444	-0.2552	0.1395	10.45
8.03	0.00661	202.77	0.0799	0.4477	0.0432	-0.2542	0.1355	10.37
8.06	0.00504	201.59	0.0468	0.4417	0.0419	-0.2492	0.1302	10.53
8.06	0.00361	199.74	0.0242	0.4204	0.0428	-0.2381	0.1229	9.83
8.04	0.00000	197.34	0.0000	0.3633	0.0345	-0.2009	0.1001	10.54
10.08	0.01037	205.04	0.1937	0.6058	0.0601	-0.3223	0.1754	10.08
10.08	0.00863	204.45	0.1351	0.5875	0.0613	-0.3206	0.1737	9.58
10.08	0.00662	203.04	0.0803	0.5645	0.0592	-0.3180	0.1698	9.54
10.10	0.00502	199.79	0.0476	0.5535	0.0568	-0.3167	0.1648	9.74
10.10	0.00379	199.57	0.0270	0.5358	0.0585	-0.3055	0.1573	9.16
10.06	0.00000	197.86	0.0000	0.4672	0.0470	-0.2600	0.1294	9.95
12.22	0.01038	205.48	0.1943	0.7168	0.0819	-0.3783	0.2068	8.76
12.23	0.00864	204.67	0.1359	0.7008	0.0839	-0.3786	0.2053	8.36
12.23	0.00660	203.51	0.0800	0.6785	0.0807	-0.3768	0.2018	8.40

1. Jet Momentum Force and moment components deducted.

ALPHA	DOTM	UTUN	CJ	CL	CD	CM	CB	L/D
12.24	0.00499	199.41	0.0474	0.6566	0.0760	-0.3742	0.1971	8.63
12.24	0.00376	199.39	0.0267	0.6333	0.0756	-0.3659	0.1896	8.37
12.21	0.00000	200.10	0.0000	0.5687	0.0617	-0.3183	0.1592	9.22
14.00	0.01017	204.68	0.1849	0.8070	0.0898	-0.4325	0.2313	8.99
14.00	0.00862	203.58	0.1346	0.7874	0.0966	-0.4312	0.2298	8.15
13.99	0.00667	202.46	0.0814	0.7602	0.0958	-0.4231	0.2258	7.94
13.99	0.00498	198.81	0.0469	0.7356	0.0892	-0.4126	0.2202	8.25
13.99	0.00354	198.48	0.0236	0.7109	0.0913	-0.3964	0.2084	7.79
13.96	0.00000	198.52	0.0000	0.6517	0.0758	-0.3532	0.1812	8.59
16.30	0.01025	204.78	0.1895	0.9160	0.1235	-0.4856	0.2632	7.42
16.30	0.00873	203.94	0.1387	0.9000	0.1286	-0.4841	0.2618	7.00
16.31	0.00669	201.62	0.0834	0.8711	0.1258	-0.4754	0.2557	6.93
16.30	0.00512	198.63	0.0501	0.8463	0.1177	-0.4723	0.2491	7.19
16.29	0.00355	198.82	0.0238	0.8103	0.1169	-0.4550	0.2366	6.93
16.25	0.00000	198.89	0.0000	0.7475	0.0976	-0.4090	0.2071	7.66
18.11	0.01030	204.67	0.1930	1.0075	0.1564	-0.5412	0.2905	6.44
18.11	0.00866	203.92	0.1373	0.9891	0.1575	-0.5368	0.2877	6.28
18.11	0.00676	200.49	0.0864	0.9615	0.1521	-0.5264	0.2805	6.32
18.10	0.00511	198.24	0.0504	0.9325	0.1447	-0.5161	0.2726	6.44
18.10	0.00376	198.33	0.0270	0.9022	0.1427	-0.5080	0.2627	6.32
18.06	0.00000	197.96	0.0000	0.8301	0.1322	-0.4784	0.2266	4.56
17.27	0.00000	0.00	0.0000	0.0000	0.0000	0.0000	0.0000	0.00

Wing 2 λ = 0.25, R = 3

IDATA	IWING	IDORF	BARM	SPFHUM	ALPHA 0		
38	2	3	30.00000	0.01100	1.30000	11-FEB-83	16:33:34

ALPHA	DOTM	UTUN	CJ	CL	CD	CM	CB	L/D
-0.39	0.00000	0.00	0.0000	0.0000	0.0000	0.0000	0.0000	0.00
-0.40	0.00774	189.84	0.1286	-0.0087	0.0075	0.0088	0.0128	-1.17
-0.40	0.00662	188.06	0.0954	-0.0050	0.0072	0.0079	0.0105	-0.70
-0.40	0.00481	187.22	0.0499	-0.0020	0.0040	0.0077	0.0062	-0.49
-0.39	0.00354	187.64	0.0260	-0.0012	0.0076	0.0073	0.0037	-0.15
-0.39	0.00264	187.41	0.0136	0.0011	0.0144	0.0063	0.0026	0.08
-0.39	0.00000	188.15	0.0027	0.0033	0.0149	0.0048	0.0019	0.22
0.54	0.00000	188.55	0.0027	0.0487	0.0128	-0.0184	0.0211	3.79
1.55	0.00000	188.81	0.0027	0.1006	0.0112	-0.0439	0.0425	9.00
1.83	0.00768	190.59	0.1289	0.1397	0.0048	-0.0848	0.0844	28.93
1.85	0.00655	189.60	0.0943	0.1399	0.0036	-0.0847	0.0794	38.40
1.87	0.00482	188.32	0.0507	0.1387	0.0016	-0.0837	0.0723	86.72
1.89	0.00344	188.43	0.0247	0.1364	0.0063	-0.0826	0.0670	21.79
1.91	0.00274	188.72	0.0148	0.1340	0.0122	-0.0821	0.0636	11.03
1.91	0.00000	188.88	0.0027	0.1194	0.0127	-0.0724	0.0512	9.37
3.85	0.00757	191.69	0.1247	0.2841	0.0033	-0.1672	0.1527	86.03
3.88	0.00649	191.39	0.0914	0.2809	0.0031	-0.1659	0.1448	90.48
3.90	0.00481	191.69	0.0490	0.2751	0.0029	-0.1626	0.1348	94.11
3.91	0.00345	190.18	0.0246	0.2691	0.0072	-0.1609	0.1268	37.52
3.92	0.00273	190.56	0.0145	0.2601	0.0127	-0.1573	0.1197	20.42
3.93	0.00000	189.20	0.0027	0.2331	0.0121	-0.1393	0.0996	19.22
5.89	0.00757	193.53	0.1234	0.4467	0.0095	-0.2644	0.2291	47.13
5.92	0.00647	193.53	0.0896	0.4404	0.0101	-0.2620	0.2193	43.66
5.92	0.00487	193.02	0.0499	0.4311	0.0090	-0.2576	0.2063	47.83
5.94	0.00340	190.00	0.0241	0.4187	0.0136	-0.2526	0.1933	30.88
5.95	0.00277	189.53	0.0153	0.4026	0.0184	-0.2441	0.1827	21.88
5.93	0.00000	190.72	0.0027	0.3621	0.0160	-0.2184	0.1538	22.67
7.96	0.00755	194.54	0.1220	0.6073	0.0195	-0.3542	0.3015	31.16
7.99	0.00649	194.15	0.0900	0.6013	0.0207	-0.3503	0.2913	29.11
8.01	0.00484	193.42	0.0494	0.5880	0.0209	-0.3435	0.2757	28.19
8.03	0.00350	189.52	0.0259	0.5712	0.0250	-0.3367	0.2612	22.88
8.03	0.00273	189.83	0.0149	0.5470	0.0291	-0.3239	0.2450	18.78
8.00	0.00000	190.06	0.0028	0.5008	0.0258	-0.2921	0.2130	19.41
10.04	0.00758	194.83	0.1237	0.7425	0.0340	-0.4174	0.3567	21.83
10.05	0.00647	194.54	0.0898	0.7373	0.0353	-0.4153	0.3461	20.90
10.07	0.00491	193.77	0.0511	0.7282	0.0373	-0.4119	0.3325	19.53
10.09	0.00350	189.96	0.0259	0.7113	0.0417	-0.4062	0.3178	17.05
10.09	0.00271	189.99	0.0147	0.6880	0.0445	-0.3955	0.3005	15.45
10.07	0.00000	190.32	0.0028	0.6448	0.0368	-0.3756	0.2699	17.52

ALPHA	DOTM	UTUN	CJ	CL	CD	CM	CB	L/D
9.45	0.00000	0.00	0.0000	0.0000	0.0000	0.0000	0.0000	0.00
12.11	0.00742	195.59	0.1167	0.8478	0.0408	-0.4679	0.3968	20.76
12.13	0.00639	195.68	0.0861	0.8431	0.0446	-0.4658	0.3862	18.91
12.15	0.00489	194.55	0.0500	0.8325	0.0478	-0.4601	0.3716	17.41
12.16	0.00350	191.76	0.0254	0.8133	0.0524	-0.4533	0.3557	15.52
12.17	0.00271	191.78	0.0144	0.7918	0.0551	-0.4467	0.3395	14.38
12.16	0.00000	191.69	0.0027	0.7523	0.0499	-0.4226	0.3106	15.06
14.22	0.00749	195.95	0.1197	0.9634	0.0600	-0.5225	0.4245	16.07
14.25	0.00641	195.98	0.0870	0.9555	0.0635	-0.5184	0.4243	15.04
14.26	0.00495	194.79	0.0516	0.9419	0.0674	-0.5112	0.4108	13.97
14.27	0.00353	192.17	0.0259	0.9204	0.0716	-0.5019	0.3928	12.86
14.28	0.00277	191.33	0.0153	0.8981	0.0740	-0.4924	0.3769	12.13
14.26	0.00000	191.89	0.0027	0.8493	0.0653	-0.4649	0.3430	13.01
16.24	0.00758	196.04	0.1232	1.0815	0.0814	-0.5806	0.4456	13.28
16.25	0.00642	195.79	0.0879	1.0690	0.0840	-0.5738	0.4453	12.73
16.25	0.00494	194.62	0.0519	1.0469	0.0885	-0.5621	0.4458	11.83
16.27	0.00352	192.00	0.0259	1.0220	0.0933	-0.5500	0.4304	10.95
16.27	0.00293	192.09	0.0173	1.0056	0.0945	-0.5435	0.4184	10.64
18.05	0.00751	191.49	0.1277	1.0738	0.2070	-0.5819	0.4581	5.19
18.09	0.00637	191.66	0.0911	1.0948	0.2070	-0.5991	0.4597	5.29
18.10	0.00481	191.62	0.0509	1.0804	0.2099	-0.5953	0.4397	5.15
18.09	0.00337	191.81	0.0238	1.0423	0.2161	-0.5754	0.4091	4.82
18.05	0.00255	191.55	0.0128	0.9742	0.2146	-0.5393	0.3699	4.54
17.92	0.00000	191.60	0.0028	0.8296	0.1901	-0.4675	0.3083	4.36
17.12	0.00000	0.00	0.0000	0.0000	0.0000	0.0000	0.0000	0.00

Wing 4 $\lambda = 0.5$, $\text{Æ} = 2$

IDATA	IWING	IDORF	BARM	SPFHUM	ALPHA O		
25	4	3	30.01000	0.00100	0.78000	11-FEB-83	16:22:49

ALPHA	DOTM	UTUN	CJ	CL	CD	CM	CB	L/D
-0.22	0.00000	188.23	0.0000	-0.0020	0.0176	-0.0002	0.0006	-0.11
3.32	0.00000	189.70	0.0000	0.1573	0.0193	-0.0664	0.0535	8.14
7.27	0.00000	189.88	0.0000	0.3512	0.0406	-0.1341	0.1187	8.66
11.76	0.01404	196.49	0.2230	0.8236	0.1027	-0.3325	0.3084	8.02
11.69	0.00000	194.54	0.0000	0.6048	0.0816	-0.2340	0.2041	7.41
16.26	0.01400	196.68	0.2223	1.0683	0.1705	-0.4351	0.3999	6.26
16.14	0.00000	192.15	0.0000	0.8186	0.1354	-0.3090	0.2769	6.05
18.27	0.00000	190.98	0.0000	0.9111	0.1606	-0.3654	0.3089	5.67
17.39	0.00000	0.00	0.0000	0.0000	0.0000	0.0000	0.0000	0.00

IDATA	IWING	IDORF	BARM	SPFHUM	ALPHA O		
26	4	3	30.05000	0.01100	0.78000	11-FEB-83	16:23:47

ALPHA	DOTM	UTUN	CJ	CL	CD	CM	CB	L/D
-1.53	0.01407	195.81	0.2301	-0.1385	0.0285	0.1266	-0.0446	-4.86
-1.53	0.01279	194.14	0.1947	-0.1364	0.0240	0.1254	-0.0432	-5.68
-1.53	0.01141	193.60	0.1568	-0.1327	0.0208	0.1210	-0.0417	-6.39
-1.52	0.00991	193.26	0.1194	-0.1281	0.0184	0.1155	-0.0396	-6.98
-1.51	0.00738	192.35	0.0674	-0.1153	0.0196	0.1024	-0.0346	-5.88
-1.46	0.00000	193.87	0.0000	-0.0643	0.0225	0.0536	-0.0154	-2.86
-0.24	0.01393	197.48	0.2271	-0.0293	0.0235	0.0611	-0.0038	-1.25
-0.22	0.01268	196.92	0.1901	-0.0295	0.0194	0.0592	-0.0035	-1.52
-0.21	0.01142	196.03	0.1560	-0.0280	0.0174	0.0570	-0.0030	-1.61
-0.21	0.00990	193.97	0.1205	-0.0273	0.0155	0.0544	-0.0024	-1.76
-0.19	0.00732	192.63	0.0672	-0.0218	0.0168	0.0457	-0.0003	-1.30
-0.15	0.00000	194.25	0.0000	-0.0067	0.0195	0.0204	0.0043	-0.35
1.12	0.01389	198.49	0.2265	0.0852	0.0214	-0.0067	0.0386	3.99
1.14	0.01268	197.90	0.1904	0.0843	0.0178	-0.0097	0.0383	4.73
1.15	0.01142	197.47	0.1555	0.0841	0.0157	-0.0109	0.0382	5.35
1.17	0.00991	196.35	0.1188	0.0812	0.0147	-0.0116	0.0375	5.52
1.17	0.00731	193.75	0.0668	0.0751	0.0165	-0.0131	0.0352	4.57

ALPHA	DOTH	UTUN	CJ	CL	CD	CM	CB	L/D
1.17	0.00000	194.72	0.0000	0.0517	0.0195	-0.0083	0.0234	2.65
3.03	0.01391	199.74	0.2262	0.2320	0.0248	-0.0856	0.0931	9.35
3.06	0.01267	199.44	0.1886	0.2285	0.0215	-0.0878	0.0917	10.65
3.05	0.01136	199.06	0.1529	0.2222	0.0200	-0.0856	0.0894	11.12
3.07	0.00995	198.18	0.1187	0.2150	0.0189	-0.0842	0.0870	11.37
3.07	0.00732	197.00	0.0654	0.1969	0.0205	-0.0793	0.0796	9.59
3.02	0.00000	194.76	0.0000	0.1384	0.0211	-0.0537	0.0512	6.54
5.17	0.01392	200.58	0.2264	0.3707	0.0351	-0.1593	0.1437	10.56
5.17	0.01142	200.08	0.1542	0.3562	0.0287	-0.1576	0.1378	12.42
5.18	0.00998	199.78	0.1186	0.3458	0.0273	-0.1545	0.1341	12.67
5.18	0.00734	198.90	0.0650	0.3182	0.0285	-0.1425	0.1228	11.15
5.11	0.00000	194.76	0.0000	0.2364	0.0260	-0.1022	0.0836	9.09
7.24	0.01385	200.50	0.2261	0.5209	0.0486	-0.2326	0.1996	10.72
7.27	0.01269	200.42	0.1906	0.5142	0.0448	-0.2291	0.1967	11.48
7.27	0.01143	200.17	0.1553	0.5031	0.0434	-0.2272	0.1923	11.59
7.28	0.01001	199.44	0.1204	0.4885	0.0418	-0.2211	0.1868	11.63
7.26	0.00735	198.76	0.0656	0.4502	0.0423	-0.2013	0.1707	10.65
7.19	0.00000	193.75	0.0000	0.3473	0.0365	-0.1503	0.1218	9.53
9.57	0.01389	201.21	0.2271	0.6930	0.0768	-0.3028	0.2631	9.02
9.59	0.01272	200.93	0.1913	0.6830	0.0732	-0.2972	0.2583	9.33
9.60	0.01148	200.34	0.1572	0.6696	0.0709	-0.2921	0.2528	9.44
9.60	0.01006	200.47	0.1210	0.6514	0.0687	-0.2834	0.2449	9.48
9.57	0.00735	197.62	0.0668	0.6024	0.0674	-0.2611	0.2239	8.93
9.48	0.00000	194.46	0.0000	0.4759	0.0555	-0.2048	0.1639	8.57
11.84	0.01391	201.49	0.2282	0.8391	0.1044	-0.3559	0.3152	8.04
11.86	0.01289	201.31	0.1970	0.8301	0.1029	-0.3514	0.3108	8.07
11.88	0.01278	200.33	0.1958	0.8327	0.1024	-0.3524	0.3114	8.13
11.87	0.01152	200.96	0.1585	0.8177	0.1000	-0.3443	0.3048	8.18
11.88	0.01016	199.46	0.1256	0.8001	0.0986	-0.3380	0.2964	8.12
11.86	0.00738	195.56	0.0692	0.7491	0.0969	-0.3173	0.2730	7.73

IDATA	IWING	IDORF	BARM	SPFHUM	ALPHA 0			
27	4	3	30.05000	0.01100	0.78000	11-FEB-83	16:25:07	

ALPHA	DOTH	UTUN	CJ	CL	CD	CM	CB	L/D
14.27	0.01404	200.45	0.2242	0.9691	0.1441	-0.3931	0.3657	6.72
14.25	0.01287	200.20	0.1900	0.9569	0.1415	-0.3865	0.3594	6.76
14.27	0.01161	199.85	0.1558	0.9396	0.1397	-0.3803	0.3509	6.73
14.26	0.01031	199.24	0.1242	0.9184	0.1385	-0.3705	0.3410	6.63
14.24	0.00739	194.59	0.0673	0.8584	0.1338	-0.3476	0.3122	6.42
14.21	0.00551	195.13	0.0375	0.8141	0.1332	-0.3315	0.2895	6.11
14.15	0.00000	196.43	0.0000	0.7340	0.1181	-0.2979	0.2507	6.22
16.51	0.01405	201.34	0.2271	1.0919	0.1834	-0.4542	0.4105	5.95
16.53	0.01296	201.06	0.1944	1.0785	0.1807	-0.4455	0.4038	5.97
16.55	0.01173	200.61	0.1606	1.0607	0.1782	-0.4380	0.3952	5.95
16.54	0.01037	199.64	0.1271	1.0375	0.1759	-0.4259	0.3837	5.90
16.49	0.00740	195.74	0.0678	0.9710	0.1679	-0.3992	0.3513	5.78
16.47	0.00559	195.54	0.0389	0.9266	0.1650	-0.3795	0.3286	5.62
16.38	0.00000	196.60	0.0000	0.8337	0.1446	-0.3399	0.2843	5.77
18.64	0.01413	201.53	0.2320	1.2167	0.2308	-0.5147	0.4340	5.27
18.65	0.01302	201.37	0.1979	1.1971	0.2268	-0.5024	0.4336	5.28
18.64	0.01180	200.66	0.1641	1.1743	0.2215	-0.4887	0.4340	5.30
18.64	0.01043	199.24	0.1306	1.1476	0.2169	-0.4797	0.4238	5.29
18.59	0.00743	194.56	0.0699	1.0776	0.2060	-0.4470	0.3890	5.23
18.57	0.00563	196.10	0.0397	1.0348	0.2008	-0.4279	0.3662	5.15
19.98	0.01416	201.87	0.2349	1.2927	0.2669	-0.5519	0.4490	4.84
19.95	0.01307	201.52	0.2012	1.2719	0.2608	-0.5387	0.4487	4.88
19.93	0.01188	200.21	0.1690	1.2486	0.2542	-0.5270	0.4501	4.91
19.90	0.01047	198.82	0.1336	1.2176	0.2466	-0.5129	0.4491	4.94
19.83	0.00743	195.34	0.0700	1.1416	0.2321	-0.4809	0.4106	4.92
19.79	0.00574	195.75	0.0417	1.1020	0.2249	-0.4599	0.3894	4.90
19.68	0.00000	196.52	0.0000	0.9822	0.1950	-0.4058	0.3337	5.04
18.73	0.00000	0.00	0.0000	0.0000	0.0000	0.0000	0.0000	0.00
18.72	0.00000	0.00	0.0000	0.0000	0.0000	0.0000	0.0000	0.00

Wing 5 $\lambda = 0.5$, $R = 4$

IDATA	IWING	IDORF	BARM	SPFHUM	ALPHA 0		
40	5	3	30.05000	0.01200	0.62000	11-FEB-83	16:36:03

ALPHA	DOTM	UTUN	CJ	CL	CD	CM	CB	L/D
-1.68	0.00000	0.00	0.0000	0.0000	0.0000	0.0000	0.0000	0.00
-0.76	0.00970	195.43	0.1638	0.0220	0.0135	-0.0091	0.0291	1.63
-0.77	0.00828	194.92	0.1211	0.0160	0.0123	-0.0071	0.0233	1.30
-0.77	0.00628	194.50	0.0710	0.0117	0.0155	-0.0059	0.0192	0.76
-0.78	0.00435	194.46	0.0353	0.0070	0.0186	-0.0049	0.0155	0.38
-0.78	0.00326	194.36	0.0208	0.0027	0.0208	-0.0032	0.0117	0.13
-0.79	0.00000	194.65	0.0018	-0.0027	0.0197	0.0001	0.0067	-0.14
3.55	0.00000	193.76	0.0018	0.2498	0.0218	-0.1002	0.1792	11.46
3.65	0.00954	196.07	0.1575	0.3565	0.0130	-0.1560	0.2935	27.43
7.80	0.00937	196.87	0.1515	0.7397	0.0254	-0.3296	0.4767	29.16
11.82	0.00000	195.64	0.0018	0.8707	0.0620	-0.3750	0.5594	14.05
12.01	0.00938	197.31	0.1523	1.0699	0.0545	-0.4688	0.5550	19.65
16.13	0.00936	197.21	0.1521	1.2718	0.0936	-0.5377	0.6031	13.59
15.95	0.00000	196.02	0.0018	1.0874	0.1008	-0.4531	0.6089	10.79

IDATA	IWING	IDORF	BARM	SPFHUM	ALPHA 0		
41	5	3	30.05000	0.01200	0.62000	11-FEB-83	16:37:54

ALPHA	DOTM	UTUN	CJ	CL	CD	CM	CB	L/D
1.36	0.00917	190.55	0.1562	0.1882	0.0111	-0.0390	0.1597	17.00
1.35	0.00797	190.32	0.1193	0.1826	0.0126	-0.0357	0.1544	14.47
1.34	0.00622	189.95	0.0743	0.1713	0.0194	-0.0288	0.1431	8.83
1.33	0.00431	190.00	0.0370	0.1549	0.0248	-0.0202	0.1276	6.25
1.29	0.00000	190.23	0.0019	0.1118	0.0280	0.0059	0.0848	3.99
3.38	0.00924	191.20	0.1604	0.3408	0.0136	-0.1065	0.2778	24.97
3.38	0.00809	191.18	0.1240	0.3358	0.0148	-0.1035	0.2720	22.69
3.36	0.00624	191.04	0.0749	0.3216	0.0226	-0.0954	0.2571	14.26
3.34	0.00434	190.54	0.0376	0.2990	0.0277	-0.0833	0.2362	10.80
3.32	0.00329	190.28	0.0227	0.2759	0.0311	-0.0707	0.2125	8.89
3.28	0.00000	190.21	0.0020	0.2364	0.0289	-0.0458	0.1710	8.17
5.32	0.00922	191.35	0.1606	0.4996	0.0175	-0.1795	0.3982	28.57
5.31	0.00805	191.40	0.1231	0.4937	0.0217	-0.1763	0.3912	22.77
5.30	0.00624	191.08	0.0753	0.4766	0.0286	-0.1669	0.3721	16.68
5.26	0.00430	190.64	0.0372	0.4429	0.0329	-0.1493	0.3398	13.44
5.23	0.00329	190.01	0.0229	0.4128	0.0367	-0.1328	0.3095	11.25
5.19	0.00000	190.35	0.0020	0.3626	0.0334	-0.1013	0.2578	10.86
7.30	0.00915	191.64	0.1587	0.6987	0.0238	-0.2737	0.4924	29.40
7.29	0.00804	191.71	0.1232	0.6884	0.0278	-0.2691	0.5012	24.77
7.26	0.00623	191.69	0.0750	0.6541	0.0376	-0.2519	0.5007	17.41
7.22	0.00434	190.34	0.0383	0.6127	0.0424	-0.2302	0.4589	14.44
7.18	0.00329	189.90	0.0230	0.5753	0.0454	-0.2098	0.4208	12.68
7.13	0.00000	190.48	0.0020	0.5150	0.0402	-0.1722	0.3608	12.82
9.33	0.00917	192.89	0.1556	0.8871	0.0355	-0.3602	0.5280	24.99
9.32	0.00804	193.00	0.1203	0.8718	0.0398	-0.3540	0.5355	21.92
9.28	0.00624	192.59	0.0739	0.8294	0.0488	-0.3336	0.5420	16.99
9.23	0.00434	191.28	0.0375	0.7779	0.0548	-0.3083	0.5453	14.21
9.19	0.00328	191.27	0.0223	0.7362	0.0572	-0.2862	0.5305	12.88
9.12	0.00000	191.43	0.0019	0.6707	0.0505	-0.2465	0.4658	13.29
11.35	0.00917	193.15	0.1565	1.0281	0.0481	-0.4178	0.5627	21.38
11.34	0.00808	192.77	0.1226	1.0134	0.0527	-0.4120	0.5717	19.23
11.30	0.00624	192.44	0.0745	0.9749	0.0625	-0.3949	0.5792	15.60
11.26	0.00436	191.34	0.0379	0.9320	0.0696	-0.3758	0.5837	13.40
11.22	0.00326	191.36	0.0222	0.8955	0.0734	-0.3578	0.5807	12.19
11.16	0.00000	191.41	0.0020	0.8299	0.0665	-0.3217	0.5725	12.48
13.41	0.00917	193.24	0.1572	1.1482	0.0660	-0.4631	0.5923	17.39
13.39	0.00805	193.24	0.1219	1.1321	0.0687	-0.4568	0.5998	16.48
13.35	0.00624	192.39	0.0749	1.0910	0.0780	-0.4386	0.6086	13.98
13.30	0.00437	191.32	0.0384	1.0423	0.0849	-0.4159	0.6118	12.28
13.27	0.00326	191.20	0.0224	1.0029	0.0869	-0.3962	0.6087	11.54

51

13.20	0.00000	191.28	0.0020	0.9308	0.0786	-0.3573	0.5992	11.C
15.45	0.00905	192.82	0.1516	1.2415	0.0793	-0.4964	0.6101	15.65
15.43	0.00798	193.01	0.1184	1.2252	0.0837	-0.4909	0.6172	14.64
15.40	0.00621	191.88	0.0737	1.1886	0.0941	-0.4757	0.6282	12.64
15.35	0.00436	191.13	0.0379	1.1397	0.0993	-0.4535	0.6306	11.48
15.31	0.00328	191.04	0.0224	1.1026	0.0999	-0.4354	0.6280	11.04
15.24	0.00000	191.43	0.0019	1.0266	0.0899	-0.3960	0.6167	11.42
17.36	0.00909	192.97	0.1541	1.3197	0.1075	-0.5319	0.6299	12.28
17.34	0.00804	192.85	0.1216	1.3000	0.1096	-0.5226	0.6371	11.86
17.30	0.00622	191.99	0.0744	1.2591	0.1172	-0.5030	0.6467	10.75
17.25	0.00432	191.01	0.0376	1.2062	0.1194	-0.4770	0.6492	10.10
17.21	0.00320	190.99	0.0217	1.1681	0.1198	-0.4577	0.6464	9.75
17.13	0.00000	191.07	0.0020	1.0826	0.1071	-0.4130	0.6339	10.11
16.09	0.00000	0.00	0.0000	0.0000	0.0000	0.0000	0.0000	0.00

Wing 6 $\lambda = 1$, $\mathcal{R} = 0.62$

IDATA	IWING	IDORF	BARM	SPFHUM	ALPHA 0		
45	6	3	30.11000	0.01000	0.14000	11-FEB-83	16:52:27

ALPHA	DOTM	UTUN	CJ	CL	CD	CM	CB	L/D
0.20	0.00000	197.85	0.0000	0.0128	0.0254	-0.0048	0.0027	0.51
0.22	0.01177	199.41	0.0826	0.0313	0.0316	-0.0107	0.0055	0.99
3.18	0.01183	200.45	0.0840	0.1467	0.0402	-0.0455	0.0244	3.65
3.11	0.00000	200.29	0.0000	0.0778	0.0296	-0.0197	0.0150	2.63
6.68	0.01179	202.06	0.0828	0.2504	0.0589	-0.0803	0.0413	4.25
6.61	0.00000	201.15	0.0000	0.1640	0.0389	-0.0440	0.0306	4.21
10.85	0.01184	202.52	0.0837	0.3526	0.0881	-0.1149	0.0579	4.00
10.78	0.00000	201.54	0.0000	0.2802	0.0610	-0.0793	0.0521	4.59
15.41	0.01178	202.29	0.0834	0.4962	0.1407	-0.1703	0.0840	3.53
15.34	0.00000	200.87	0.0000	0.4281	0.1033	-0.1301	0.0797	4.14
14.94	0.00000	0.00	0.0000	0.0000	0.0000	0.0000	0.0000	0.00

IDATA	IWING	IDORF	BARM	SPFHUM	ALPHA 0		
46	6	4	30.18000	0.01000	0.14000	11-FEB-83	16:53:05

ALPHA	DOTM	UTUN	CJ	CL	CD	CM	CB	L/D
0.19	0.00000	0.00	0.0000	0.0000	0.0000	0.0000	0.0000	0.00
0.25	0.01562	195.35	0.1486	0.0641	0.0367	-0.0218	0.0103	1.75
0.27	0.01731	195.35	0.1833	0.0804	0.0373	-0.0264	0.0130	2.16
0.24	0.01397	195.45	0.1204	0.0499	0.0350	-0.0164	0.0085	1.43
0.23	0.01225	195.33	0.0932	0.0368	0.0352	-0.0118	0.0066	1.05
0.22	0.00973	192.92	0.0606	0.0260	0.0347	-0.0077	0.0048	0.75
0.21	0.00823	193.08	0.0435	0.0215	0.0350	-0.0063	0.0040	0.61
0.21	0.00644	193.02	0.0267	0.0169	0.0353	-0.0054	0.0035	0.48
0.20	0.00000	194.43	0.0000	0.0105	0.0328	-0.0034	0.0027	0.32
2.28	0.01730	196.18	0.1862	0.1766	0.0467	-0.0575	0.0286	3.78
2.26	0.01562	196.44	0.1521	0.1572	0.0449	-0.0515	0.0253	3.50
2.24	0.01405	196.49	0.1235	0.1396	0.0430	-0.0461	0.0227	3.24
2.23	0.01211	196.25	0.0923	0.1211	0.0408	-0.0402	0.0200	2.97
2.21	0.01062	195.29	0.0720	0.1081	0.0395	-0.0362	0.0182	2.74
2.19	0.00824	194.79	0.0437	0.0896	0.0377	-0.0300	0.0152	2.38
2.18	0.00636	195.09	0.0261	0.0750	0.0370	-0.0250	0.0130	2.03
2.16	0.00000	194.79	0.0000	0.0529	0.0341	-0.0157	0.0099	1.55
2.16	0.00000	196.21	0.0000	0.0579	0.0319	-0.0188	0.0116	1.81
4.26	0.01728	196.95	0.1869	0.2576	0.0593	-0.0859	0.0416	4.35
4.24	0.01565	197.02	0.1537	0.2370	0.0568	-0.0791	0.0382	4.17
4.21	0.01399	197.25	0.1230	0.2129	0.0534	-0.0714	0.0345	3.99
4.20	0.01257	197.06	0.0998	0.1940	0.0511	-0.0648	0.0316	3.79
4.18	0.01096	197.24	0.0761	0.1753	0.0478	-0.0581	0.0289	3.67
4.17	0.00954	197.80	0.0574	0.1609	0.0461	-0.0531	0.0268	3.49
4.14	0.00664	197.39	0.0281	0.1323	0.0432	-0.0430	0.0226	3.06
4.11	0.00370	194.77	0.0090	0.1021	0.0393	-0.0301	0.0178	2.60
4.11	0.00000	196.38	0.0000	0.1047	0.0333	-0.0317	0.0199	3.14

6.30	0.01725	197.16	0.1875	0.3299	0.0755	-0.1111	0.0532	4.37
6.28	0.01547	197.49	0.1509	0.3029	0.0708	-0.1020	0.0487	4.23
6.25	0.01393	197.78	0.1225	0.2750	0.0666	-0.0927	0.0444	4.13
6.23	0.01217	197.82	0.0938	0.2498	0.0620	-0.0835	0.0408	4.03
6.21	0.01073	198.22	0.0728	0.2261	0.0574	-0.0746	0.0374	3.94
6.19	0.00896	198.43	0.0508	0.2075	0.0543	-0.0674	0.0347	3.82
6.16	0.00653	197.48	0.0273	0.1800	0.0497	-0.0568	0.0307	3.62
6.14	0.00438	194.67	0.0127	0.1547	0.0443	-0.0459	0.0271	3.49
6.14	0.00000	197.08	0.0000	0.1532	0.0382	-0.0447	0.0290	4.01
8.24	0.01716	197.63	0.1862	0.3904	0.0939	-0.1325	0.0632	4.16
8.21	0.01550	197.82	0.1522	0.3628	0.0883	-0.1235	0.0585	4.11
8.19	0.01425	198.00	0.1287	0.3356	0.0633	-0.1139	0.0542	4.03
8.16	0.01242	198.31	0.0978	0.3057	0.0766	-0.1028	0.0496	3.99
8.13	0.01086	198.77	0.0747	0.2790	0.0698	-0.0925	0.0459	4.00
8.12	0.00942	198.74	0.0563	0.2583	0.0655	-0.0841	0.0429	3.94
8.09	0.00671	197.87	0.0289	0.2276	0.0584	-0.0706	0.0389	3.90
8.06	0.00412	194.95	0.0113	0.1962	0.0518	-0.0559	0.0344	3.79
8.07	0.00000	197.53	0.0000	0.2044	0.0448	-0.0589	0.0383	4.57
10.37	0.01708	197.56	0.1858	0.4546	0.1170	-0.1549	0.0742	3.89
10.34	0.01554	198.31	0.1531	0.4222	0.1089	-0.1449	0.0685	3.88
10.31	0.01417	198.62	0.1274	0.3886	0.1008	-0.1325	0.0630	3.05
10.28	0.01256	199.00	0.0999	0.3578	0.0923	-0.1206	0.0582	3.83
10.25	0.01107	198.91	0.0780	0.3287	0.0847	-0.1087	0.0538	3.83
10.23	0.00918	199.08	0.0537	0.2993	0.0769	-0.0959	0.0497	3.89
10.20	0.00654	198.51	0.0275	0.2687	0.0679	-0.0811	0.0460	3.96
10.18	0.00360	195.84	0.0086	0.2464	0.0598	-0.0689	0.0435	4.12
10.19	0.00000	198.14	0.0000	0.2644	0.0580	-0.0770	0.0494	4.54
12.16	0.01707	198.11	0.1857	0.5159	0.1412	-0.1779	0.0951	3.65
12.12	0.01556	198.51	0.1541	0.4783	0.1309	-0.1662	0.0783	3.65
12.09	0.01392	198.66	0.1236	0.4411	0.1209	-0.1523	0.0721	3.65
12.05	0.01215	198.77	0.0944	0.4004	0.1085	-0.1361	0.0656	3.69
12.01	0.01022	198.96	0.0669	0.3626	0.0966	-0.1198	0.0599	3.76
11.98	0.00713	199.03	0.0327	0.3217	0.0824	-0.0994	0.0547	3.90
11.96	0.00384	196.13	0.0098	0.3023	0.0729	-0.0874	0.0531	4.14
11.97	0.00000	198.06	0.0000	0.3195	0.0716	-0.0946	0.0598	4.46
14.27	0.01707	197.69	0.1872	0.5937	0.1734	-0.2083	0.0998	3.42
14.23	0.01559	197.99	0.1562	0.5572	0.1627	-0.1964	0.0931	3.42
14.20	0.01446	198.25	0.1343	0.5224	0.1520	-0.1842	0.0870	3.44
14.17	0.01281	198.42	0.1056	0.4859	0.1393	-0.1700	0.0806	3.49
14.13	0.01102	198.70	0.0783	0.4425	0.1237	-0.1511	0.0740	3.58
14.10	0.00935	198.85	0.0563	0.4100	0.1122	-0.1354	0.0692	3.65
14.07	0.00729	198.96	0.0343	0.3856	0.1016	-0.1222	0.0661	3.80
14.06	0.00395	198.47	0.0102	0.3733	0.0929	-0.1110	0.0657	4.02
14.07	0.00000	197.04	0.0000	0.3860	0.0914	-0.1164	0.0724	4.22
16.23	0.01704	197.26	0.1859	0.6652	0.2060	-0.2343	0.1137	3.23
16.19	0.01564	197.47	0.1568	0.6267	0.1938	-0.2213	0.1067	3.23
16.16	0.01451	197.76	0.1350	0.5932	0.1818	-0.2097	0.1008	3.26
16.12	0.01286	198.19	0.1060	0.5528	0.1660	-0.1945	0.0937	3.33
16.09	0.01155	198.43	0.0856	0.5214	0.1540	-0.1809	0.0884	3.39
16.07	0.01029	198.60	0.0680	0.4920	0.1419	-0.1676	0.0836	3.47
16.04	0.00866	198.67	0.0483	0.4673	0.1308	-0.1545	0.0801	3.57
16.02	0.00653	198.56	0.0275	0.4479	0.1201	-0.1428	0.0777	3.73
16.02	0.00000	198.41	0.0000	0.4442	0.1125	-0.1348	0.0787	3.95
16.03	0.00000	197.15	0.0000	0.4537	0.1120	-0.1401	0.0847	4.05
18.14	0.01700	197.45	0.1863	0.7396	0.2422	-0.2639	0.1284	3.05
18.10	0.01575	197.51	0.1603	0.7044	0.2299	-0.2513	0.1221	3.06
18.06	0.01422	197.70	0.1307	0.6589	0.2127	-0.2355	0.1139	3.10
18.03	0.01284	197.56	0.1071	0.6243	0.1981	-0.2227	0.1076	3.15
18.00	0.01158	198.54	0.0864	0.5907	0.1832	-0.2082	0.1018	3.22
17.97	0.01018	198.52	0.0670	0.5601	0.1694	-0.1937	0.0968	3.31
17.94	0.00817	198.82	0.0432	0.5311	0.1539	-0.1772	0.0922	3.45
17.93	0.00667	198.82	0.0289	0.5200	0.1475	-0.1695	0.0908	3.53
17.93	0.00393	198.78	0.0101	0.5145	0.1421	-0.1613	0.0909	3.62
17.93	0.00000	198.38	0.0000	0.5181	0.1380	-0.1631	0.0974	3.76
17.44	0.00000	0.00	0.0000	0.0000	0.0000	0.0000	0.0000	0.00

Wing 7 $\lambda = 1$, $\mathcal{R} = 1.24$

IDATA	IWING	IDORF	BARM	SPFHUM	ALPHA 0		
12	7	3	30.00000	0.00900	0.47000	11-FEB-83	16:39:55

ALPHA	DOTH	UTUN	CJ	CL	CD	CM	CB	L/D
-0.19	0.00000	205.42	0.0043	0.0000	0.0217	0.0126	0.0005	0.00
1.90	0.00000	206.09	0.0043	0.0692	0.0216	-0.0006	0.0216	3.21
3.94	0.00000	205.89	0.0044	0.1395	0.0233	-0.0192	0.0428	6.00
8.11	0.00000	206.51	0.0044	0.3018	0.0354	-0.0714	0.0915	8.53
10.18	0.00000	206.78	0.0044	0.3931	0.0471	-0.1008	0.1195	8.34
12.42	0.00000	205.89	0.0044	0.4950	0.0665	-0.1359	0.1510	7.44
14.51	0.00000	206.90	0.0044	0.5982	0.0913	-0.1719	0.1835	6.55
16.55	0.00000	208.25	0.0044	0.7009	0.1205	-0.2095	0.2169	5.82
-0.17	0.00464	203.46	0.0236	0.0096	0.0162	0.0156	-0.0008	0.59
-0.18	0.00398	203.81	0.0164	0.0033	0.0190	0.0185	0.0001	0.17
-0.18	0.00295	204.50	0.0071	0.0001	0.0197	0.0189	0.0003	0.01
-0.18	0.00231	204.90	0.0027	-0.0041	0.0204	0.0203	0.0006	-0.20
-0.16	0.00548	203.70	0.0352	0.0190	0.0133	0.0175	-0.0003	1.43
-0.16	0.00612	203.16	0.0451	0.0258	0.0109	0.0172	-0.0004	2.36
-0.15	0.00668	202.25	0.0552	0.0307	0.0097	0.0185	-0.0009	3.16
-0.15	0.00700	202.85	0.0607	0.0336	0.0088	0.0190	-0.0011	3.80
-0.14	0.00743	202.78	0.0691	0.0378	0.0070	0.0198	-0.0016	5.42
-0.14	0.00775	202.54	0.0758	0.0403	0.0066	0.0211	-0.0021	6.10
1.99	0.00771	206.27	0.0727	0.1519	0.0091	-0.0135	0.0327	16.62
1.98	0.00693	206.27	0.0581	0.1416	0.0123	-0.0123	0.0327	11.54
1.97	0.00634	205.78	0.0482	0.1350	0.0132	-0.0112	0.0328	10.21
1.97	0.00578	204.70	0.0398	0.1288	0.0151	-0.0103	0.0329	8.53
1.95	0.00486	204.87	0.0269	0.1158	0.0173	-0.0077	0.0323	6.71
1.94	0.00425	204.82	0.0196	0.1033	0.0190	-0.0042	0.0304	5.45
1.93	0.00359	205.10	0.0127	0.0920	0.0197	0.0003	0.0277	4.67
1.92	0.00286	205.00	0.0065	0.0795	0.0201	0.0044	0.0245	3.95
1.91	0.00237	205.57	0.0031	0.0695	0.0204	0.0072	0.0225	3.41
1.91	0.00000	205.75	0.0046	0.0675	0.0183	0.0065	0.0242	3.69
12.47	0.00759	206.93	0.0694	0.5955	0.0838	-0.1604	0.1667	7.11
12.44	0.00674	206.93	0.0541	0.5672	0.0798	-0.1528	0.1606	7.11
12.43	0.00627	206.83	0.0465	0.5567	0.0794	-0.1512	0.1589	7.01
12.40	0.00549	206.68	0.0348	0.5325	0.0759	-0.1437	0.1535	7.02
12.38	0.00473	206.59	0.0247	0.5063	0.0714	-0.1373	0.1477	7.09
12.37	0.00408	204.84	0.0176	0.4940	0.0684	-0.1345	0.1459	7.22
12.37	0.00304	204.80	0.0079	0.4955	0.0650	-0.1389	0.1482	7.62
12.37	0.00260	204.66	0.0046	0.5000	0.0651	-0.1413	0.1512	7.68
12.37	0.00228	204.95	0.0026	0.4988	0.0640	-0.1419	0.1519	7.79
12.37	0.00000	206.49	0.0046	0.4989	0.0651	-0.1441	0.1557	7.67
11.88	0.00000	0.00	0.0000	0.0000	0.0000	0.0000	0.0000	0.00

IDATA	IWING	IDORF	BARM	SPFHUM	ALPHA 0		
15	7	3	29.98000	0.00900	0.47000	11-FEB-83	16:45:56

ALPHA	DOTH	UTUN	CJ	CL	CD	CM	CB	L/D
-0.19	0.00000	0.00	0.0000	0.0000	0.0000	0.0000	0.0000	0.00
-0.16	0.01146	203.24	0.1621	0.0277	0.0286	0.0187	0.0057	0.97
-0.16	0.01051	204.38	0.1349	0.0306	0.0294	0.0245	0.0071	1.04
-0.17	0.00932	204.52	0.1056	0.0208	0.0305	0.0241	0.0051	0.68
-0.17	0.00802	204.45	0.0775	0.0243	0.0303	0.0160	0.0078	0.80
-0.17	0.00663	204.70	0.0518	0.0193	0.0301	0.0107	0.0076	0.64
-0.18	0.00456	206.71	0.0220	0.0088	0.0309	0.0093	0.0052	0.28
0.00	0.00000	207.55	0.0043	0.0146	0.0280	0.0072	0.0062	0.52
1.43	0.01227	208.77	0.1827	0.1823	0.0294	-0.0049	0.0534	6.21
1.41	0.01142	208.99	0.1579	0.1642	0.0309	-0.0017	0.0484	5.32
1.39	0.01045	209.30	0.1316	0.1426	0.0312	0.0003	0.0427	4.57
1.42	0.00936	209.34	0.1052	0.1249	0.0320	-0.0031	0.0386	3.91
1.43	0.00799	209.14	0.0761	0.1085	0.0313	-0.0072	0.0350	3.46
1.43	0.00661	209.21	0.0508	0.1009	0.0315	-0.0112	0.0344	3.21

ALPHA	DOTM	UTUN	CJ	CL	CD	CM	CB	L/D
1.44	0.00464	207.49	0.0234	0.0876	0.0323	-0.0101	0.0313	2.71
1.43	0.00000	208.66	0.0044	0.0630	0.0288	0.0004	0.0229	2.19
3.44	0.01241	210.14	0.1887	0.2988	0.0393	-0.0352	0.0897	7.59
3.44	0.01131	210.38	0.1565	0.2757	0.0389	-0.0345	0.0836	7.08
3.45	0.01034	210.35	0.1306	0.2534	0.0387	-0.0344	0.0777	6.54
3.46	0.00929	210.22	0.1049	0.2340	0.0390	-0.0332	0.0726	6.00
3.46	0.00804	210.17	0.0779	0.2139	0.0385	-0.0315	0.0675	5.55
3.45	0.00655	209.83	0.0506	0.1895	0.0378	-0.0290	0.0612	5.02
3.46	0.00452	207.63	0.0224	0.1703	0.0373	-0.0268	0.0564	4.57
3.45	0.00000	209.74	0.0045	0.1384	0.0298	-0.0117	0.0448	4.65
5.57	0.01111	198.28	0.1683	0.3919	0.0491	-0.0646	0.1173	7.99
5.57	0.01031	198.57	0.1442	0.3665	0.0492	-0.0632	0.1107	7.45
5.56	0.00928	198.53	0.1163	0.3372	0.0482	-0.0625	0.1030	7.00
5.56	0.00807	198.57	0.0870	0.3080	0.0477	-0.0618	0.0953	6.45
5.55	0.00655	198.73	0.0559	0.2738	0.0465	-0.0595	0.0862	5.88
5.53	0.00454	196.31	0.0251	0.2421	0.0430	-0.0547	0.0775	5.63
5.53	0.00000	198.11	0.0050	0.2139	0.0340	-0.0430	0.0686	6.29

IDATA IWING IDORF BARM SPFHUM ALPHA 0
14   7   3   29.98000   0.00900   0.47000   11-FEB-83   16:43:12

ALPHA	DOTM	UTUN	CJ	CL	CD	CM	CB	L/D
8.88	0.00000	0.00	0.0000	0.0000	0.0000	0.0000	0.0000	0.00
5.65	0.01171	209.18	0.1591	0.3661	0.0434	-0.0664	0.1072	8.44
5.64	0.01067	209.25	0.1324	0.3431	0.0437	-0.0583	0.1004	7.85
5.63	0.00948	209.19	0.1045	0.3165	0.0428	-0.0555	0.0932	7.40
5.61	0.00814	209.76	0.0762	0.2897	0.0419	-0.0534	0.0862	6.91
5.60	0.00670	209.43	0.0508	0.2628	0.04?0	-0.0537	0.0792	6.57
5.59	0.00470	207.01	0.0236	0.2345	0.0363	-0.0511	0.0713	6.46
5.58	0.00000	209.04	0.0043	0.2105	0.0287	-0.0407	0.0637	7.34
7.50	0.01158	210.31	0.1605	0.4594	0.0582	-0.0834	0.1360	7.89
7.48	0.01064	210.65	0.1349	0.4300	0.0567	-0.0806	0.1276	7.58
7.47	0.00945	210.82	0.1056	0.3971	0.0556	-0.0783	0.1186	7.15
7.45	0.00813	210.83	0.0773	0.3629	0.0533	-0.0746	0.1087	6.80
7.42	0.00670	210.47	0.0515	0.3294	0.0492	-0.0711	0.0990	6.69
7.40	0.00487	206.24	0.0264	0.2928	0.0447	-0.0649	0.0884	6.54
7.41	0.00000	209.89	0.0044	0.2815	0.0363	-0.0580	0.0859	7.76
9.58	0.01159	211.17	0.1620	0.5661	0.0775	-0.1196	0.1700	7.30
9.56	0.01058	211.30	0.1345	0.5311	0.0755	-0.1148	0.1598	7.04
9.54	0.00943	211.34	0.1062	0.4932	0.0726	-0.1119	0.1491	6.80
9.52	0.00815	211.18	0.0788	0.4530	0.0693	-0.1039	0.1369	6.53
9.48	0.00655	210.58	0.0498	0.4085	0.0636	-0.0960	0.1234	6.43
9.46	0.00493	207.18	0.0274	0.3682	0.0568	-0.0909	0.1114	6.49
9.48	0.00000	210.67	0.0044	0.3734	0.0465	-0.0875	0.1135	8.04

IDATA IWING IDORF BARM SPFHUM ALPHA 0
16   7   3   29.98000   0.00900   0.47000   11-FEB-83   16:48:04

ALPHA	DOTM	UTUN	CJ	CL	CD	CM	CB	L/D
11.10	0.00000	0.00	0.0000	0.0000	0.0000	0.0000	0.0000	0.00
11.79	0.01136	197.59	0.1738	0.7061	0.1015	-0.1758	0.2111	6.95
11.78	0.01038	197.71	0.1447	0.6629	0.0991	-0.1697	0.1984	6.69
11.76	0.00935	197.43	0.1173	0.6216	0.0969	-0.1631	0.1860	6.41
11.75	0.00819	197.10	0.0895	0.5783	0.0912	-0.1497	0.1721	6.34
11.72	0.00659	196.90	0.0566	0.5210	0.0834	-0.1453	0.1552	6.24
11.70	0.00491	196.79	0.0295	0.4828	0.0760	-0.1332	0.1428	6.35
11.73	0.00000	196.05	0.0050	0.4786	0.0633	-0.1359	0.1434	7.56
13.93	0.01203	198.65	0.1972	0.8524	0.1377	-0.2263	0.2594	6.19
13.89	0.01135	198.68	0.1753	0.8170	0.1341	-0.2162	0.2481	6.09
13.85	0.01043	198.53	0.1478	0.7726	0.1299	-0.2075	0.2348	5.95
13.83	0.00940	198.22	0.1197	0.7258	0.1247	-0.1997	0.2205	5.82
13.81	0.00819	198.24	0.0899	0.6768	0.1186	-0.1862	0.2050	5.71
13.78	0.00660	197.66	0.0572	0.6234	0.1096	-0.1730	0.1875	5.69
13.77	0.00475	197.30	0.0276	0.5813	0.0994	-0.1643	0.1745	5.85

13.77	0.00000	196.25	0.0050	0.5772	0.0858	-0.1629	0.1741	6.73
16.05	0.01208	199.03	0.1998	0.9558	0.1710	-0.2597	0.2935	5.59
16.01	0.01127	198.93	0.1740	0.9155	0.1672	-0.2554	0.2818	5.47
15.98	0.01033	198.80	0.1458	0.8734	0.1625	-0.2428	0.2682	5.37
15.97	0.00932	198.27	0.1188	0.8314	0.1576	-0.2294	0.2546	5.28
15.94	0.00813	198.07	0.0896	0.7808	0.1502	-0.2252	0.2399	5.20
15.93	0.00660	197.55	0.0578	0.7332	0.1402	-0.2098	0.2233	5.23
15.90	0.00475	197.14	0.0279	0.6858	0.1257	-0.2007	0.2083	5.45
15.93	0.00000	197.17	0.0050	0.6846	0.1155	-0.1983	0.2089	5.93
15.26	0.00000	0.00	0.0000	0.0000	0.0000	0.0000	0.0000	0.00

Wing 8 $\lambda = 1$, $\mathit{R} = 2$

IDATA	IWING	IDORF	BARM	SPFHUM	ALPHA 0		
34	8	3	30.00000	0.01000	0.54000	11-FEB-83	16:30:26

ALPHA	DOTM	UTUN	CJ	CL	CD	CM	CB	L/D
1.06	0.00701	191.49	0.0967	0.0600	0.0148	0.0056	0.0088	4.05
1.07	0.00770	191.71	0.1147	0.0697	0.0118	0.0152	0.0122	5.93
1.06	0.00667	191.59	0.0885	0.0584	0.0150	0.0118	0.0108	3.90
1.06	0.00644	191.45	0.0834	0.0581	0.0161	0.0090	0.0105	3.60
1.06	0.00552	190.79	0.0642	0.0575	0.0180	0.0024	0.0129	3.20
1.06	0.00434	190.62	0.0433	0.0598	0.0205	-0.0088	0.0159	2.92
1.06	0.00363	190.72	0.0331	0.0592	0.0207	-0.0167	0.0156	2.86
1.06	0.00284	191.66	0.0235	0.0608	0.0207	-0.0205	0.0176	2.94
1.05	0.00000	192.52	0.0089	0.0542	0.0191	-0.0165	0.0152	2.84
1.09	0.00768	192.04	0.1154	0.0684	0.0128	0.0219	0.0126	5.35
1.08	0.00644	191.99	0.0840	0.0567	0.0166	0.0150	0.0108	3.42
1.12	0.00483	190.63	0.0521	0.0609	0.0207	-0.0051	0.0156	2.95
1.14	0.00351	191.98	0.0313	0.0619	0.0213	-0.0200	0.0170	2.91
3.18	0.00771	194.70	0.1143	0.2152	0.0168	-0.0168	0.0913	12.82
3.17	0.00647	194.20	0.0836	0.1882	0.0201	-0.0258	0.0776	9.35
3.18	0.00434	194.91	0.0422	0.1823	0.0247	-0.0552	0.0747	7.39
3.20	0.00356	195.12	0.0313	0.1869	0.0258	-0.0680	0.0774	7.24
3.22	0.00290	194.52	0.0239	0.1870	0.0240	-0.0776	0.0762	7.79
3.22	0.00000	193.28	0.0090	0.1648	0.0182	-0.0690	0.0617	9.06
5.28	0.00764	195.73	0.1124	0.3617	0.0240	-0.0587	0.1676	15.08
5.27	0.00640	196.12	0.0812	0.3283	0.0283	-0.0723	0.1471	11.59
5.27	0.00472	195.82	0.0484	0.3079	0.0319	-0.0985	0.1323	9.64
5.31	0.00472	195.96	0.0484	0.3101	0.0319	-0.0986	0.1335	9.73
5.29	0.00356	195.20	0.0317	0.2976	0.0316	-0.1112	0.1240	9.43
5.30	0.00294	194.94	0.0244	0.2919	0.0293	-0.1183	0.1176	9.94
5.31	0.00000	192.69	0.0091	0.2745	0.0214	-0.1137	0.1050	12.80
7.36	0.00769	195.49	0.1151	0.5065	0.0369	-0.0922	0.2408	13.72
7.32	0.00641	195.67	0.0825	0.4676	0.0409	-0.1179	0.2124	11.43
7.28	0.00483	195.64	0.0507	0.4291	0.0416	-0.1393	0.1842	10.31
7.27	0.00356	194.76	0.0320	0.4054	0.0383	-0.1469	0.1670	10.57
7.31	0.00356	194.81	0.0319	0.4071	0.0385	-0.1459	0.1678	10.57
7.31	0.00281	195.12	0.0233	0.3898	0.0346	-0.1447	0.1560	11.26
7.34	0.00000	192.16	0.0092	0.3842	0.0266	-0.1339	0.1527	14.46
9.28	0.00772	196.00	0.1160	0.6418	0.0523	-0.1368	0.3056	12.27
9.27	0.00642	196.02	0.0830	0.5948	0.0560	-0.1600	0.2712	10.62
9.24	0.00485	195.47	0.0515	0.5455	0.0546	-0.1713	0.2355	9.98
9.24	0.00371	195.09	0.0340	0.5206	0.0517	-0.1819	0.2178	10.07
9.24	0.00279	195.00	0.0231	0.4917	0.0462	-0.1683	0.2007	10.64
9.28	0.00000	192.30	0.0093	0.4934	0.0399	-0.1618	0.2028	12.37
10.61	0.00000	0.00	0.0000	0.0000	0.0000	0.0000	0.0000	0.00
11.38	0.00757	195.49	0.1097	0.7874	0.0741	-0.2046	0.3744	10.63
11.36	0.00635	195.09	0.0803	0.7387	0.0743	-0.2234	0.3375	9.94
11.33	0.00487	194.18	0.0516	0.6800	0.0728	-0.2167	0.2991	9.34
11.32	0.00362	194.37	0.0324	0.6391	0.0684	-0.2071	0.2742	9.34
11.32	0.00298	194.49	0.0249	0.6197	0.0650	-0.1990	0.2622	9.54
11.35	0.00000	194.58	0.0089	0.6188	0.0578	-0.1911	0.2630	10.71
11.57	0.00765	196.14	0.1125	0.8122	0.0777	-0.2354	0.3810	10.45
13.56	0.00764	196.31	0.1125	0.9333	0.0991	-0.2618	0.4458	9.42
13.54	0.00639	194.93	0.0827	0.8831	0.1034	-0.2695	0.4093	8.54
13.53	0.00484	194.15	0.0517	0.8215	0.1032	-0.2724	0.3671	7.96
13.49	0.00366	194.26	0.0334	0.7818	0.0974	-0.2597	0.3425	8.02
13.50	0.00300	194.42	0.0254	0.7557	0.0932	-0.2491	0.3261	8.11
13.50	0.00000	195.16	0.0089	0.7510	0.0821	-0.2362	0.3252	9.15
15.38	0.00773	195.98	0.1161	1.0470	0.1253	-0.3119	0.5010	8.36
15.36	0.00643	194.86	0.0843	0.9917	0.1295	-0.3203	0.4597	7.66

56

15.34	0.00494	194.64	0.0536	0.9282	0.1267	-0.3023	0.4181	7.32
15.30	0.00374	194.33	0.0347	0.8868	0.1217	-0.2863	0.3918	7.28
15.31	0.00294	194.79	0.0248	0.8551	0.1144	-0.2724	0.3716	7.48
15.34	0.00000	194.96	0.0090	0.8535	0.1067	-0.2619	0.3728	8.00
17.59	0.00773	194.33	0.1162	1.0842	0.1764	-0.3351	0.5320	6.15
17.65	0.00632	193.47	0.0817	1.1104	0.1590	-0.3290	0.5203	6.98
17.62	0.00492	193.13	0.0534	1.0449	0.1572	-0.3160	0.4760	6.65
17.59	0.00370	193.55	0.0341	1.0017	0.1515	-0.3070	0.4469	6.61
17.60	0.00287	193.79	0.0241	0.9730	0.1451	-0.2949	0.4283	6.71
17.63	0.00000	194.29	0.0090	0.9722	0.1414	-0.2893	0.4304	6.87
19.44	0.00769	194.10	0.1172	1.1353	0.2270	-0.3623	0.5604	5.00
19.40	0.00636	193.88	0.0834	1.0888	0.2190	-0.3339	0.5236	4.97
19.36	0.00489	193.90	0.0531	1.0512	0.2123	-0.3169	0.4908	4.95
19.38	0.00374	193.66	0.0349	1.0296	0.2056	-0.3090	0.4713	5.01
19.39	0.00288	193.81	0.0244	1.0124	0.1961	-0.2985	0.4570	5.16
19.46	0.00000	194.18	0.0091	1.0584	0.1752	-0.2806	0.4779	6.04
18.43	0.00000	0.00	0.0000	0.0000	0.0000	0.0000	0.0000	0.00

Wing 10 $\lambda = 1.0$, $\mathcal{R} = 4$

IDATA	IWING	IDORF	BARM	SPFHUM	ALPHA 0		
42	10	3	30.05000	0.01100	0.34000	11-FEB-83	16:55:24

ALPHA	DOTH	UTUN	CJ	CL	CM	CB
-0.33	0.00000	0.00	0.0000	0.000	0.0000	0.0000
-0.33	0.00000	0.00	0.0000	0.000	0.0000	0.0000
-0.33	0.00000	186.95	0.0010	0.010	-0.0191	-0.0005
-0.29	0.01177	192.56	0.1442	0.010	-0.0360	0.0371
-0.26	0.01362	193.19	0.1920	0.010	-0.0469	0.0555
-0.29	0.01178	193.49	0.1448	0.010	-0.0350	0.0390
-0.31	0.00939	193.44	0.0929	0.010	-0.0243	0.0218
-0.32	0.00708	194.03	0.0533	0.010	-0.0168	0.0113
-0.33	0.00504	194.48	0.0276	0.010	-0.0127	0.0063
-0.34	0.00000	192.88	0.0010	0.010	-0.0046	0.0034
2.34	0.00000	0.00	0.0000	0.000	0.0000	0.0000
9.55	0.00000	189.81	0.0010	0.634	-0.1594	0.5983
9.89	0.01362	191.72	0.1971	0.914	-0.3446	0.8009
9.85	0.01187	192.53	0.1497	0.888	-0.3061	0.7849
9.78	0.00944	192.61	0.0956	0.842	-0.2643	0.7659
9.71	0.00710	192.30	0.0550	0.783	-0.2295	0.7461
9.65	0.00503	190.38	0.0289	0.736	-0.2120	0.6965
9.57	0.00000	191.60	0.0010	0.655	-0.1783	0.6039

IDATA	IWING	IDORF	BARM	SPFHUM	ALPHA O		
43	10	3	30.05000	0.01100	0.34000	11-FEB-83	16:57:25

ALPHA	DOTM	UTUN	CJ	CL	CM	CB
10.81	0.00000	0.00	0.0000	0.000	0.0000	0.0000
11.86	0.01280	190.27	0.1758	1.021	-0.3197	0.8333
11.87	0.01362	190.31	0.1997	1.018	-0.3361	0.8386
11.85	0.01179	191.09	0.1496	1.022	-0.3011	0.8306
11.80	0.00945	191.22	0.0969	0.989	-0.2669	0.8157
11.74	0.00712	190.30	0.0565	0.942	-0.2361	0.8029
11.68	0.00506	189.05	0.0297	0.896	-0.2121	0.7935
11.60	0.00000	190.12	0.0010	0.821	-0.1737	0.7413
13.90	0.01350	189.89	0.1999	1.102	-0.3499	0.8758
13.86	0.01179	190.69	0.1520	1.086	-0.3162	0.8606
13.82	0.00946	191.17	0.0983	1.066	-0.2793	0.8464
13.77	0.00712	190.56	0.0568	1.037	-0.2462	0.8368
13.72	0.00499	189.71	0.0289	0.989	-0.2221	0.8244
13.64	0.00000	190.64	0.0010	0.914	-0.1824	0.7960
15.93	0.01354	190.13	0.2020	1.189	-0.3654	0.9075
15.89	0.01181	191.09	0.1531	1.175	-0.3332	0.8917
15.84	0.00936	191.18	0.0971	1.143	-0.2951	0.8755
15.79	0.00713	190.68	0.0574	1.110	-0.2628	0.8635
15.66	0.00000	190.65	0.0010	0.997	-0.1938	0.8249
19.27	0.01355	190.08	0.2036	1.264	-0.4011	0.9371
19.23	0.01177	190.84	0.1533	1.243	-0.3716	0.9198
19.13	0.00944	190.76	0.0997	1.161	-0.3226	0.8874
19.09	0.00713	189.79	0.0582	1.135	-0.2937	0.8803
19.05	0.00495	189.33	0.0289	1.102	-0.2714	0.8701
19.00	0.00000	190.77	0.0010	1.064	-0.2314	0.8499
-0.56	0.00000	0.00	0.0000	0.0	0.0000	0.0000
1.91	0.01345	191.74	0.1946	0.193	-0.0843	0.2782
1.88	0.01170	192.20	0.1478	0.183	-0.0599	0.2502
1.84	0.00931	191.80	0.0948	0.167	-0.0348	0.2153
1.81	0.00710	190.21	0.0568	0.147	-0.0167	0.1805
1.78	0.00505	189.53	0.0297	0.132	-0.0045	0.1549
1.75	0.00000	190.80	0.0010	0.108	0.0143	0.1191
3.89	0.01349	192.24	0.1977	0.362	-0.1530	0.4618
3.85	0.01172	191.94	0.1504	0.346	-0.1221	0.4241
3.81	0.00942	190.60	0.0995	0.324	-0.0914	0.3798
3.76	0.00707	189.84	0.0574	0.291	-0.0658	0.3284
3.73	0.00506	189.78	0.0301	0.265	-0.0490	0.2887
3.68	0.00000	191.14	0.0010	0.227	-0.0201	0.2330
5.90	0.01345	191.88	0.1989	0.551	-0.2422	0.6347
5.85	0.01169	191.36	0.1519	0.529	-0.2057	0.5885
5.80	0.00940	192.52	0.0979	0.495	-0.1686	0.5305
5.74	0.00707	192.17	0.0564	0.451	-0.1373	0.4697
5.70	0.00516	191.25	0.0310	0.418	-0.1141	0.4246
5.64	0.00000	191.88	0.0010	0.359	-0.0682	0.3507
7.88	0.01351	192.10	0.2012	0.752	-0.2900	0.7601
7.82	0.01173	192.97	0.1511	0.718	-0.2449	0.7402
7.75	0.00937	193.50	0.0968	0.672	-0.1993	0.6915
7.69	0.00707	192.83	0.0563	0.622	-0.1694	0.6210
7.64	0.00494	191.17	0.0286	0.581	-0.1515	0.5614
7.56	0.00000	191.66	0.0010	0.507	-0.1081	0.4793
7.07	0.00000	0.00	0.0000	0.0	0.0000	0.0000
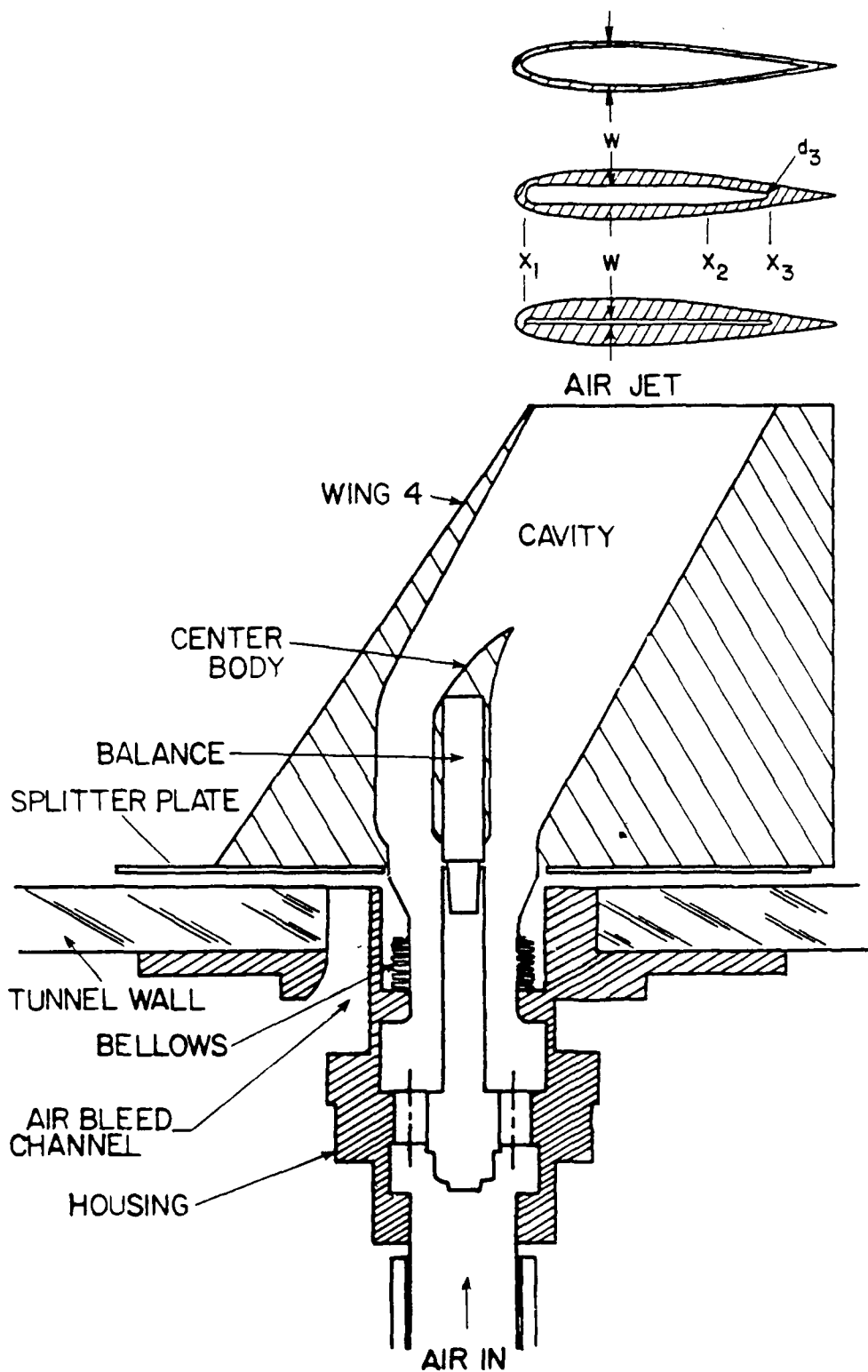
Figure 1.- Longitudinal sectional view of wing model installation.
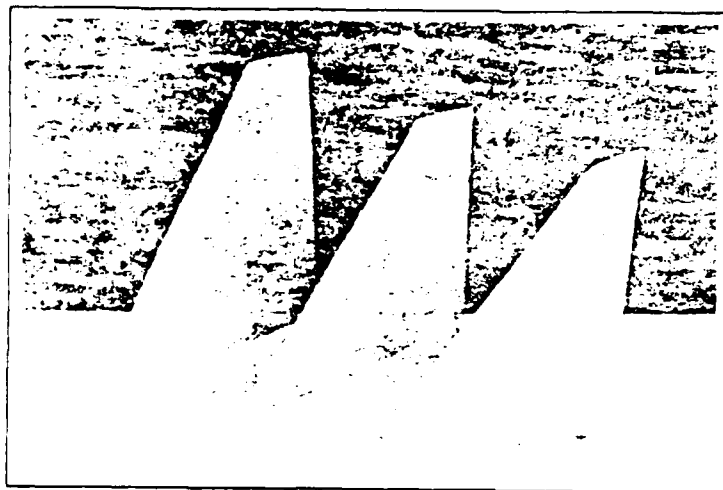
a. Wings 1, 2, and 5
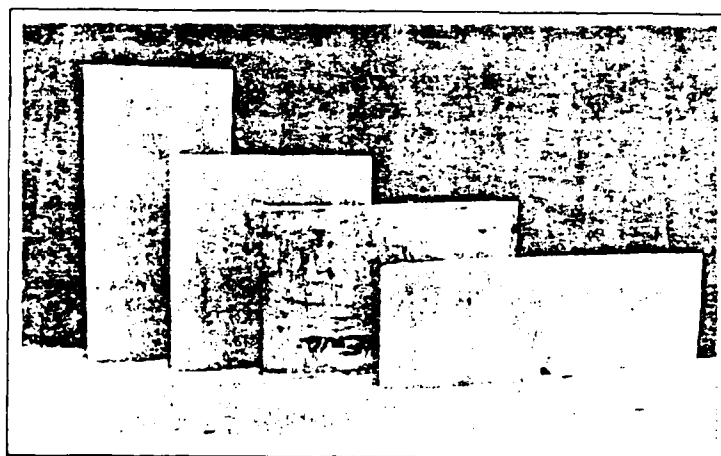
b. Wings 10, 8, 7 (mold), and 6
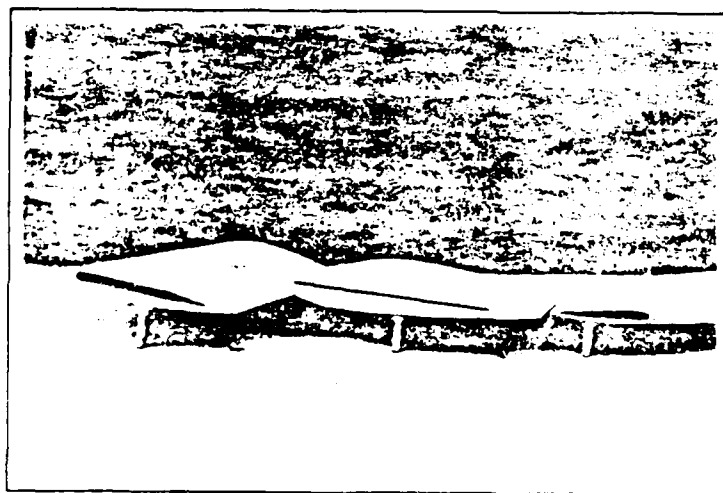
c. End view of wings 10, 7, and 1

Figure 2.- Semispan wing models.

60
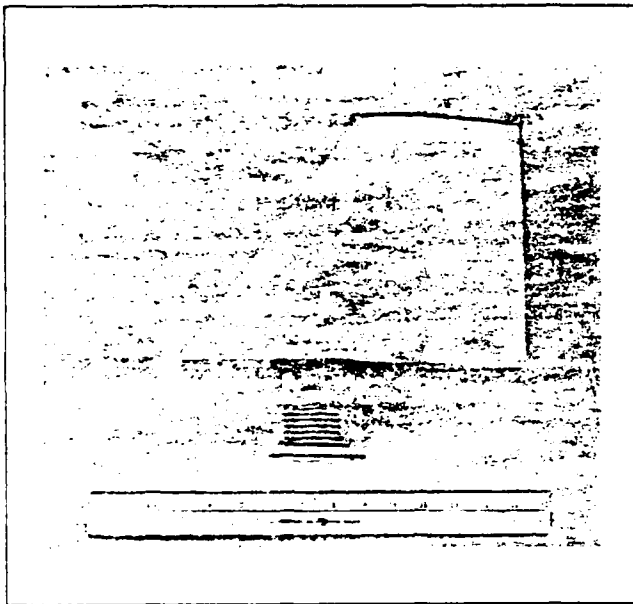
Figure 3.- Wing 4 with
bellows attached.
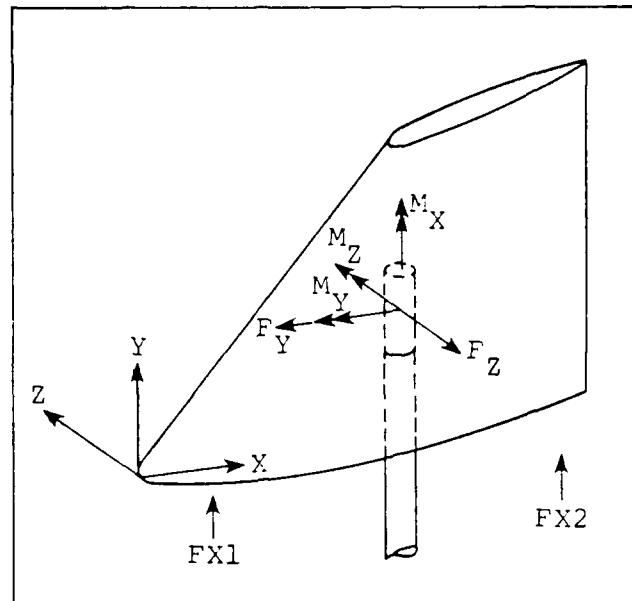
Figure 4.- Wing coordinates and
balance force and
moment system.
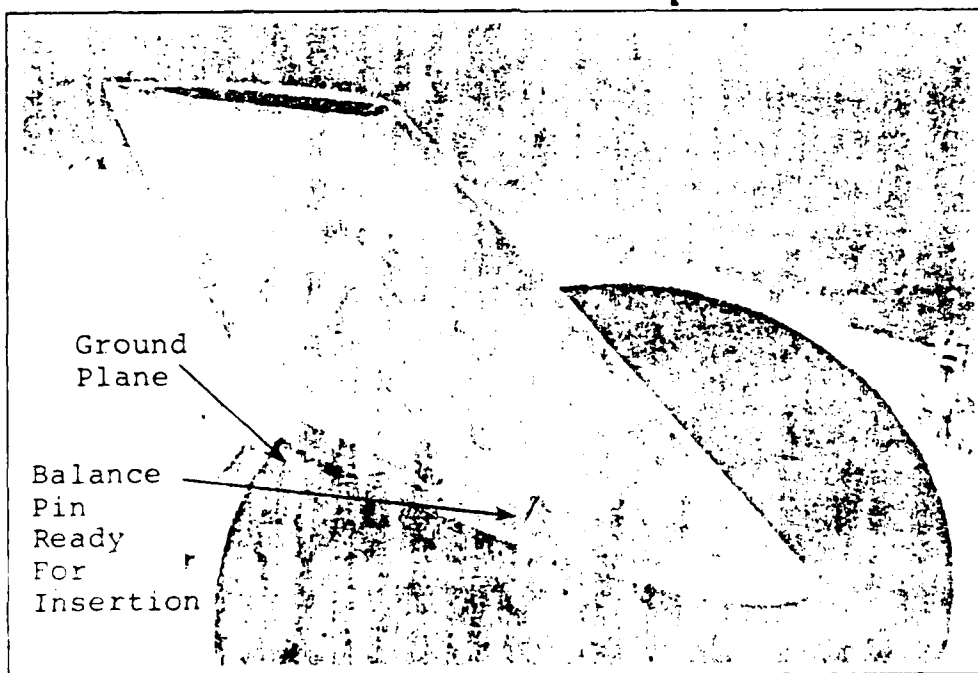
Figure 5.- Wing 4 mounted in the wind tunnel.

61
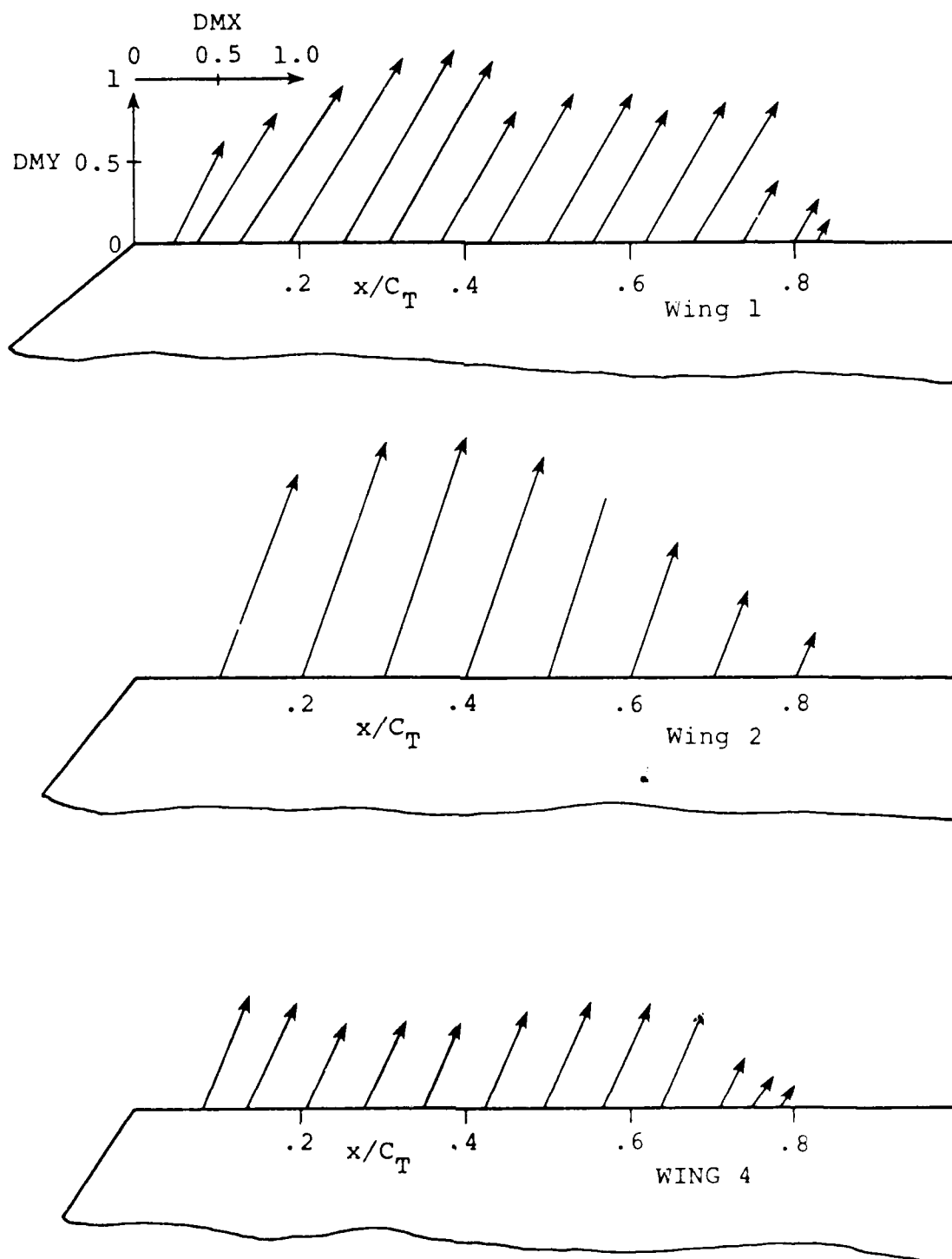
Figure 6.- Tip blowing momentum vectors.
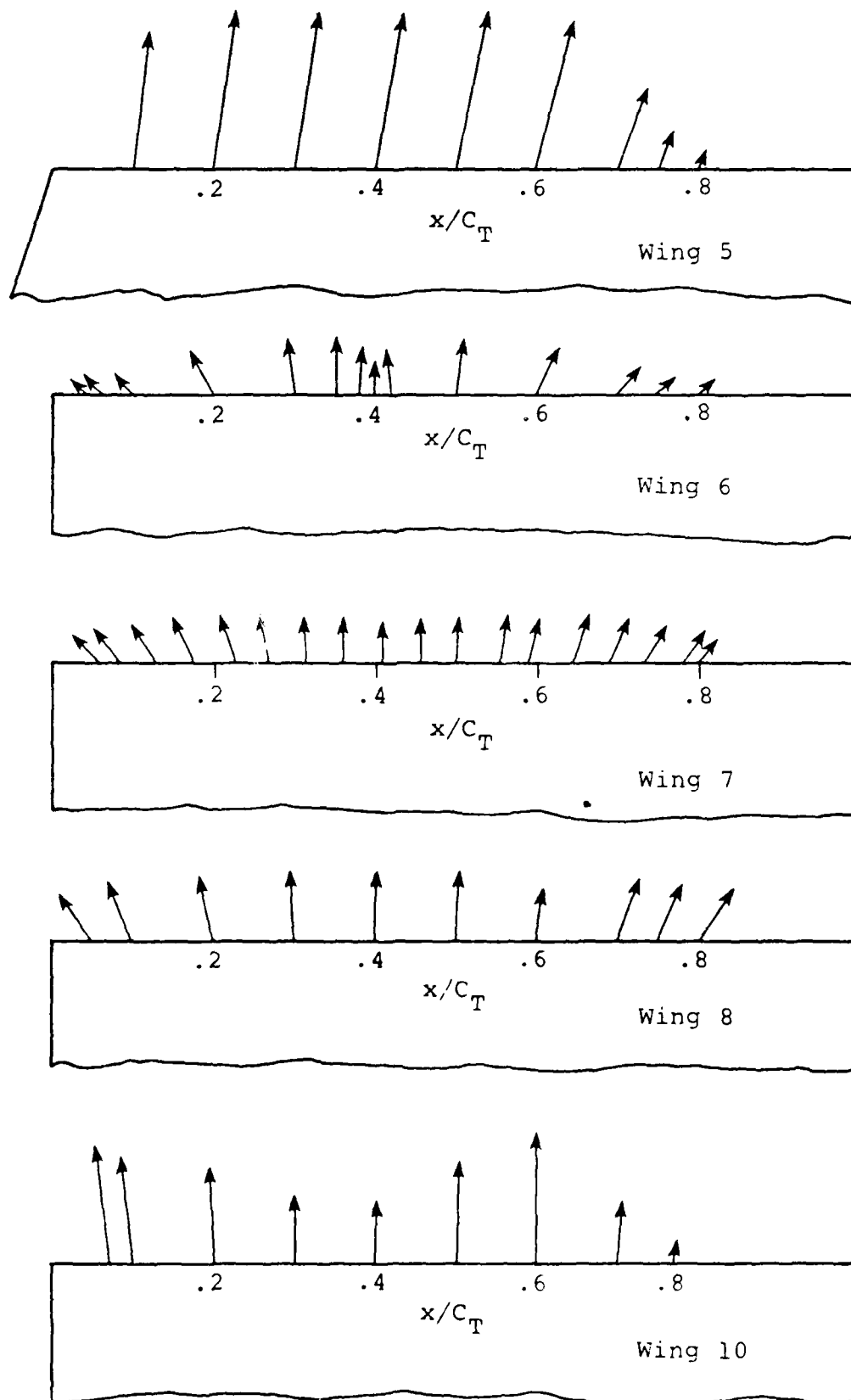
Figure 6.- Concluded.
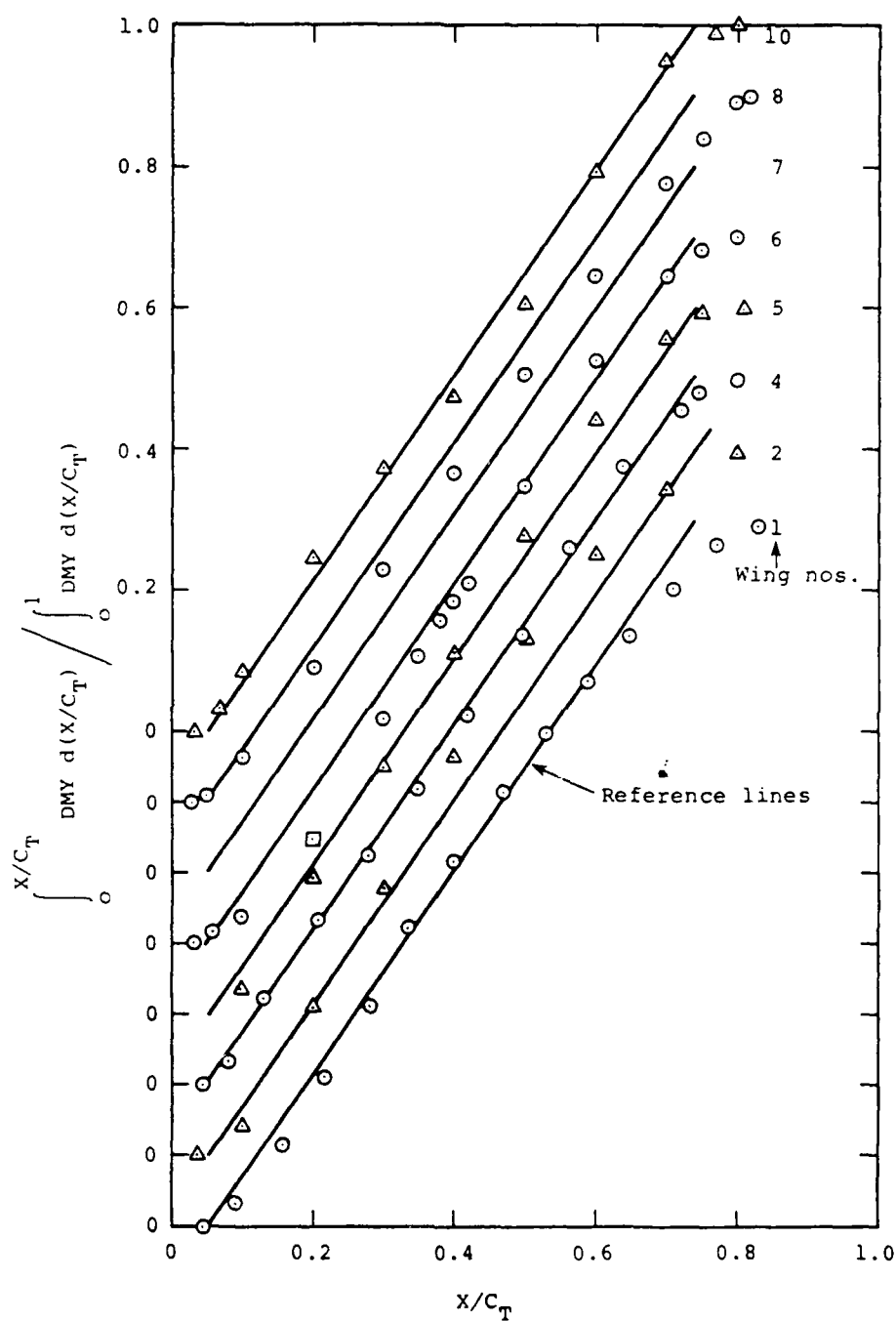
Figure 7.- Comparison of jet Y-momentum distribution along the wing tips.

64
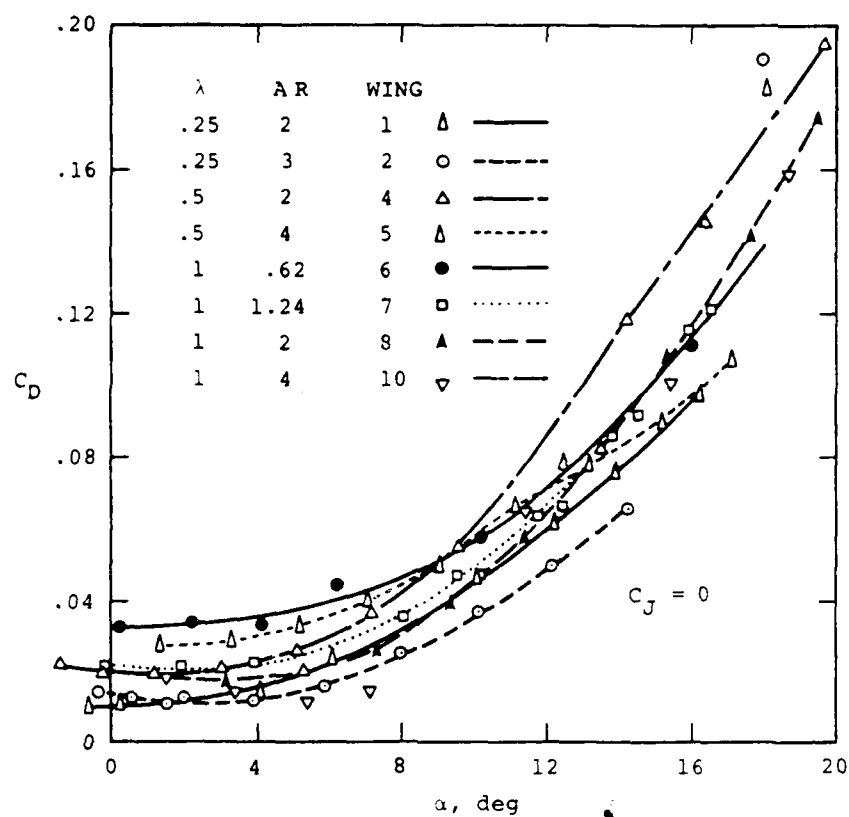
Figure 8.- Drag coefficients versus angle of attack, no blowing.
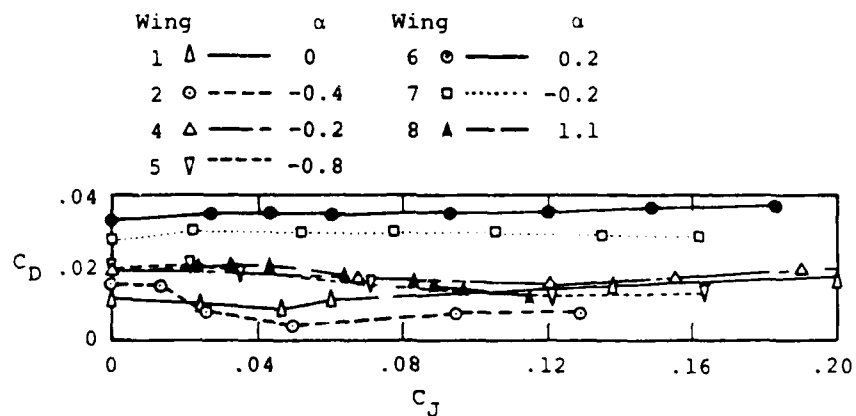
Figure 9.- Drag coefficients near zero angle of attack
versus jet momentum coefficient.
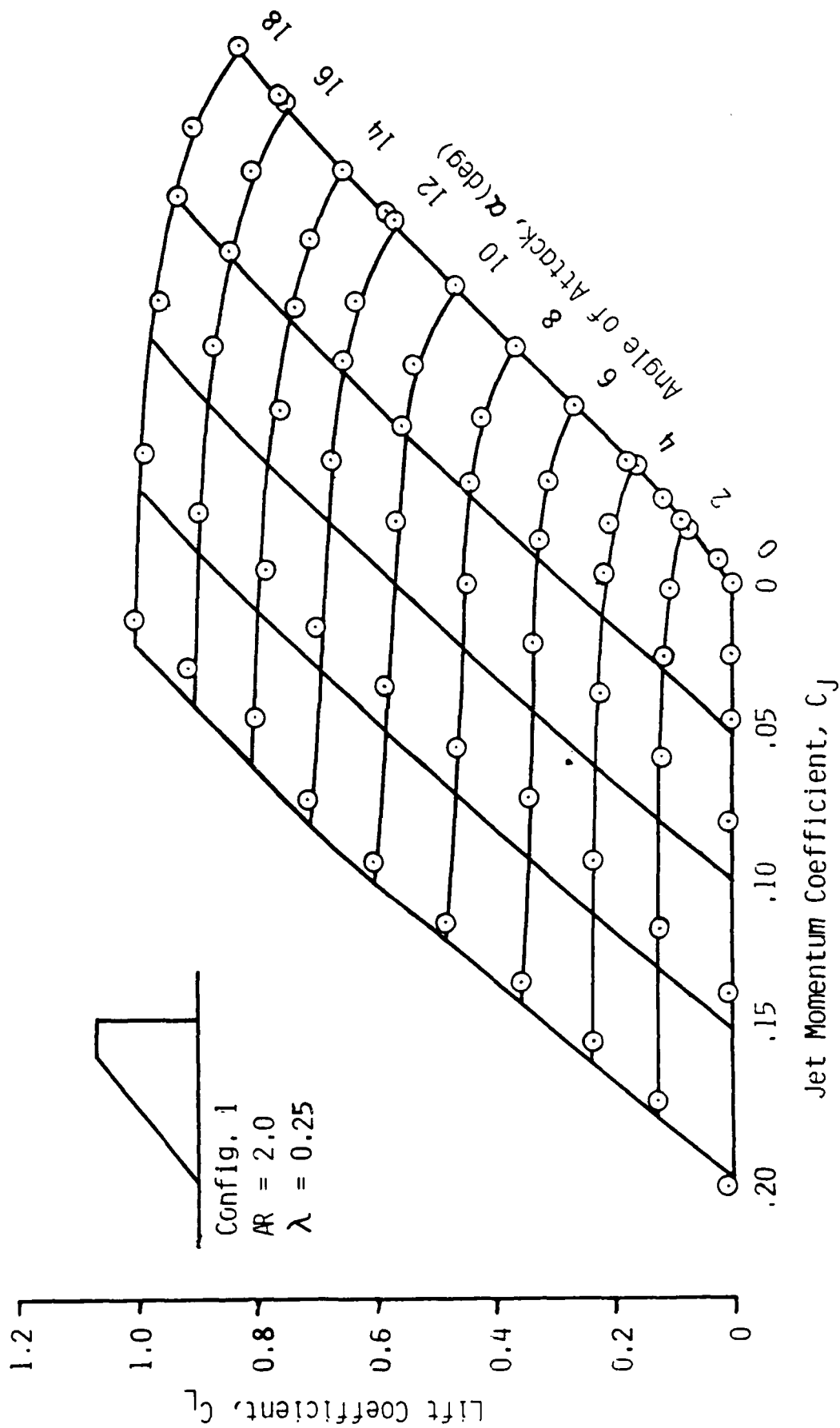
Figure 10.- Effect of wing-tip blowing and angle of attack upon lift coefficient, Wing 1.

66
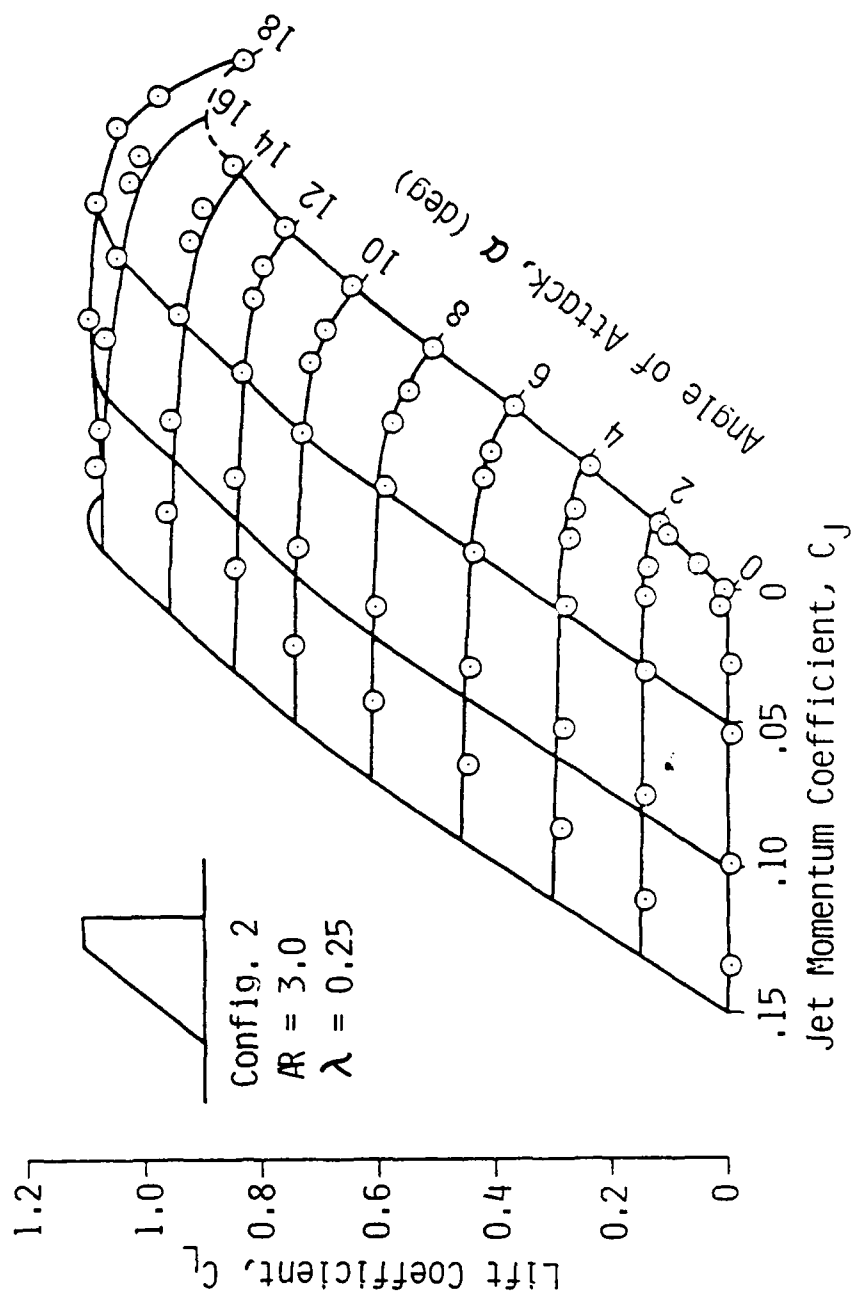
Figure 10.- Continued, Wing 2.

67
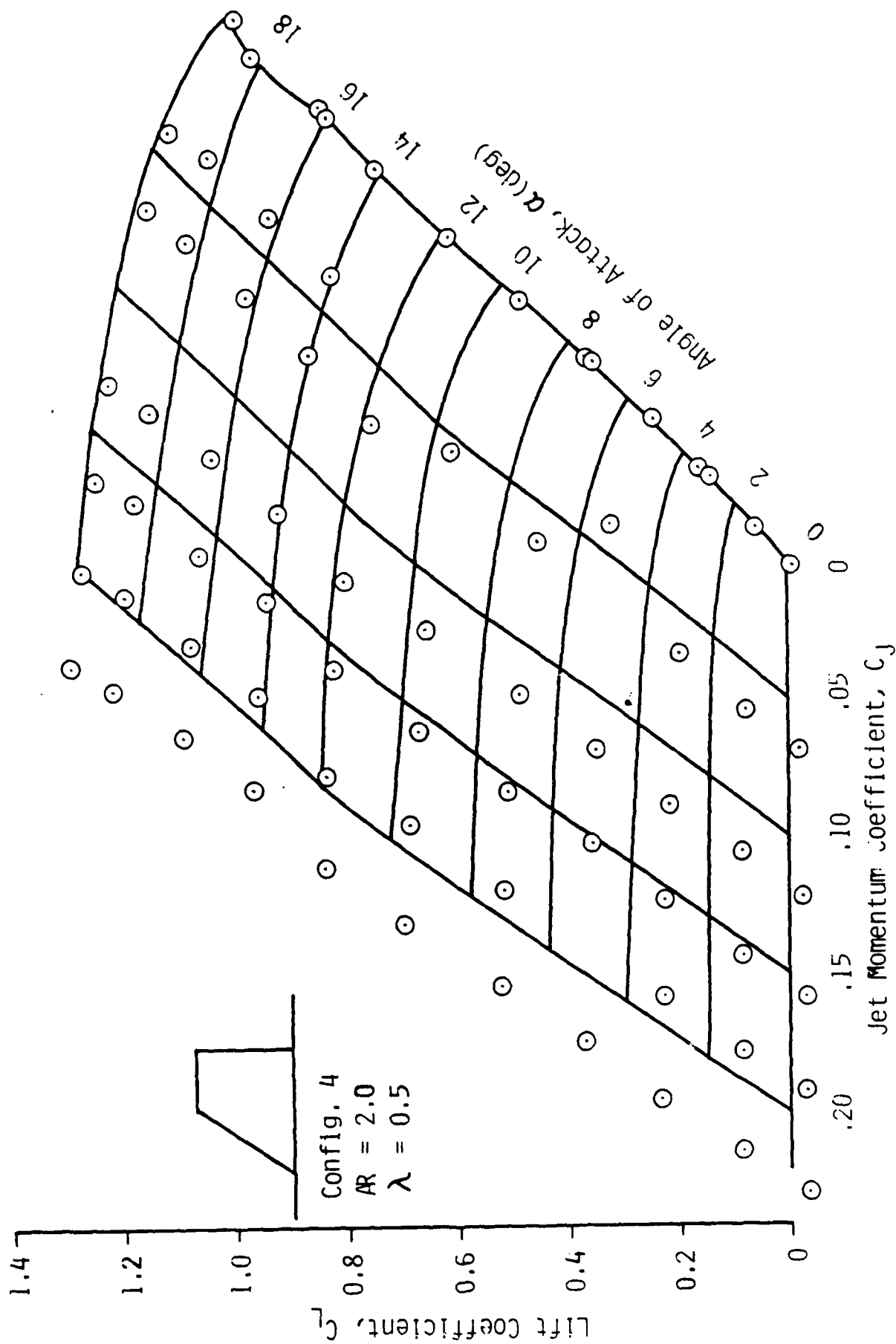
Figure 10.- Continued, Wing 4.

68
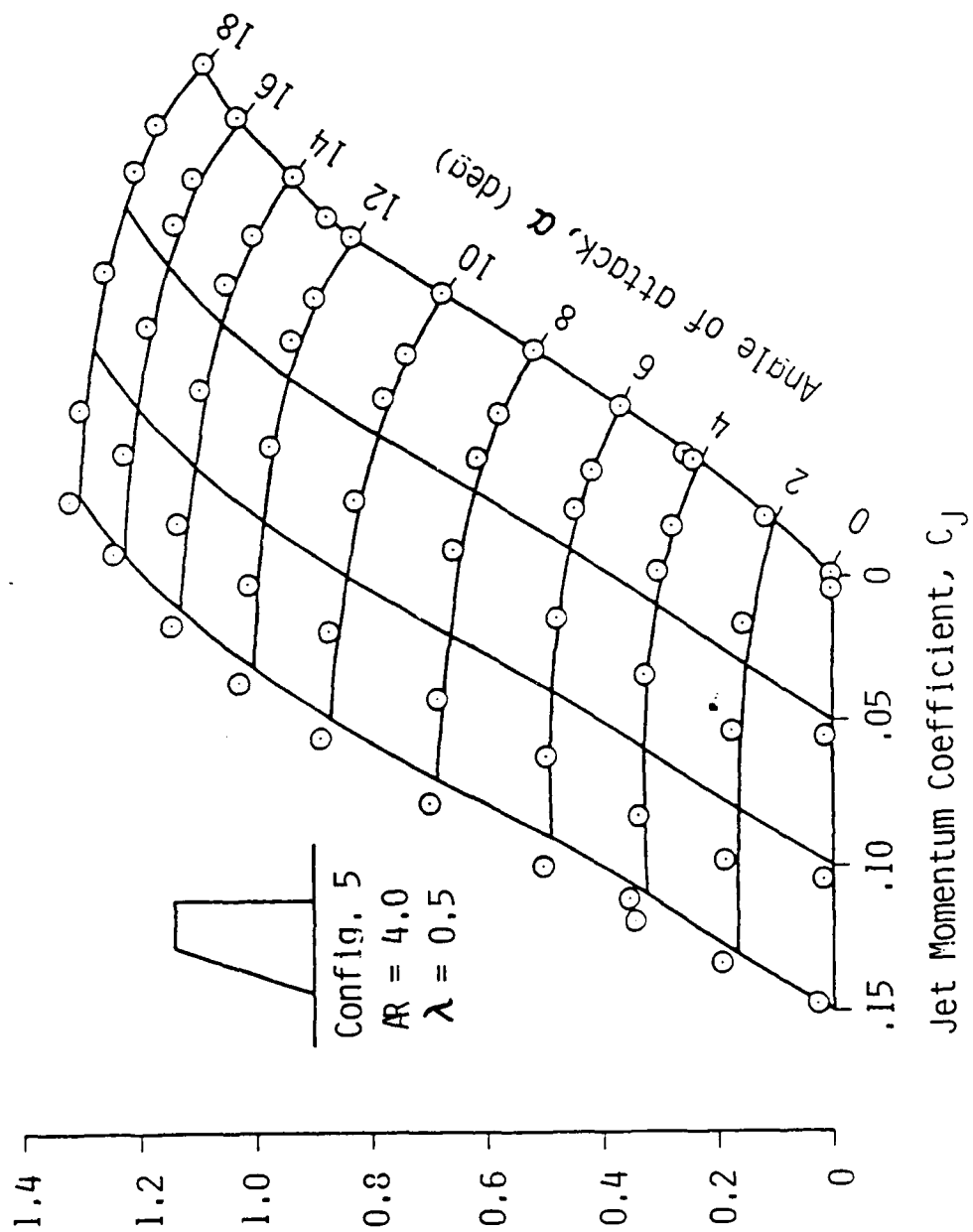
Figure 10.- Continued, Wing 5

69
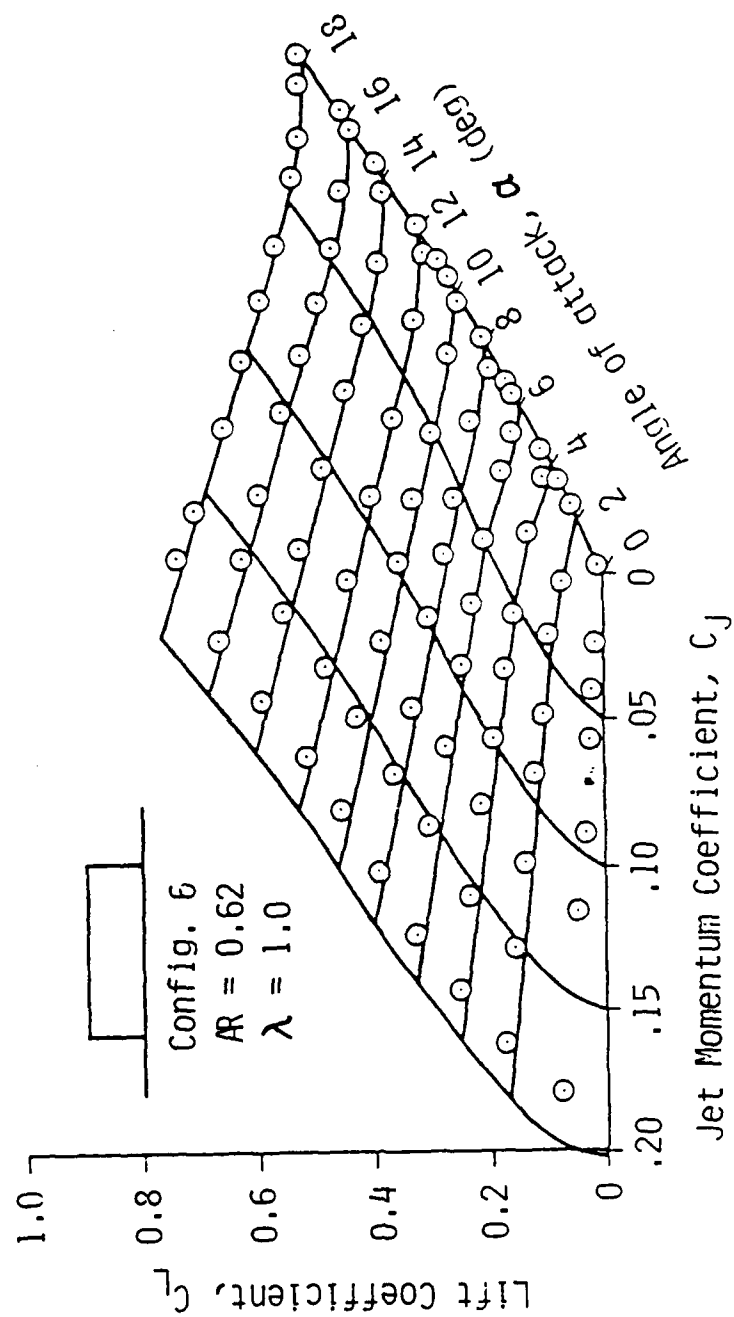
Figure 10.- Continued, Wing 6.

70
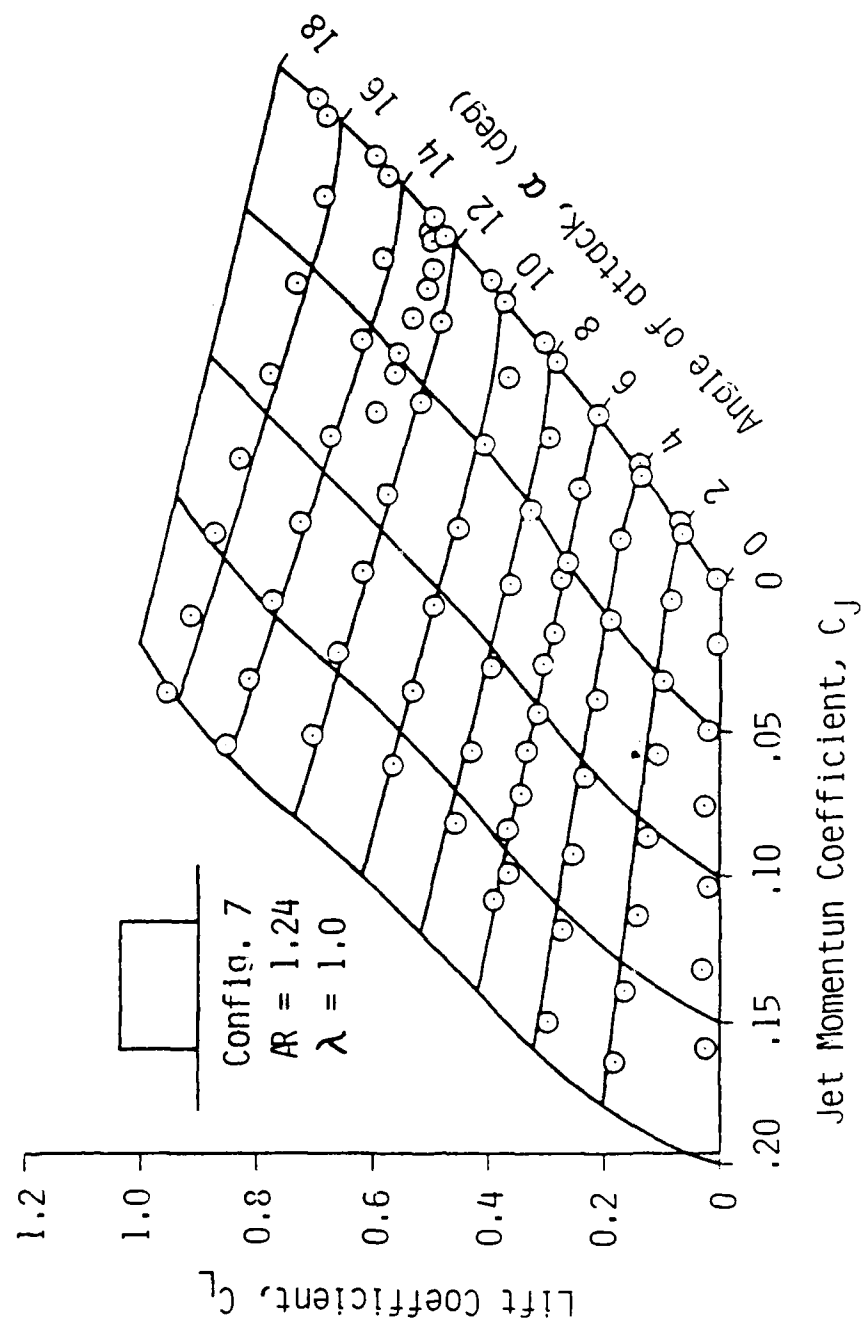
Figure 10.- Continued, Wing 7
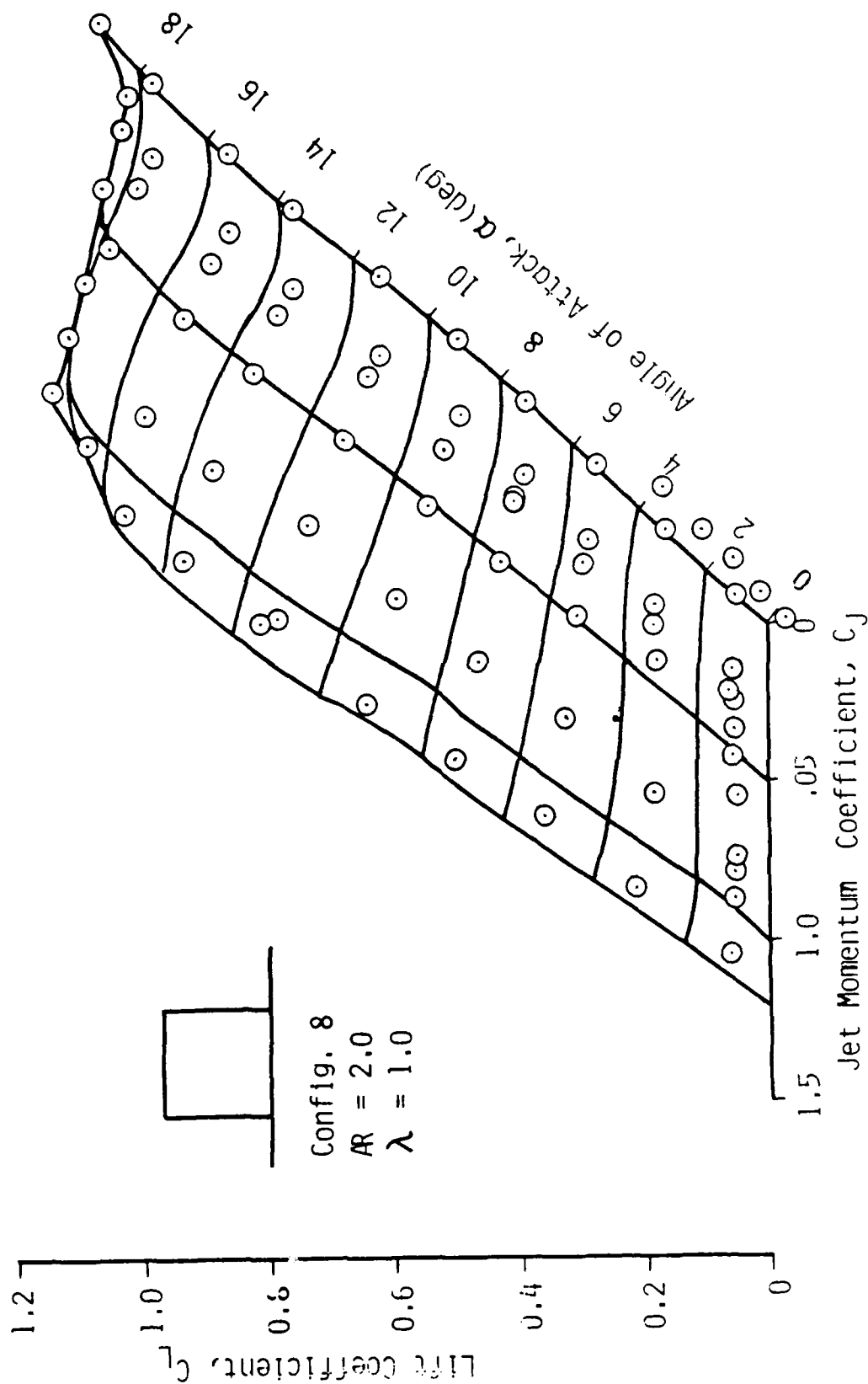
Figure 10.- Continued, Wing 8.

72
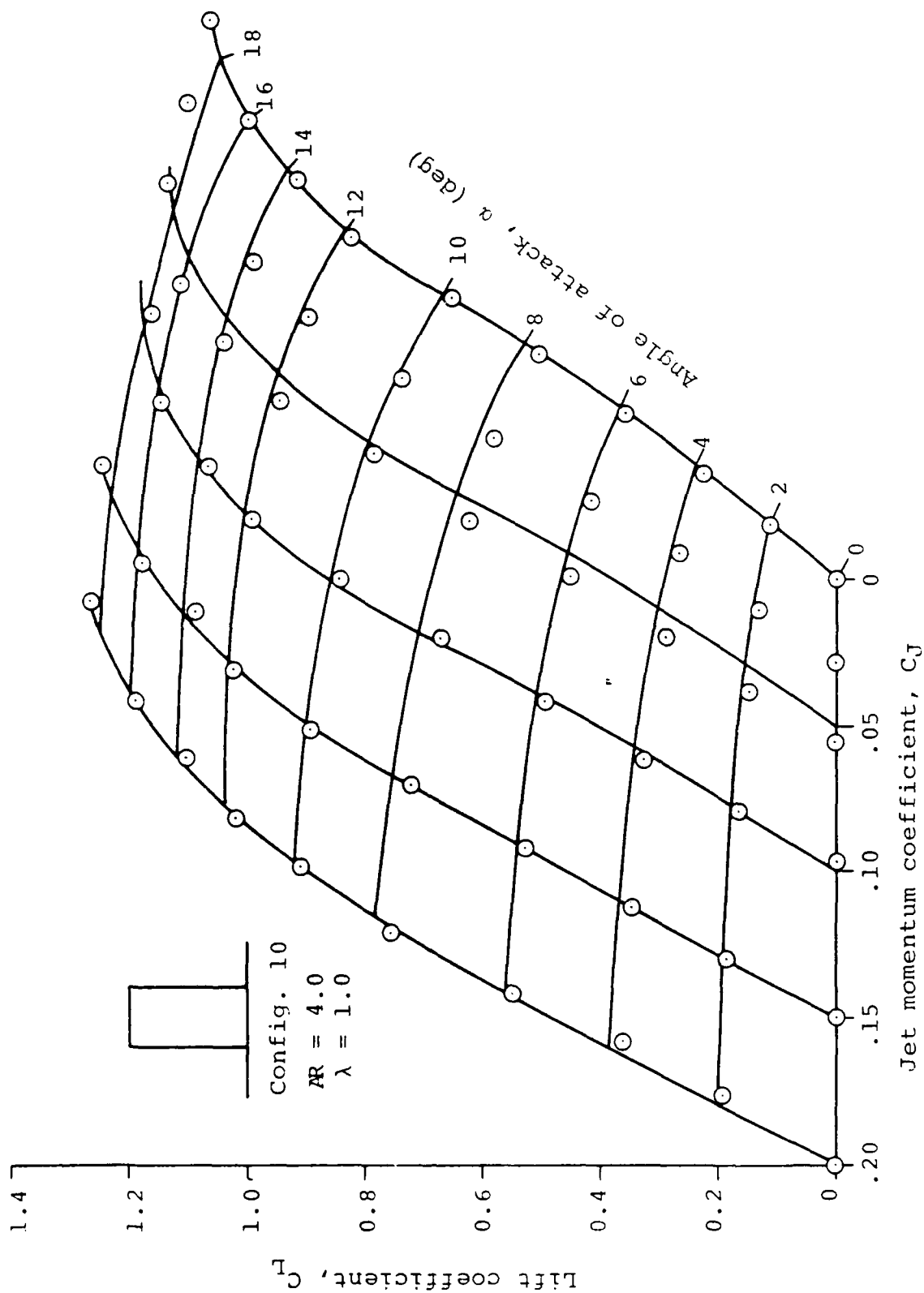
Figure 10.- Concluded, Wing 1.0
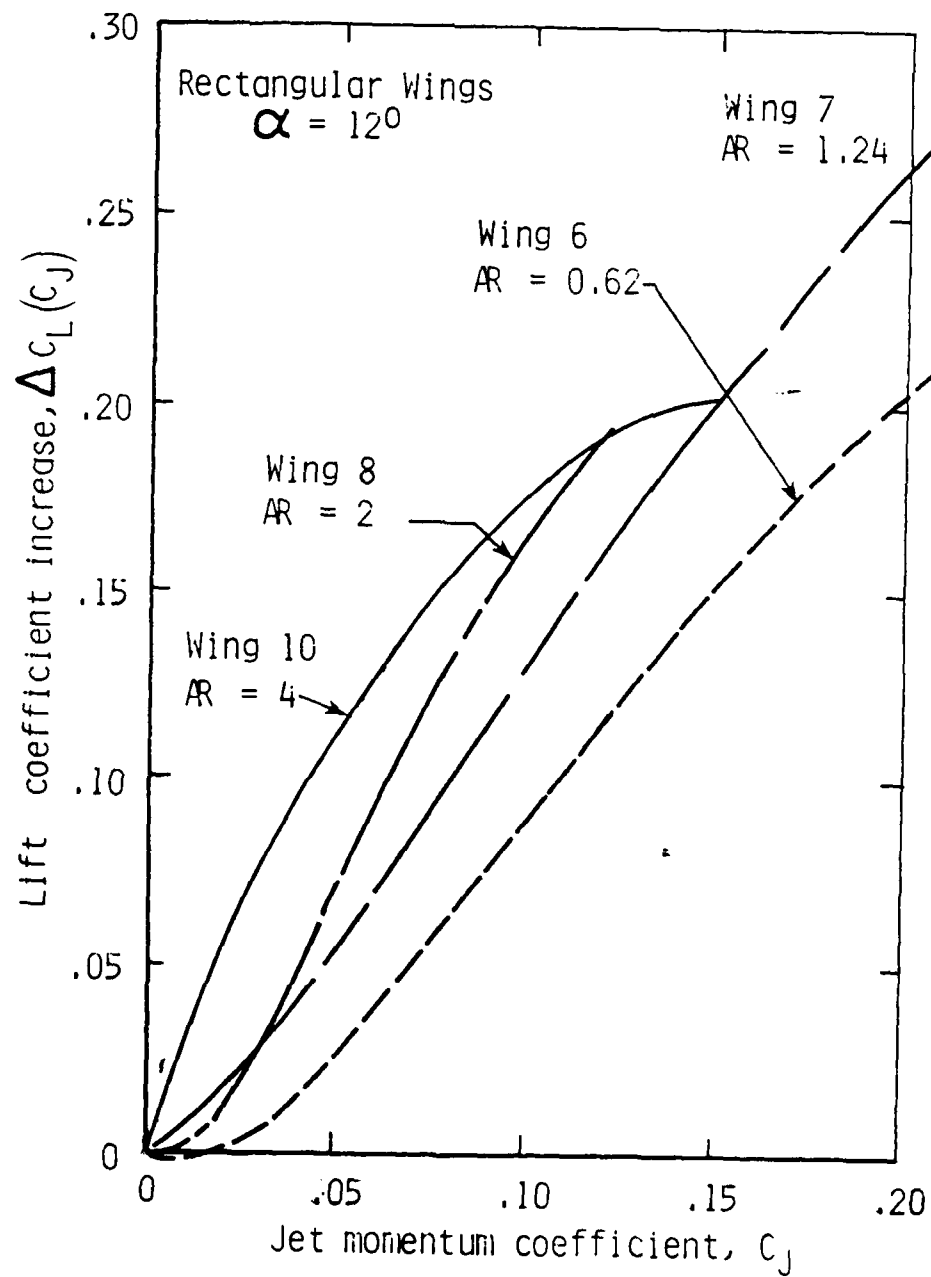
Figure 11.- Lift coefficient increase associated with jet blowing for rectangular wings.
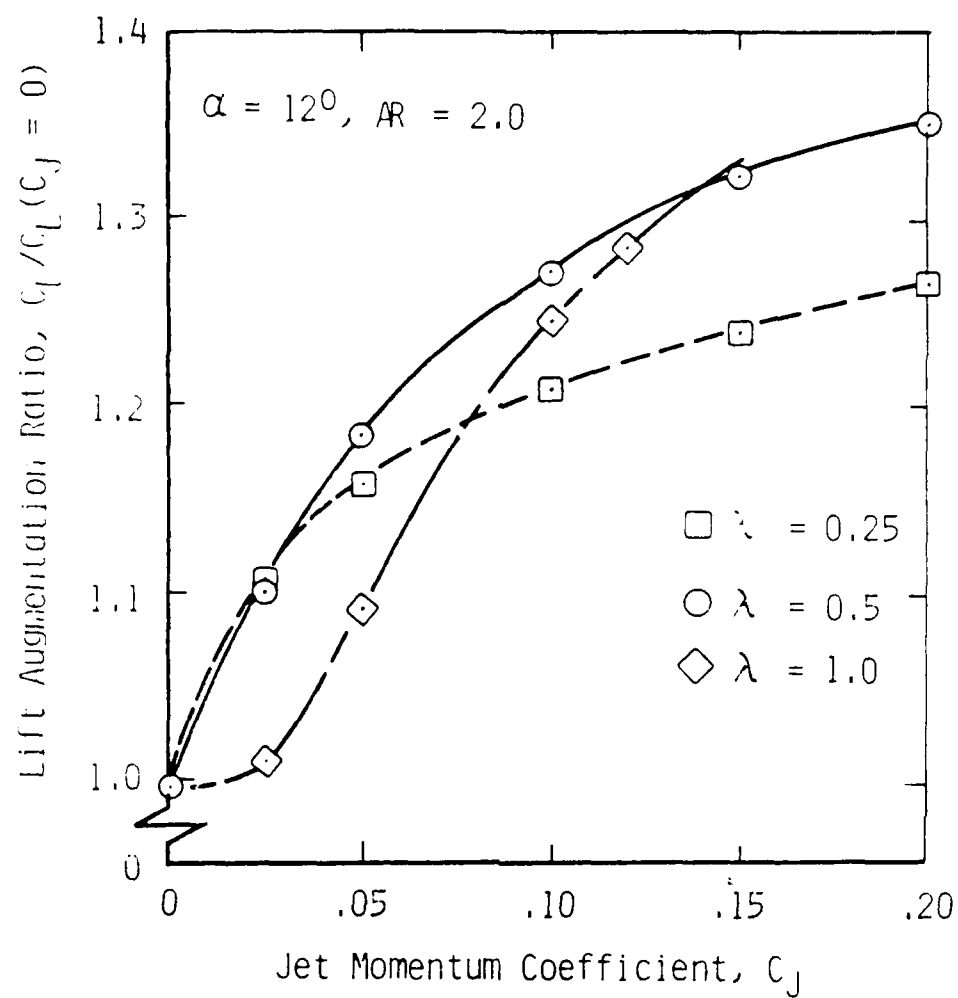
Figure 12.- Wing-tip blowing lift augmentation for AR = 2
wings at α = 12°.
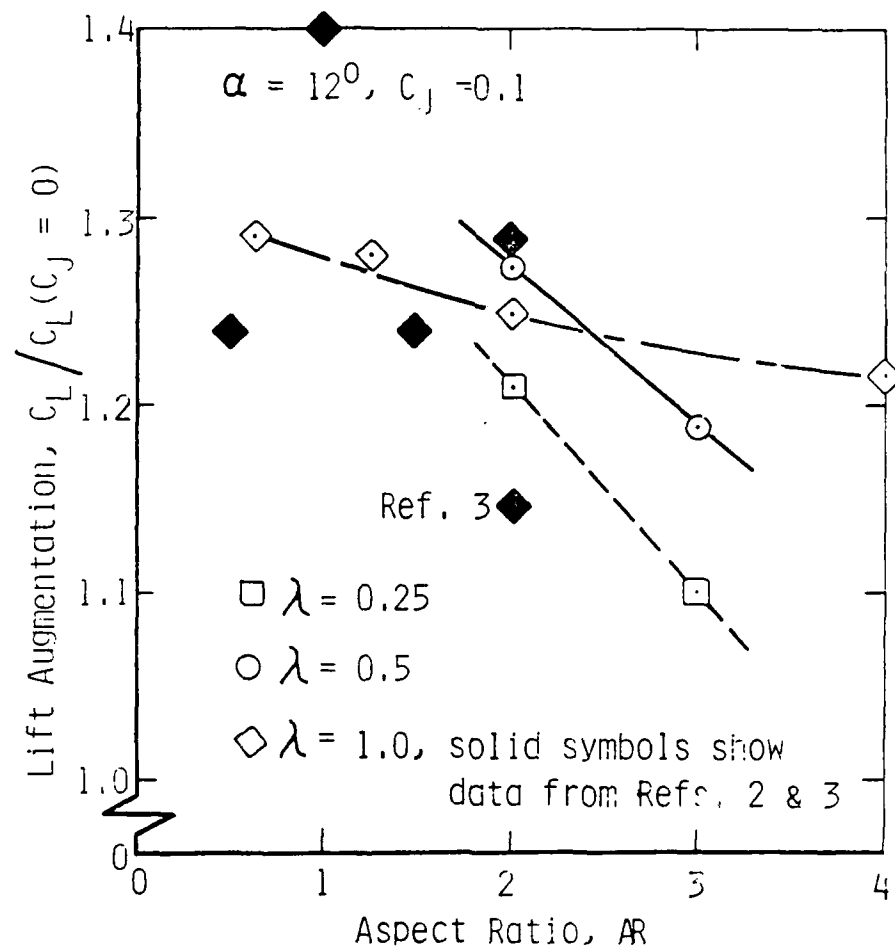
Figure 13.-Effect of aspect ratio upon lift augmentation
ratio for α = 12°, C_J = 0.1.

76
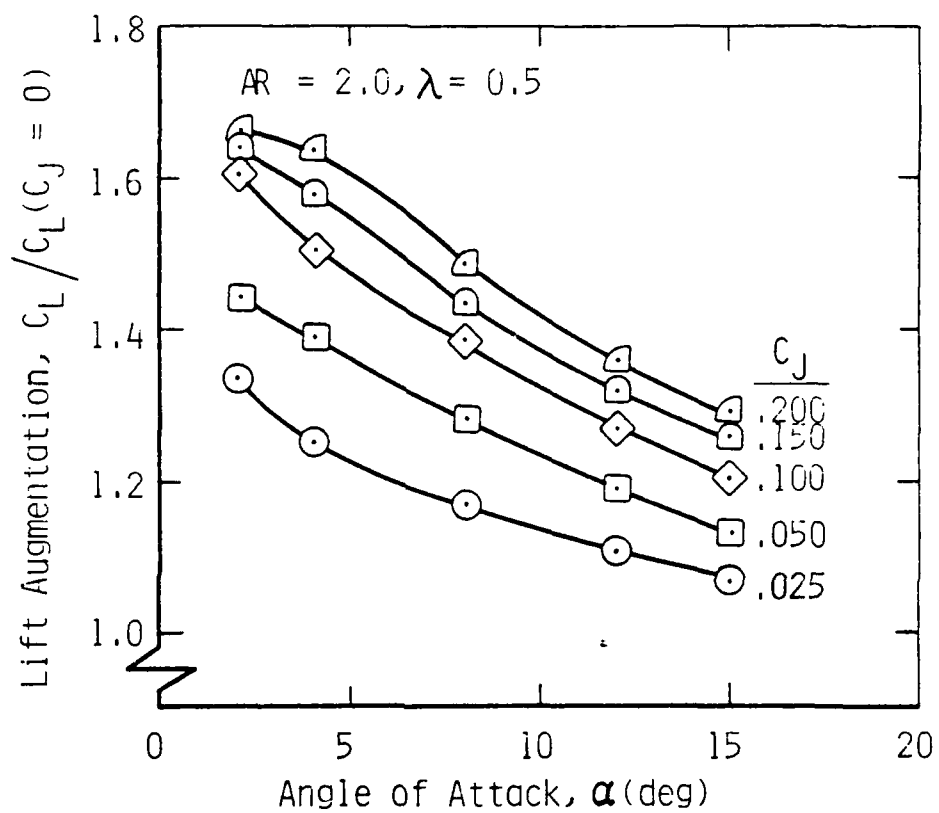
Figure 14.- Lift augmentation ratio of wing 4 as affected by angle of attack and jet momentum coefficient,
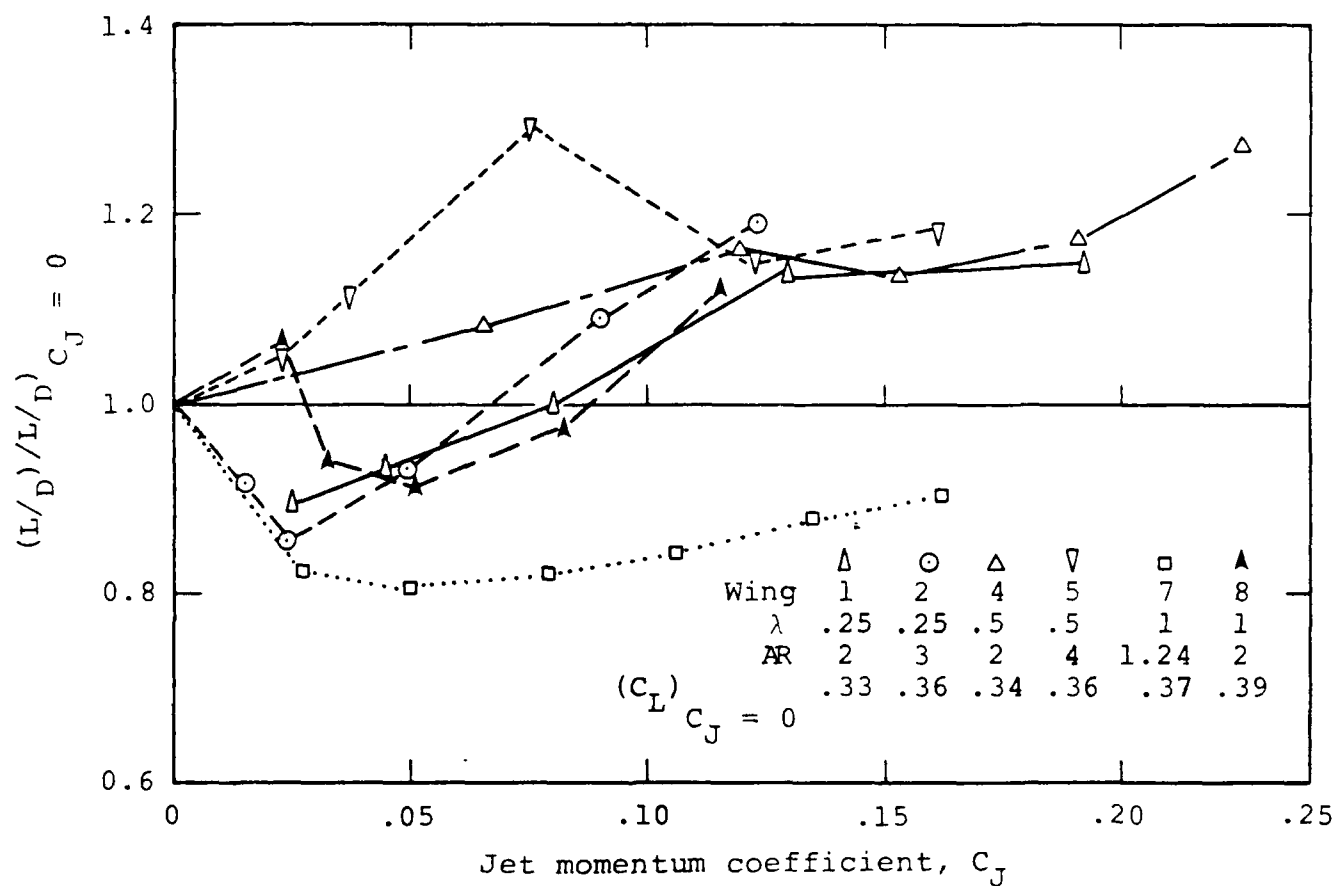
Figure 15.- Approximate lift-to-drag ratio versus jet
momentum coefficient at $C_L \approx 0.35$.
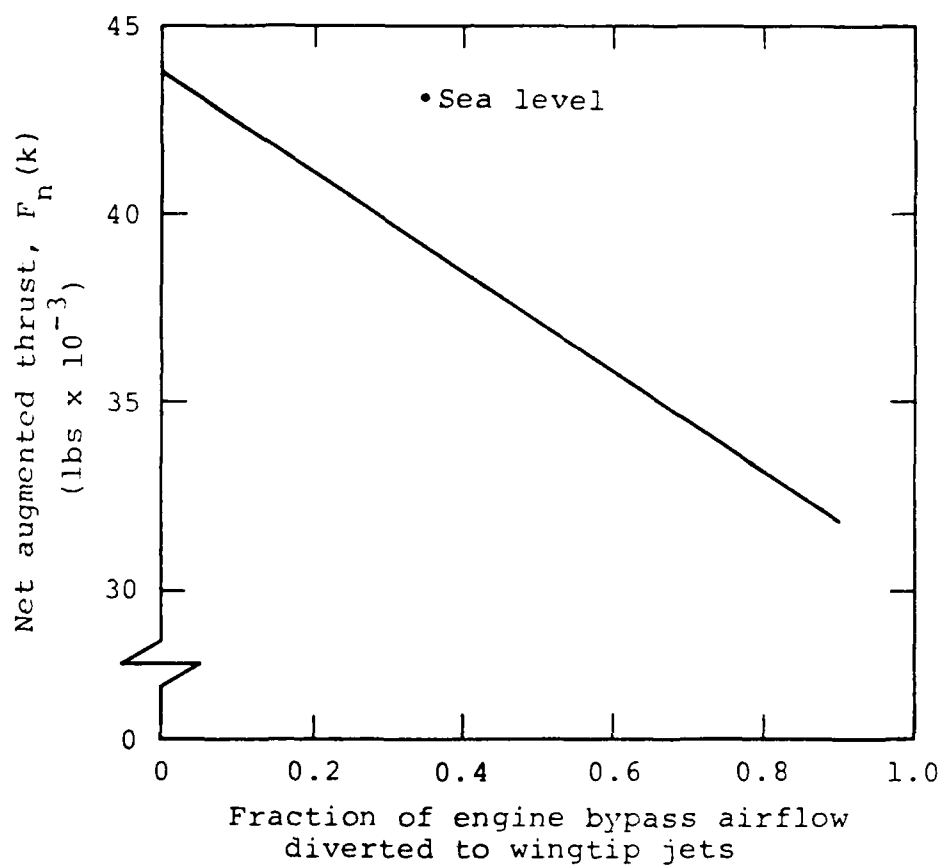
Figure 16.- Thrust degradation due to diverting engine
bypass airflow to wingtip jets (engine exhaust
nozzle adjected to provide same
exit velocity).

79

- Interceptor takeoff weight = 41,500 lbs.
- 210 ft/sec velocity.
- No winds, 1000 ft. altitude.
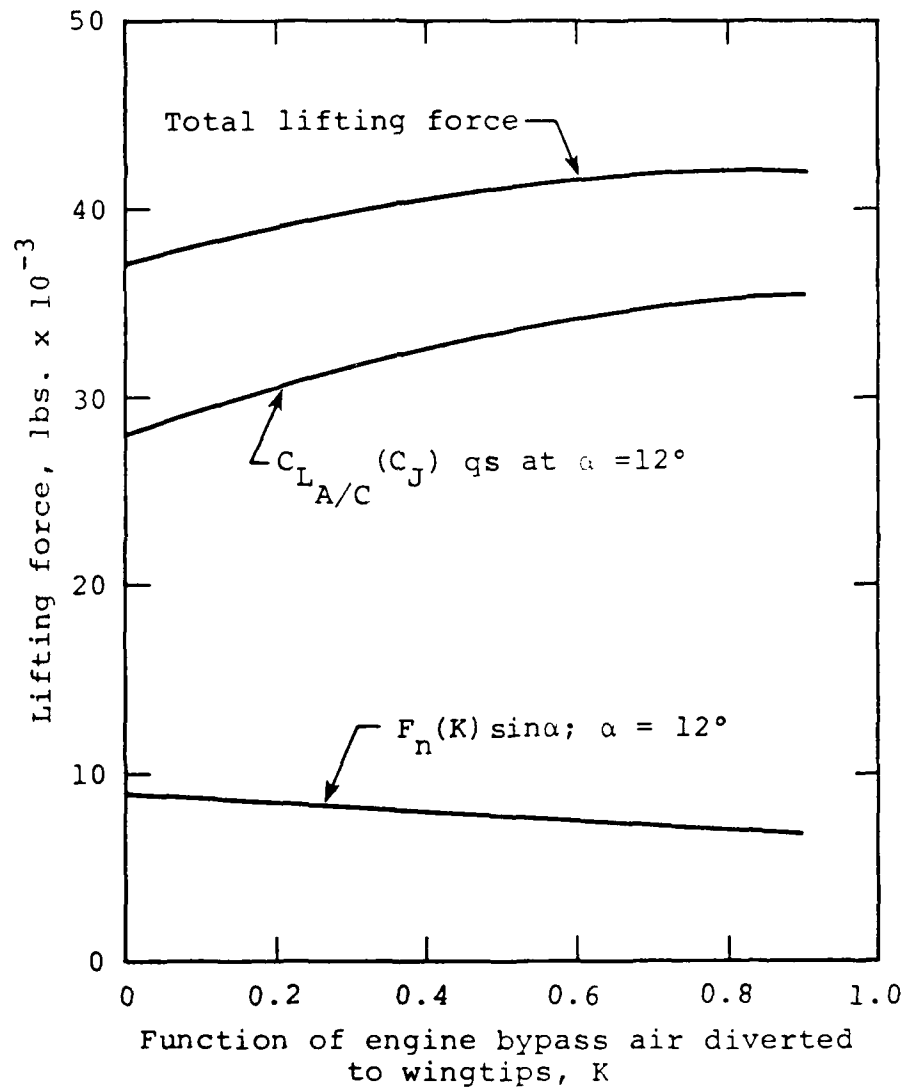
Figure 17.- Effect of diverting bypass air to the wingtip jets when runway speed = 210 ft/sec.
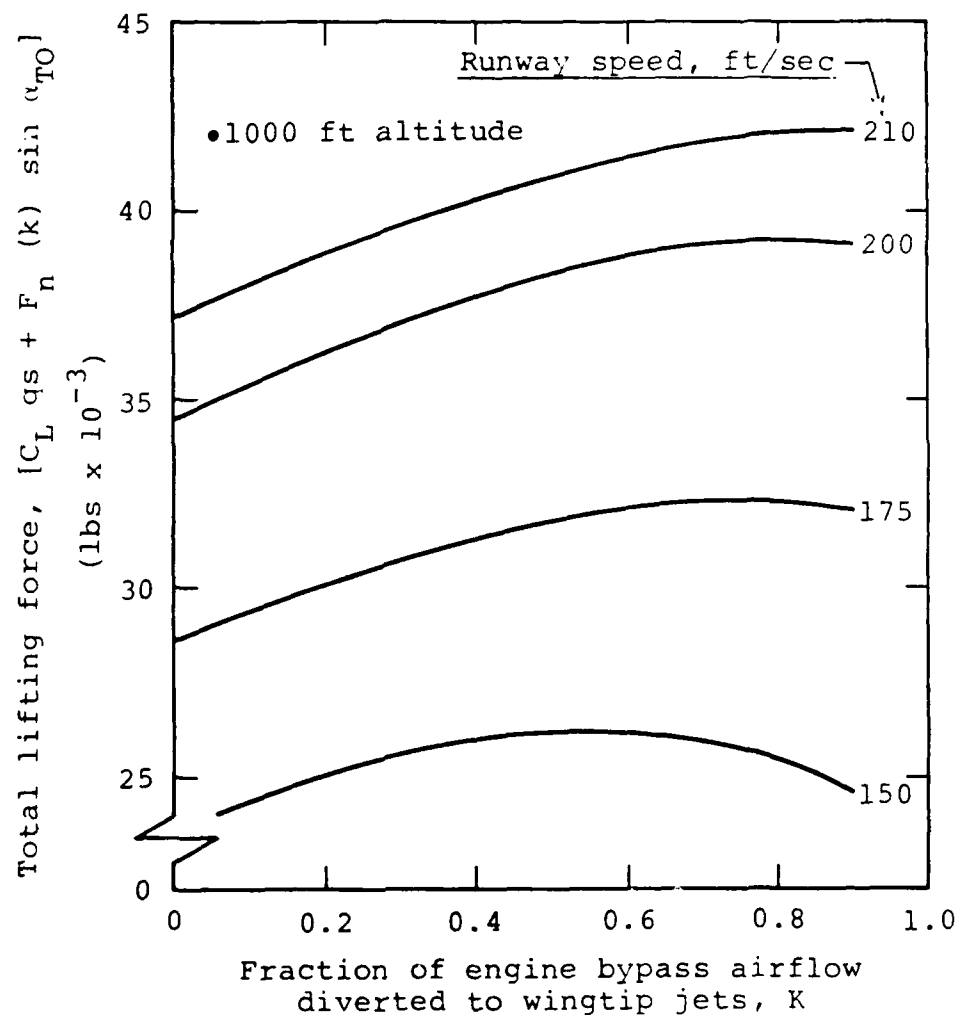
Figure 18.- Variation of total liftoff force with fraction of engine bypass airflow diverted to wing tip jets.
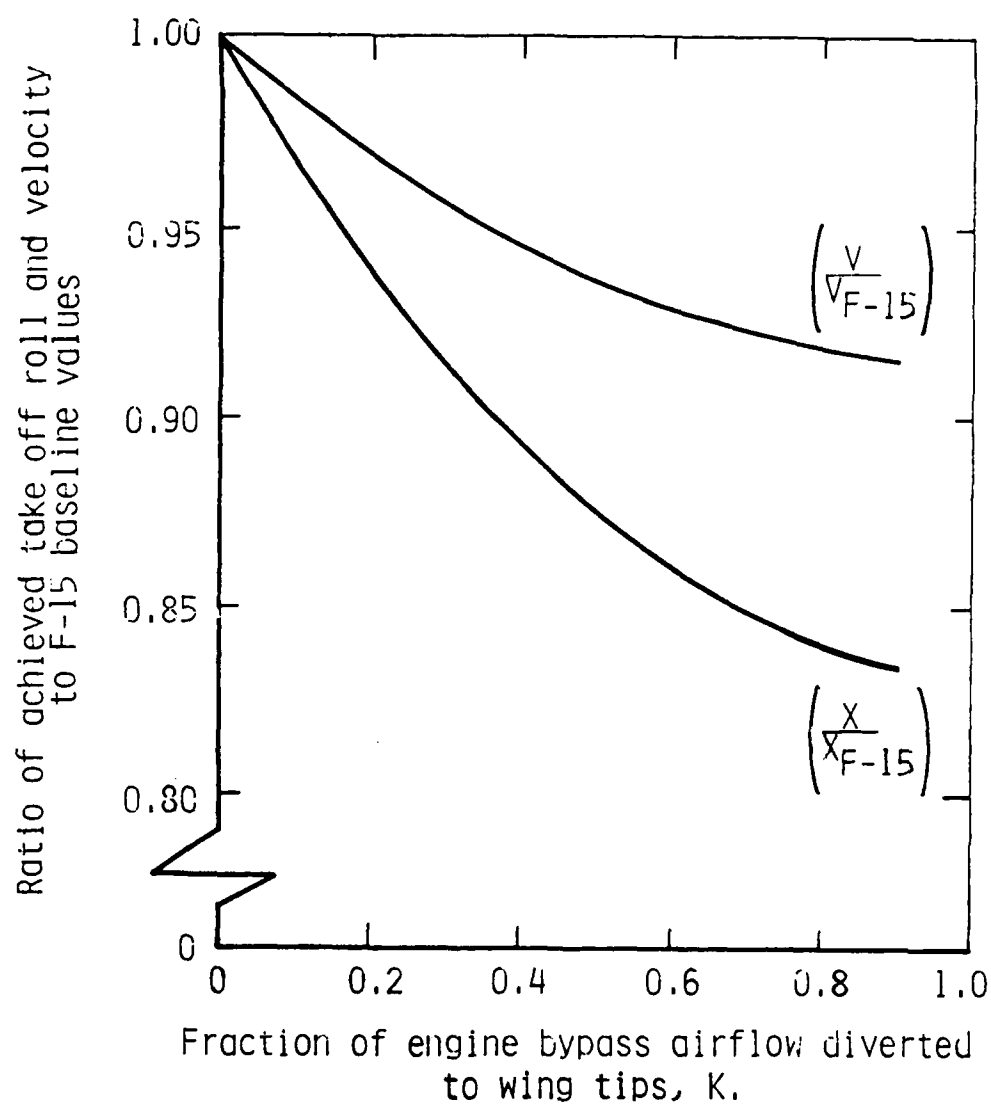
Figure 19.- Reduction in takeoff roll achieved by application of wing-tip blowing to an F-15 in interceptor configuration.
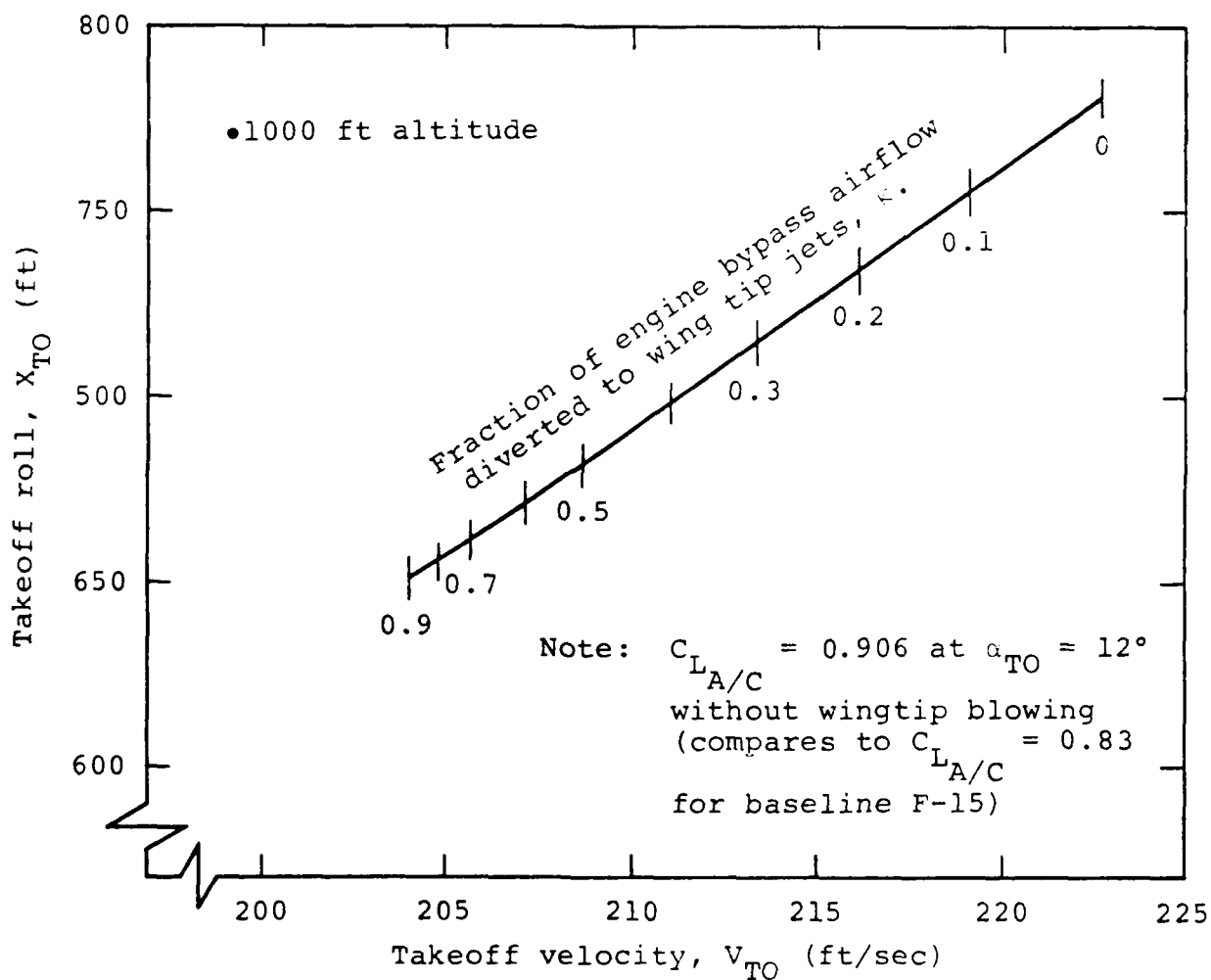
Figure 20.- Takeoff performance of an F-15 airplane fitted with
aspect ratio 2.0, taper ratio 0.5 wing panels,
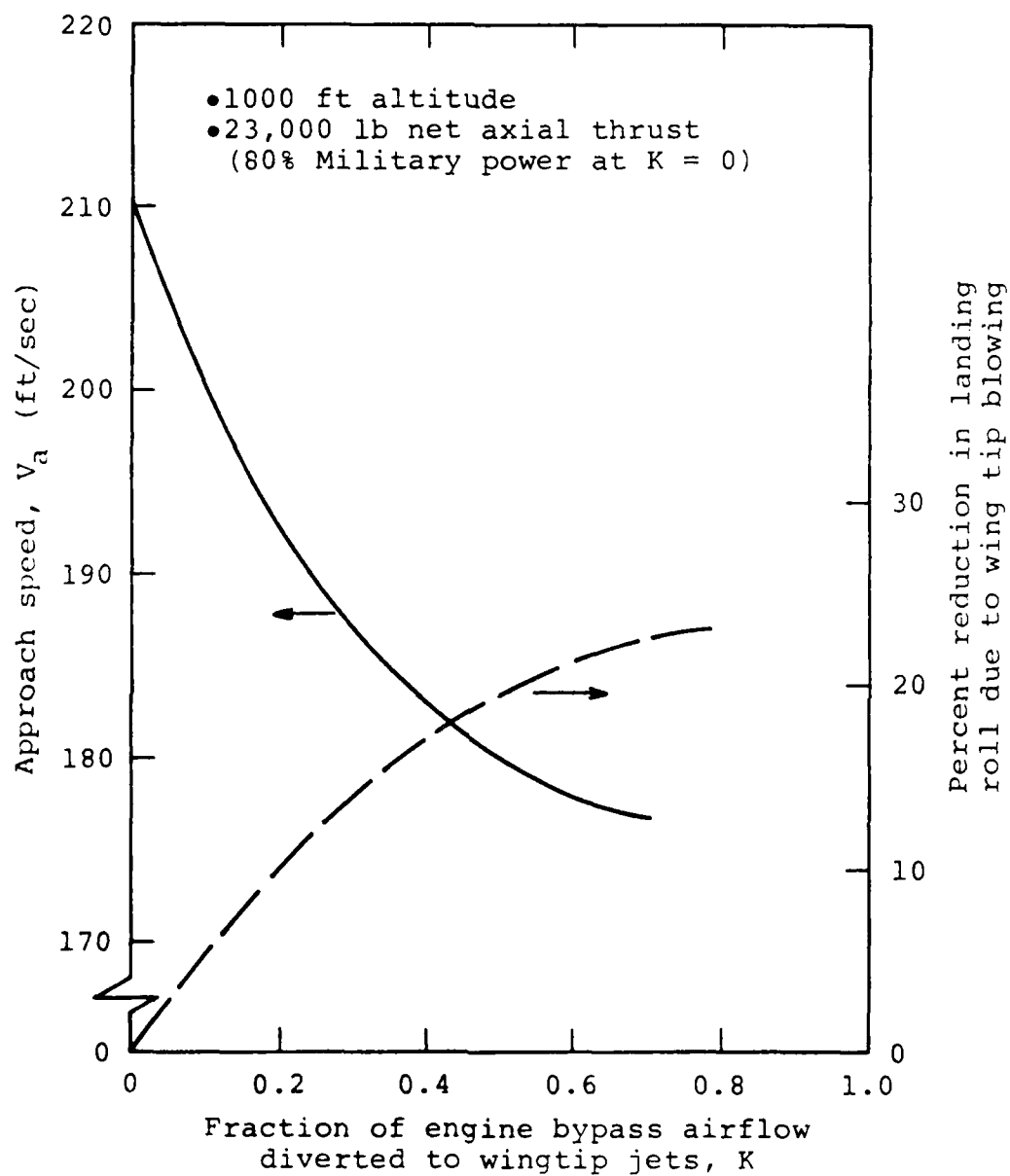and with blowing outboard from the wing
tips to augment lift.

83

Figure 21.- Landing roll reduction associated
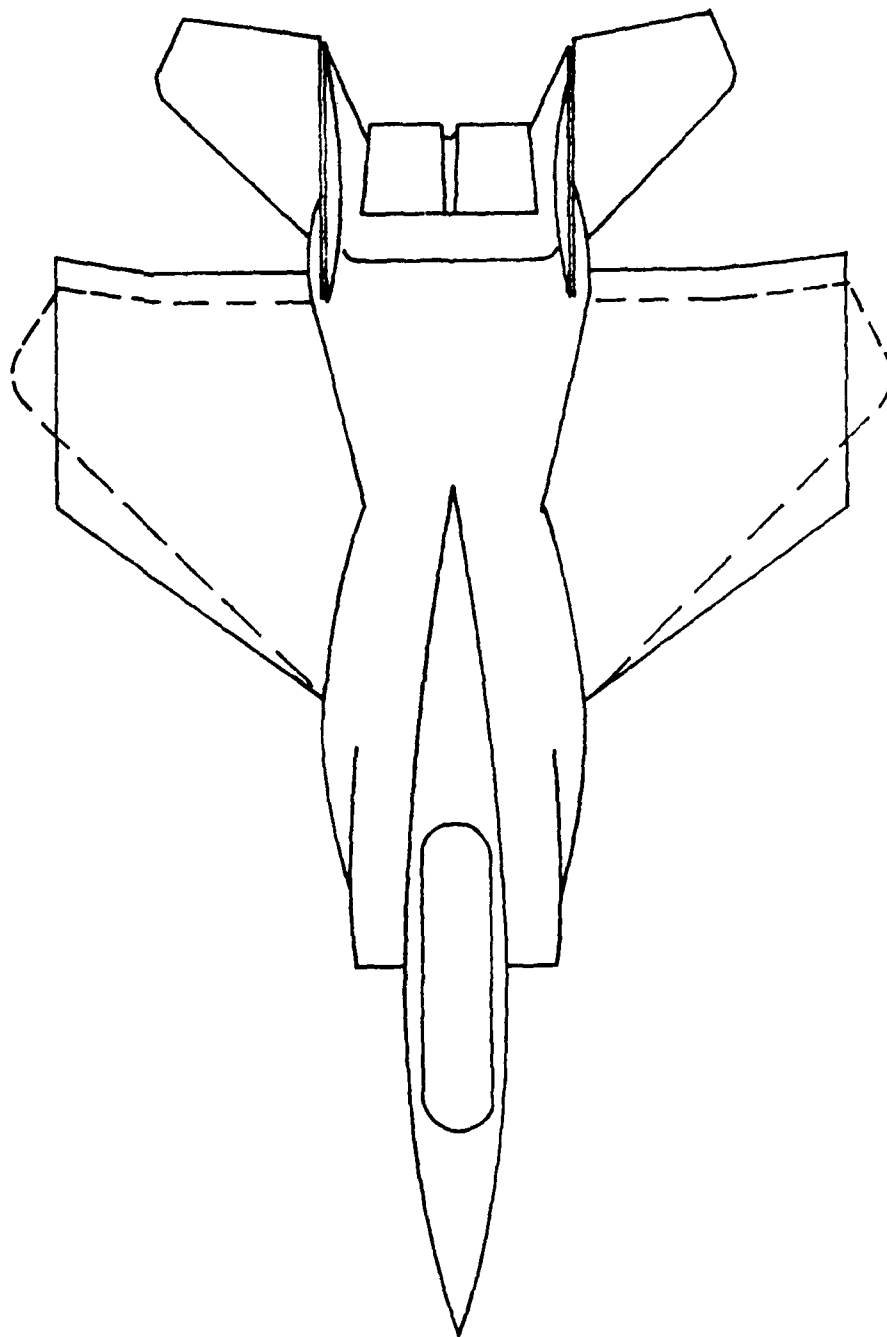with wingtip blowing,

Figure 22.– Recommended wing planform provides less taper, more tip chord for blowing.
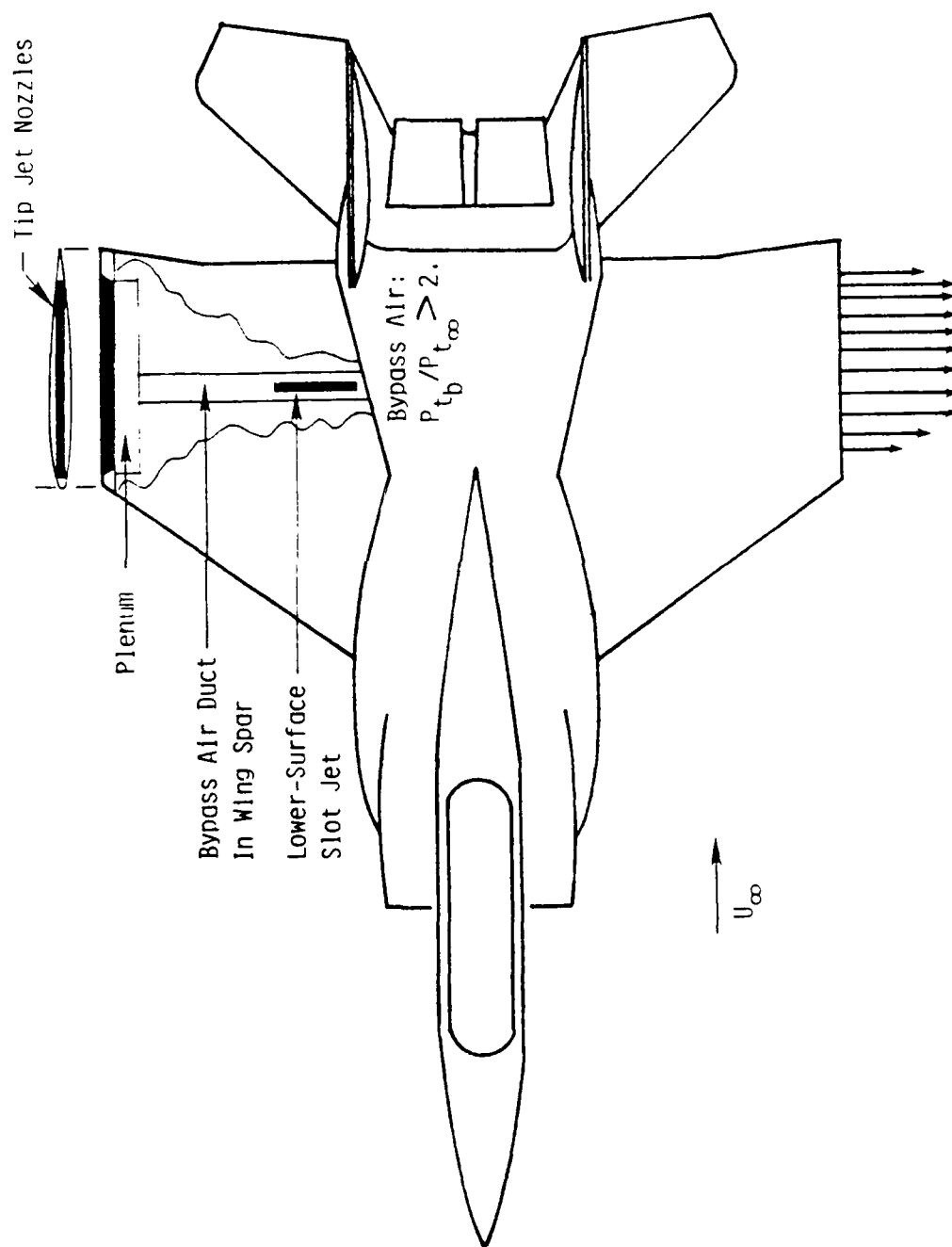
Figure 23.– Implementation of wing tip and lower surface blowing.

Tip Jet Nozzles

Plenum

Bypass Air Duct
In Wing Spar

Lower-Surface
Slot Jet

Bypass Air:
$P_{t_b}/P_{t_\infty} > 2.$

U_∞

END

FILMED

1-84

DTIC